THE FLUID REGIME OF METAMORPHISM AND THE CHARNOCKITE REACTION IN GRANULITES: A REVIEW

L. L. Perchuk and *T. V. Gerya*
(Institute of Experimental Mineralogy,
Russian Academy of Sciences, Chernogolovka)

From: "Flyuidnyy rezhim metamorfizma i reaktsii charnokitizatsii granulitov: obzor," *Izvestiya AN, seriya geologiya*, 1992 (forthcoming).

Several parameters (T, P_s, $\mu^{fl}_{K_2O}$, $\mu^{fl}_{CO_2}$, $\mu^{fl}_{H_2O}$, f_{O_2} and the bulk composition of rocks) govern the charnockite reaction,

$$\underset{\text{biotite}}{KMg_3AlSi_3O_{10}(H)_2} + \underset{\text{quartz}}{3SiO_2} = \underset{\text{orthopyroxene}}{3MgSiO_3} + \underset{\text{K-feldspar}}{KAlS_3O_8} + \underset{\text{water}}{(H_2O)},$$

in Precambrian gneiss complexes, which is effected by the introduction of alkali-carbon dioxide fluids during the retrograde phase of metamorphism. In the usual case, these fluids promote dehydration reactions due to the high μ_{K_2O} and low μ_{H_2O}. In the zoned *metamafite-enderbite-charnockite* complexes of Ukraine, East Siberia and Central Finland, the reactions

(i) $CaAl_2Si_2O_8 \cdot n NaAlSi_3O_8 + (0.5\ mK_2O) = CaAl_2Si_2O_8 \cdot (n\text{-}m)NaAlSi_3O_8 + mKAlSi_3O_6 + (0.5\ mNa_2O)$,

(ii) $(Fe, Mg)_2Si_2O_6 \cdot (1\text{-}n)Al_2Al_2O_6 + (1\text{-}n)\ (K_2O) = (1\text{-}n)KAlSi_3O_8 + (Mg, Fe)_2Si_2O_6$

and

(iii) $3K(Mg, Fe)_2Al_3Si_2O_{10}(OH)_2 + 21SiO_2 + 2(K_2O) = 7KAlSi_3O_8 + 2K(Mg, Fe)_3AlSi_3O_{10}(OH)_2 + (H_2O)$,

unambiguously indicate the fully mobile behavior of alkalies (Korzhinskiy, 1962), especially potassium. This shows up in a negative correlation between Al in Bt and/or Opx and N^{Pl}_{An}. In the case of introduction of fluid into a metamafic rock, the reaction

(iv) $NaCa_2Mg_5AlSi_7O_{22}(OH)_2 + 4SiO_2 + (^1/_2K_2O) = Ca_2Mg_5Si_8O_{22}(OH)_2 + KAlSi_3O_8 + (^1/_2Na_2O)$

International Geology Review, 1992, **34**, No. 1, pp. 1-58.

is an independent indicator of the effect of μ_{K_2O} on equilibrium in the metamafic rock, if reaction (i) proceeds at the same time. The associations Kfs + Opx (charnockite) and Pl + Opx (enderbite) form if the temperature is constant or decreasing (along retrograde *T-P* paths). It has been found that a_{H_2O} is higher in the formation of charnockites than in the metamorphism of associated gneisses; carbonates form in charnockites during decharnockitization, in the andalusite stability field as indicated by associated metapelites.

In the *arrested charnockites* of southern India and Sri Lanka, a negative correlation between the content of Al in Bt, Am and/or Opx and N_{An}^{Pl} is not found (i.e., potassium is inert). Nor has the leading role of CO_2 in charnockitization (Newton's model) been confirmed. However, replacement of hypersthene by biotite and/or cummingtonite in these rocks is almost ubiquitous. This indicates that decharnockitization reactions have taken place (high $\mu_{H_2O}^{fl}$). Estimates of the thermodynamic parameters and of the correlation between N_{Fe} and SiO_2 in arrested charnockites point to the possibility of melting in the cores of the patches with preliminary (or simultaneous) metasomatic alteration of the outer zones of the columns, with a shift of the bulk composition of the gneisses toward the granite eutectic. This promotes a water-carbon dioxide composition of the fluid, which sharply reduces the temperature of the charnockite eutectic (Peterson and Newton, 1990). Geologic observations of dikes and small bodies unequivocally prove the local migration of charnockite and enderbite melts. From the kinetic point of view, arrested charnockites can serve as a model of the charnockitization process, including that occurring in metamafites and metatonalites in zoned complexes.

Conventional Symbols

Minerals

Ab	=	albite	Gr	=	graphite
Act	=	actinolite	Gru	=	grunerite
Alm	=	almandine	Hbl	=	hornblende
Aln	=	allanite	Ilm	=	ilmenite
Am	=	amphibole	Kfs	=	K-feldspar
An	=	anorthite	Maf	=	dark minerals
Ank	=	ankerite	Mag	=	magnetite
Ann	=	annite	Ms	=	muscovite
Brn	=	breunherite	oCrn	=	"orthocorundum"
Bt	=	biotite	Opx	=	orthopyroxene
Cal	=	calcite	Or	=	orthoclase
Chl	=	chlorite	Prg	=	pargasite
Crd	=	cordierite	Phl	=	phlogopite
Crd	=	carbonate-cordierite	Pl	=	plagioclase
Cum	=	cummingtonite	Prp	=	pyrope
Dol	=	dolomite	Qtz	=	quartz
Eas	=	eastonite	San	=	sanidine
Ed	=	edenite	Sid	=	siderophyllite
En	=	enstatite	Sil	=	sillimanite
Fa	=	fayalite	Spl	=	spinel
Fs	=	ferrosilite	Tr	=	tremolite
Gln	=	glaucophane	Ts	=	tschermakite
Grt	=	garnet			

Thermodynamic Parameters

μ_i^{fl} = chemical potential of component i in fluid
X_i = mole fraction of component i
a_i^{fl} = activity of component i in fluid
γ_{En}^{Opx} = coefficient of activity in En in Opx solid solution
W_i = parameter of interaction of isomorphous components in solid solution
G_i^{α} = excess partial molar free energy of component i in phase α
ΔH^0, ΔS^0 and ΔV^0 = standard enthalpy, entropy and volume of reaction

Introduction

A half century ago, Korzhinskiy [1940] formulated the problem of the behavior of CO_2 during metamorphism. Using the rocks of the Aldan shield as an example, he demonstrated that P_{CO_2} increases with increasing depth of metamorphism, promoting the carbonatization of calcium silicates. He also distinguished the depth facies of carbonate-silicate rocks. Perchuk [1973; 1977] confirmed the pattern by calculating a_{CO_2} for complexes of different depths of metamorphism. As it turned out, the results contraindicated with the possibility of charnockitization of gneisses at shallow depths. However, this conflict is only apparent. Figure 1 shows the *generalized P-T* trends of the retrograde stage of metamorphism at four granulite complexes. The linear relationship of the *P-T* parameters is unequivocal and the paths themselves are close enough to lead to the derivation of a general equation for the relationship of the *P-T* parameters for the retrograde phase of metamorphism [Perchuk and Gerya, 1990]:

$$P, \text{kbar} = 0.0176\ (\pm 0.00376) \cdot t^{\circ}\text{C} - 6.774\ (\pm 2.529) \quad (1)$$

Despite the closeness of the paths in Figure 1, within each metamorphic complex a_{H_2O} increases isothermally from the relatively high-pressure Sutam complex [Marakushev, 1965] to the shallow Sharyzhalgay complex. This is seen in Figure 2, plotted from the data in Table 1, using very simple models of the activity of the components in Opx, Bt and Grt [Perchuk, 1991; Perchuk and Gerya, 1990].

The problem of the origin of rocks of the charnockite series has been discussed and rediscussed, by Allen, Weaver, Janardhan, Condie, Korzhinskiy, Levitskiy, Marakushev, Nalivkina, Newton, Petrova, Santosh, Friend, Hansen, and many other petrologists.

Sudovikov [1954] proposed a model of granitization (including charnockitization) of gneisses, in which metasomatism by fluids changes the composition of the rocks to the eutectic, and they are melted under granulite-facies conditions. This model would seem to explain the origin of the arrested charnockites formed after orthogneisses and khondalites in the granulite complexes of southern India and Sri Lanka, as will be discussed below.

Korzhinskiy [1962] developed a model of charnockitization of gneisses and metamorphic rocks in line with the concept of granitization as magmatic replacement, caused by fluids with a high chemical potential of potassium. Santosh et al. [1991] studied the composition of fluid inclusions in minerals in the Closepet granite at Kabbaldurga, southern India. This enabled them to ascertain the evolution of the fluid, and in essence, to confirm Korzhinskiy's idea that charnockites are related to granite magmatism, which serves as the carrier of heat and volatiles.

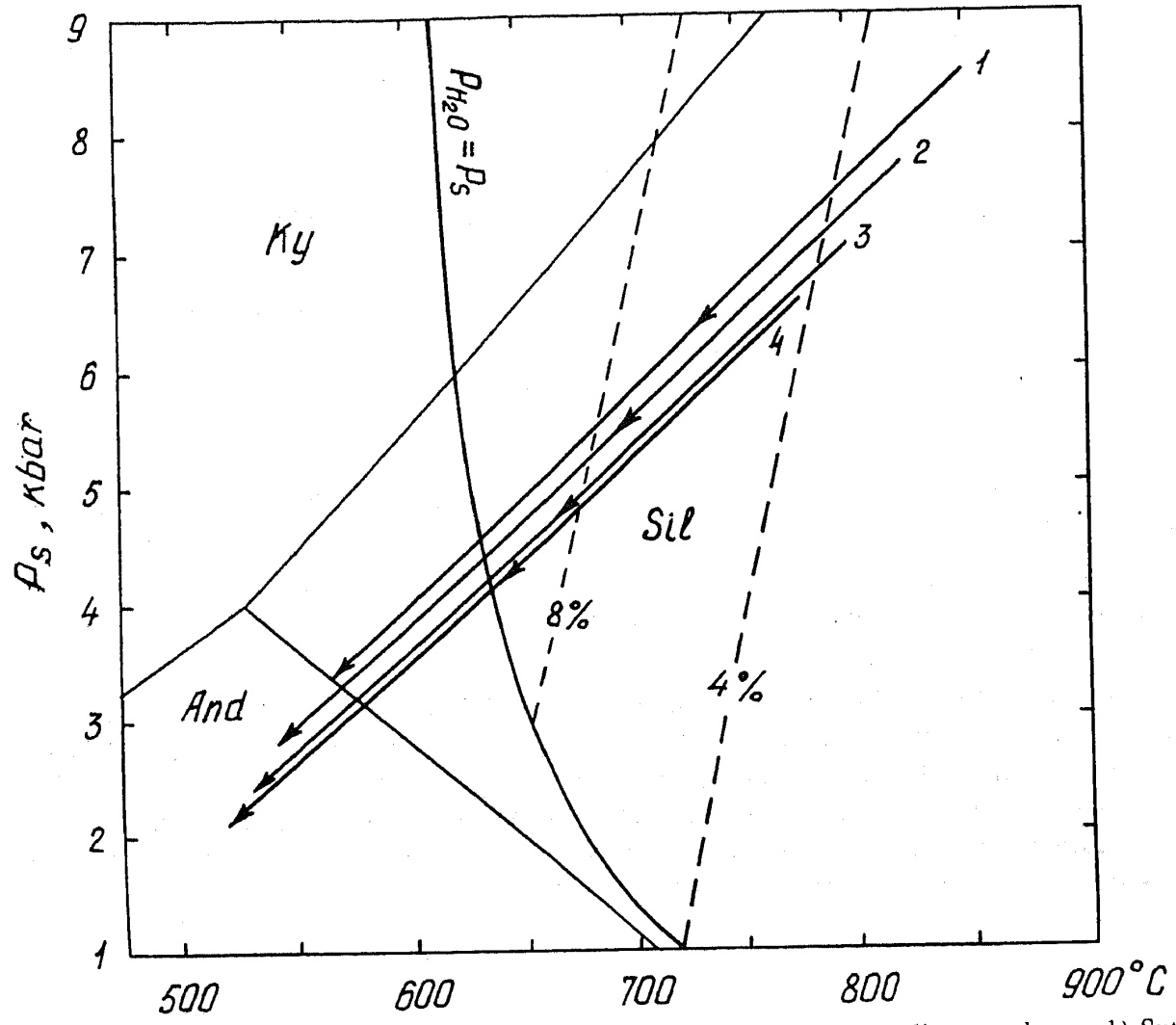

FIGURE 1. Generalized *P-T* paths of retrograde metamorphism in four granulite complexes: 1) Sutam complex, Aldan Shield; 2) West Aldan [Perchuk et al., 1985]; 3) Khankay pluton, Primor'ye [Russian Far East] [Perchuk, 1987]; 4) Sharyzhalgay complex, southeastern Cisbaikalia [Perchuk, 1987, 1989].

Studying the so-called arrested charnockites of southern India, Janardhan et al. [1979, 1982], Friend [1981, 1983, 1985], and then Condie et al. [1982] and Raith et al. [1989] concluded that CO_2 plays an essential part in dehydration of biotite gneisses to form charnockites under granulite-facies conditions. The idea also emerged that boundaries between zones of granulite- and amphibole-facies metamorphism during charnockitization are local [Janardhan et al., 1982; Santosh et al., 1990]. Lamb and Valley [1984] proposed a model of anhydrous prograde metamorphism of granulites, at a low partial pressure of carbon dioxide, as a result of which dehydration reactions occurred, with the formation, in particular, of a stable paragenesis of orthopyroxenes with K-feldspar. The essence of this idea had earlier been expressed by Korikov and Kislyakova [1975], who found Opx + Fsp reaction rims around biotite grains in granulite of the Sutam complex of the Aldan Shield, and related these textures to the prograde stage of metamorphism. Finally, Waters and Whales [1985] developed the idea of dehydration of granulites as a result of extraction of granitic partial melts.

In one way or another, all authors relate charnockitization to the introduction of subalkaline carbon-dioxide juvenile fluids during the prograde stage of metamorphism. Moreover, after systematic investigations of many granulite complexes, Perchuk [1985, 1986, 1989] showed that

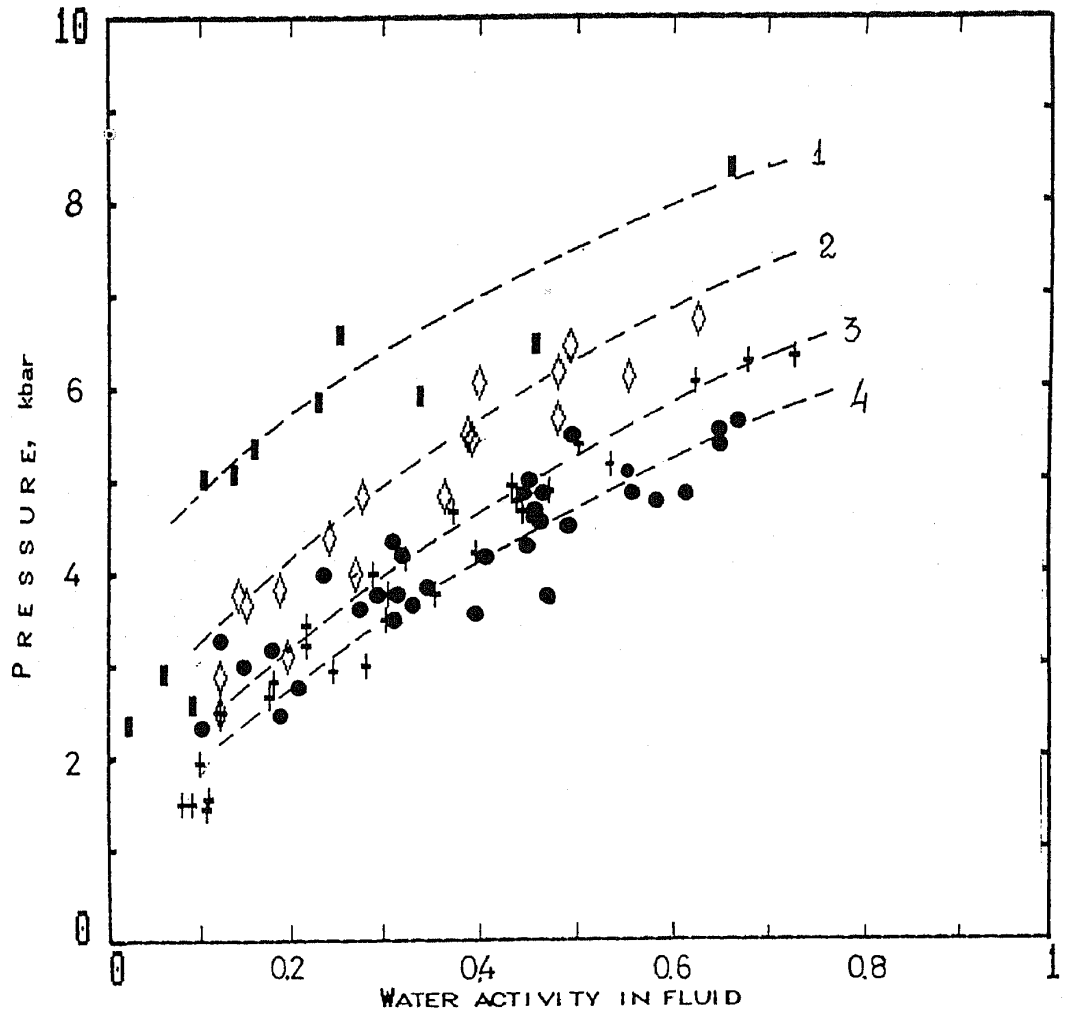

FIGURE 2. Variation in activity of water during retrograde metamorphism of the four granulite complexes along *P-T* paths of Figure 1 [Perchuk, 1987].

the reaction textures of the prograde phase of metamorphism are hardly ever preserved, and the activity of CO_2 can also increase in the retrograde phase. In this case, biotite gneisses and some metamafic rocks are transformed into rocks of the charnockite series (enderbite and charnockite), and carbonate-cordierite is extensively developed in interbedded metapelites [Perchuk, 1989]:

$$Grt + Qtz + (CO_2) = Opx + Crd \cdot CO_2 \quad (2)$$

$$Bt + Grt + Qtz + (CO_2) = Opx + Kfs + Crd \cdot CO_2 + H_2O \quad (3)$$

Marakushev [1965, 1969] examined reaction (3) in detail, but without the participation of CO_2. Stressing its extreme nature (maximum chemical potential of H_2O in the P_s-μ_{H_2O} diagram), he attributed to this reaction a special role as the boundary between two mineral facies independent of the total pressure P_s. However, as mentioned above, μ_{CO_2} can substantially reduce the temperature limit of stability of the paragenesis Bt + Grt + Qtz, i.e., it can shift reactions (3) and (2) to the right. In fact, by determining the *P-T* parameters during regressive metamorphism in the metapelites of the Sharyzhalgay granulite complex in southwestern Cisbaikalia, Perchuk

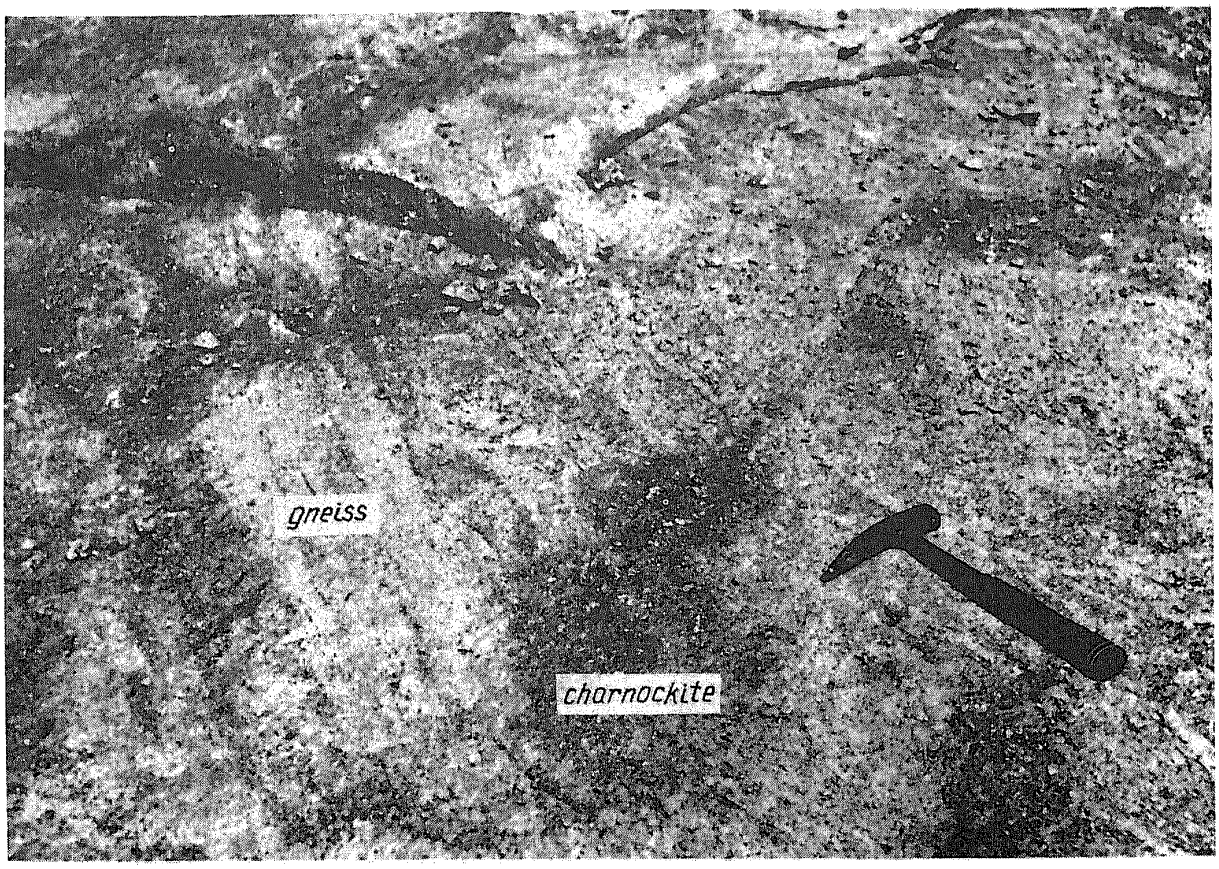

Fig. 3a

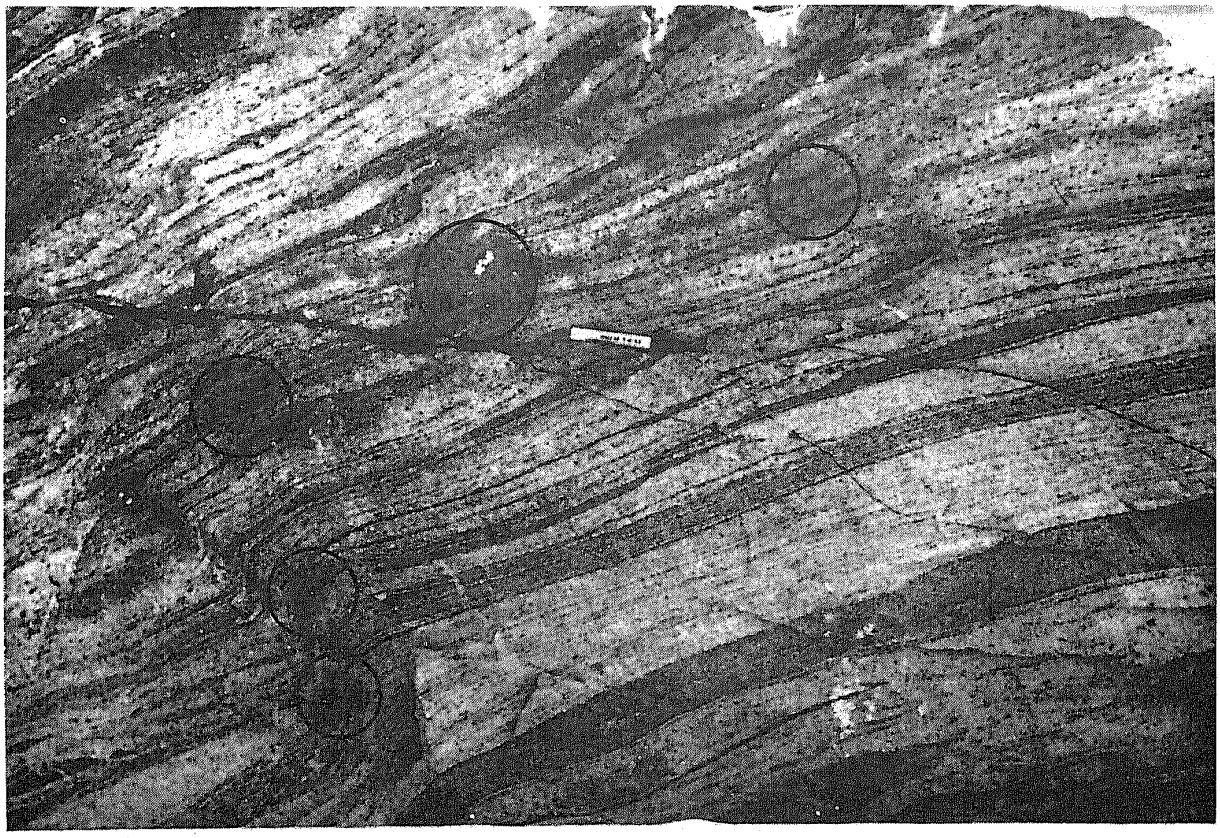

Fig. 3b

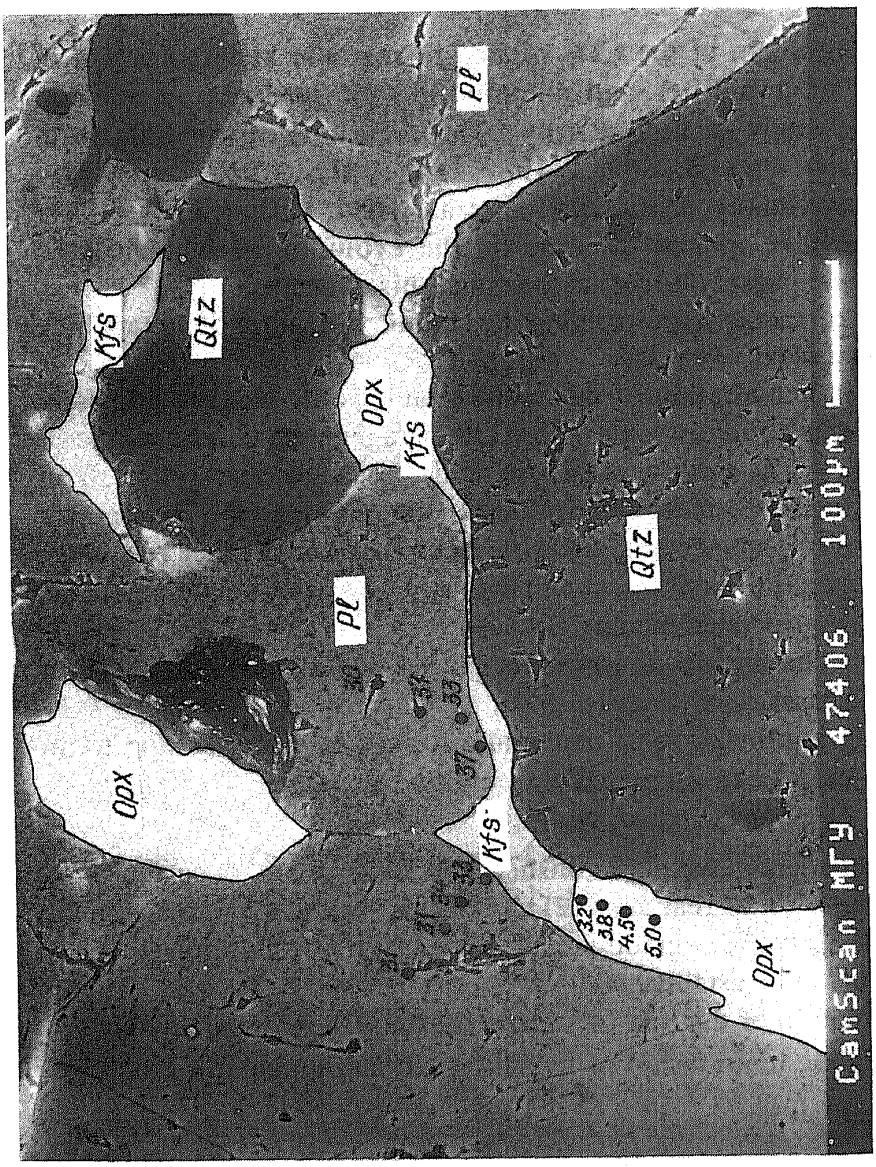

FIGURE 3. Structural homogenization of gneisses during charnockitization in the Kabbaldurga area, southern India. Circles indicate areas in which the primary banding and metamorphic foliation gradually disappear.

Fig. 3c

[1987, 1989]unambiguously determined the stability of the Opx + Crd · CO_2 paragenesis to a temperature of 550° C and pressure of ~2.5 kbar. Virtually the same conclusion can be drawn from comparison of the data of Chacko et al. [1987, p. 350] based on estimation of the *P-T* parameters of formation of the garnet-cordierite gneisses (khondalites) and charnockites developed after them in the state of Kerala, southern India. For charnockites, these parameters are lower everywhere. Hiroi et al. [1990] studied the structural relationships and mineral composition of the associated gneisses and arrested charnockites of Sri Lanka and concluded that charnockitization took place at low pressures and moderate temperatures. In particular, retrograde andalusite and siderite were found in the gneisses and migmatites. Moreover, in outcrops in central Sri Lanka, on the slopes of Mt. Kabbal in the state of Karnataka, India, in central Finland, and in the Baikal section of the Sharyzhalgay complex, it is seen that metasomatic transformation of gneisses into charnockite involves the disappearance of inherited signs of deformation in the rocks, i.e., they become texturally homogenized (see Fig. 3) at relatively shallow depths. All these observations indicate that in some cases charnockitization of biotite gneisses and amphibolites can occur at shallow depths and over a wide temperature range.

At one time it seemed that the problem of the CO_2 regime in regional metamorphism in general, and in charnockitization of granulites and amphibolites in particular, had been unequivocally solved, thanks to the study of high-density CO_2 inclusions in minerals from granulite-facies rocks, including charnockites [Berdnikov, 1987; Dolgov et al., 1967; Kurdyukov and Berdnikov, 1987; Tomilenko and Chupin, 1983; Hansen et al., 1984; Rudnik et al., 1987; Touret, 1981, 1971]. However, the development of ideas on the evolution of metamorphic complexes, especially in the retrograde phase, obliges us to amend this concept.

Thus, at present the following phenomena accompanying the charnockitization of metapelites and metamafic rocks have been established:

1) CO_2 plays an essential role in dehydration of metapelites and biotite-bearing gneisses, with the formation of the Opx + Pl + Qtz and/or Opx + Kfs + Qtz parageneses, characteristic of enderbite and charnockite, respectively. The activity of CO_2 in many cases increases precisely in the *retrograde phase* of metamorphism (this is indicated by direct estimates of the *P-T* parameters in rocks, as well as by the appearance of muscovite, ankerite, breunnerite and other relatively low-temperature carbonates in charnockite gneisses simultaneously with the development of carbonate-cordierite and andalusite in associated metapelites).

2) The activity of H_2O during the charnockitization of metapelites and gneisses may remain constant, and in some cases even increases.

3) Charnockites can form during granitization of metamafic rocks and gneisses due to an increase in μ_{K_2O} in the fluids migrating from a crystallizing granite magma into surrounding mafic rocks [Korzhinskiy, 1962].

4) Detailed observations in thin-section have established the widespread occurrence of decharnockitization, i.e., a shift to the right of reactions (2) and (3), as well as the development of oxidation-reduction reactions during the retrograde metamorphism; their relationship to the charnockitization process still remains to be established.

This paper is devoted to determination of the role of various thermodynamic parameters (T, P_s, $\mu^{fl}_{K_2O}$, $\mu^{fl}_{CO_2}$, $\mu^{FL}_{H_2O}$, f_{O_2}), as well as the relationship of metamorphic and magmatic processes during charnockitization of gneiss complexes.

Terminology and Classification of Rocks of the Charnockite Series

1. *Relationships between the amphibolite and granulite metamorphic facies: terminology.*

In metamorphic complexes where charnockitization of biotite and amphibole gneisses occurs, one sees a local change (sometimes within a few centimeters) from parageneses typical of the amphibolite facies (Bt + Qtz + Pl, Am + Qtz + Pl) to those typical of the granulite facies (Opx + Kfs + Qtz, Opx + Pl + Qtz). As mentioned above, in recent years a tendency has been observed to identify the principles of mineral facies with metamorphic facies. This has led to meaningless study of the so-called transition zone between granulite and amphibolite facies, just because the Opx + Kfs paragenesis develops in the former instead of Bt + Qtz ± Hbl. It is generally accepted that the stability field of a mineral and its association, the rock composition being constant, is determined by a multitude of thermodynamic parameters: T, P_s, $\mu^{fl}_{H_2O}$, $\mu^{fl}_{CO_2}$, f_{O_2}, etc. (mineral facies), while rocks metamorphosed at $T \geq 650°$ and $P_s \geq 3$ kbar belong to the granulite facies [*Glossary of Geology*, 1978]. Even in a recent textbook on metamorphism [Yardley, 1989, p. 93], granulite-facies metamorphism is treated in the classic interpretation.

2. *Classification of rocks of the charnockite series.*

The classification of rocks of the charnockite series put together at the beginning of the century underwent many changes for a number of objective reasons. The main one was the

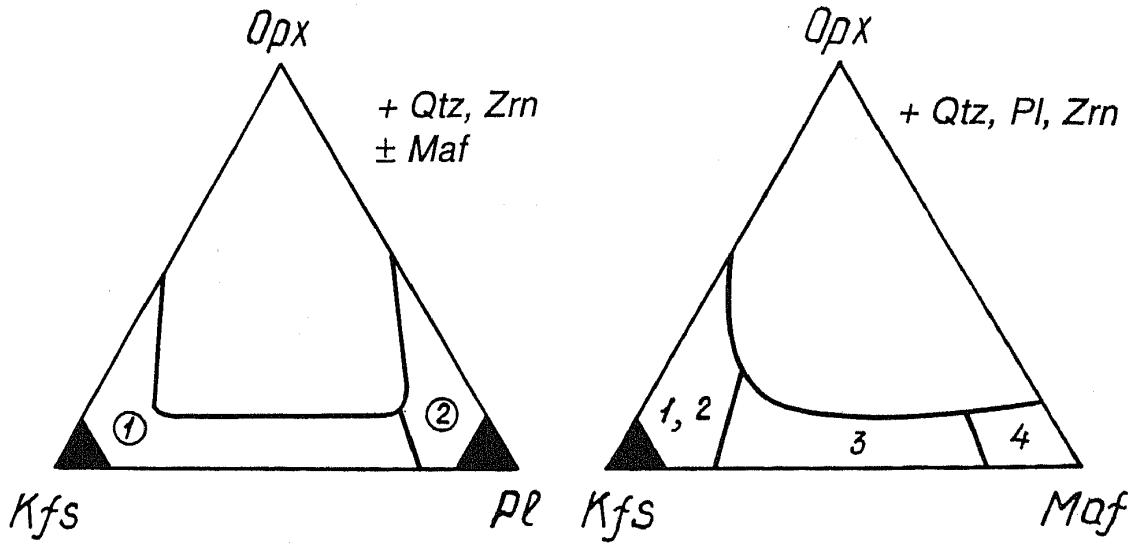

FIGURE 4. Classification of rocks of the charnockite series based on mineralogic composition (vol%): 1) charnockites; 2) enderbites; 3) norites; 4) metamafites and mafic schists.

rather widespread occurrence of the Opx + Kfs paragenesis in metamorphic rocks of different compositions. To some extent, that was what caused Korzhinskiy [1962] to turn his attention to the problem of charnockitization of gneisses. In addition, introduction of the term enderbite (from Enderby Land in Antarctica) largely contributed to terminological chaos.

Rocks of the charnockite series may be igneous, metamorphic or metasomatic. The differences between them are relatively easy to establish on the basis of textural and geological relationships. The *Glossary of Geology* [1978] defines charnockites as hypersthene granites containing about 20% quartz, with K-feldspar making up from 35 to 90% of the total of all felsic components. According to other definitions, the amount of quartz may range from 10 to 60%. Enderbite is considered a member of the charnockite series rich in antiperthitic plagioclase (up to 87.5% of all felsic components), in which the quartz content reaches 65% of the leucocratic fraction. In addition to Opx, magnetite is found in it. For instance, the Sharyzhalgay complex contains not only typical metamorphic enderbites, but also medium-grained leucocratic igneous rocks with hypidiomorphic-granular texture. These form independent bodies, in the marginal parts of which are xenoliths and relicts of the metamorphic host rocks; sometimes fairly thick (up to 5 m) giant-grained veins of pegmatoid enderbite are encountered, in which content of Mag and Opx do not exceed 8-10%; the rest (60-70%) is quartz. The texture and composition of these rocks are very persistent and therefore we can say they are of allochthonous igneous origin.

Because the nomenclature of the rocks fo the charnockite series has not been perfected, hypersthene-bearing rocks with various contents of Kfs and Pl are called enderbo-charnockites or charno-enderbites (see, for instance, Petrova and Livitskiy [1984]). To avoid terminological confusion, we have chosen very simple mineralogical and chemical classifications of the rocks of the charnockite series and will hold to them in this paper. These classifications are presented in Figures 4 and 5. They are based on the classic definitions of charnockite, enderbite, monzonite and norite and are independent of genetic considerations.

Geologic Position of Charnockites and Enderbites

Three groups of rocks are distinguished in the charnockite series:

1) The genetic series granite-charnockite-enderbite-metatonalite (or metamafite). Depending

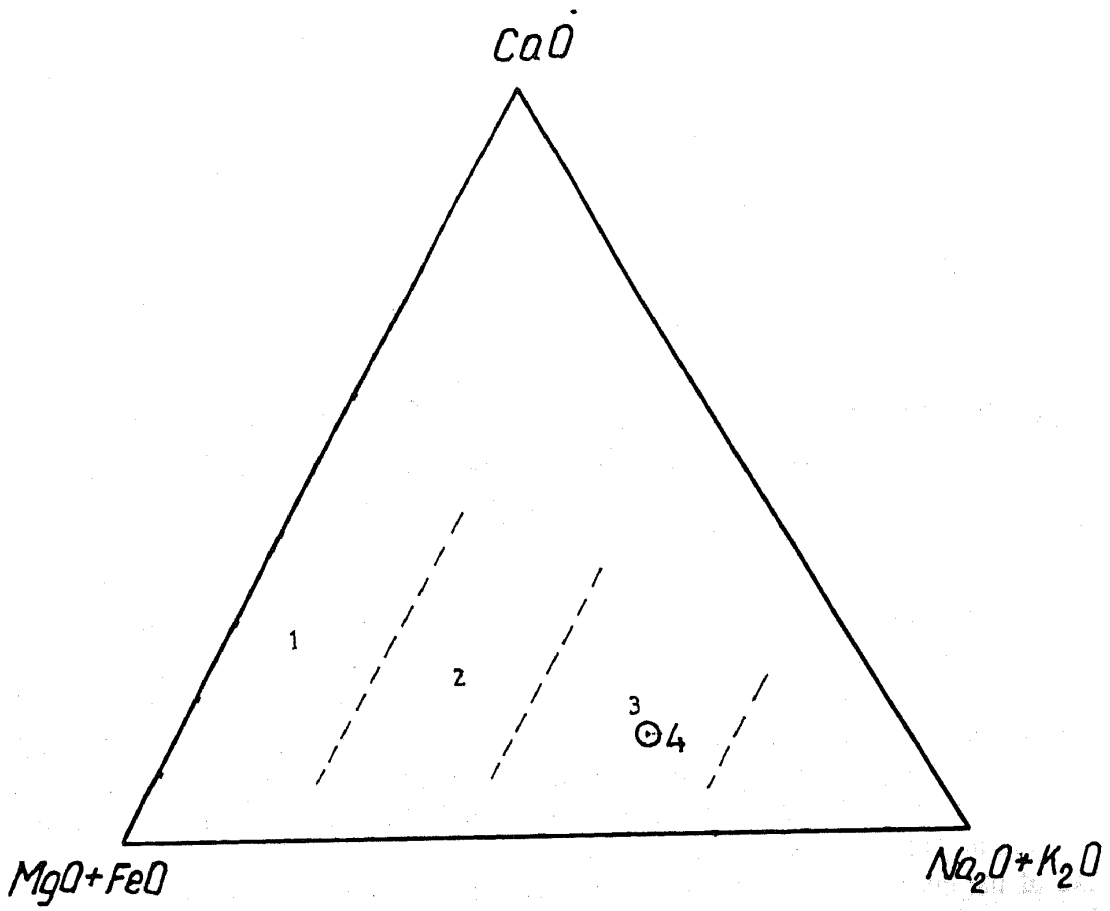

FIGURE 5. Classification of rocks of the charnockite series based on chemical composition (wt%): 1) norites, schists, and metamafites; 2) enderbites and monzonites; 3) charnockites; 4) average composition of near-eutectic Precambrian granites [Zavaritskiy, 1960].

on the character and nature of the charnockitization process, norites, monzonites, and various migmatites may appear in this series. The last, as a rule, surround granite-gneiss domes in metamafites and/or metatonalites metamorphosed to various degrees, but chiefly to the granulite facies. The transitions between members of the series are gradual, but occur within fairly narrow zones. Very typical examples are the Baikal section of the Sharyzhalgay granulite complex [Petrova and Levitskiy, 1984] in eastern Siberia, and the charnockite complex on the Bug River in Ukraine [Nalivkina, 1964].

2) The so-called patchy or arrested charnockites (Fig. 6), formed after biotite or amphibole gneisses as the result of attack by carbon dioxide fluids [Newton, 1986]. The charnockites of southern India, Sri Lanka and central Finland are such.

3) Metamorphic charnockites, and enderbites, produced from various gneisses at their contacts with carbonate rocks, in the Adirondacks [McLelland et al., 1988], southwest Cisbaikalia [Petrova and Levitskiy, 1984], on the Aldan shield [Perchuk et al., 1985], and in many other regions.

The relationships between all the members of the charnockite series in various geologic settings have been studied fairly well. There is abundant information on their mineralogic and chemical composition, structural and textual features, absolute age, composition of fluid inclusions and their isotopic characteristics. These data absolutely help solve the problem of

FIGURE 6. Arrested charnockites (dark) developed after biotite orthogneisses (light), Wanni complex, Kurunegala area, Sri Lanka.

charnockitization, but there are gaps in the investigation of the reactions between minerals, as well as in analysis of the changes in their composition during the charnockitization process.

Thermodynamic Factors in Charnockitization

1. **Biotite gneisses and metapelites**

T, P and activities of H_2O and CO_2. The reaction

$$KMg_3AlSi_3O_{10}(OH)_2 + 3SiO_2 = 3MgSiO_3 + KAlSi_3O_8 + H_2O \quad (4)$$

or

$$Bt + Qtz = Opx + Kfs + H_2O$$

is the key to the process of metamorphic charnockitization of gneisses and metapelites. It is shifted to the right by changes in several thermodynamic parameters: (1) by an increase in T or decrease in P; (2) by an increase in $X^{fl}_{CO_2}$ or a decrease in $X^{fl}_{H_2O}$ (when $X^{fl}_{H_2O} + X^{fl}_{CO_2} = 1$); and (3) by a decrease in X^{rock}_{Al} or X^{rock}_{Mg}.

Reaction (4) can be calculated as a function of these variables using GEOPATH thermodynamic data [Gerya and Perchuk, 1990]. The standard values of enthalpy, entropy and

TABLE 1. Mutually Consistent Standard Thermodynamic Data for Mineral Equilibria in Which Ms, Bt, Sil, Opx and Grt Take Part

Reaction	ΔH°_{1000} cal	ΔS°_{1000} cal/K	ΔV cal/bar	Reference
$Ms + Prp = Phl + 2Sil + Qtz$	-10066 ±357	-1.948 ±0.406	0.437	This paper
	-8435 ±342	-1.747 ±0.394	0.432	[6]*
	-16868 ±147	-1.233	0.339	[17]*
$Prp + San + H_2O = Phl + Sil + 2Qtz$	-32955 ±857	-40.884 ±2.406	0.550	This paper
	-36530 ±750	-45.50	0.604	[6]
	-7738 ±408	-42.460	0.599	[17]
$San + Sil + H_2O = Ms + Qtz$	-22889 ±345	-38.936 ±2.923	0.130	This paper
	-24270 ±253	-43.75	0.130	[6]
	-24635 ±352	-43.55	0.153	[17]
$Phl + Qtz = En + San + H_2O$	24048 ±707	36.000 ±2.103	-0.406	This paper
	28512 ±869	45.94 ±3.04	-0.43	[6]
	24850 ±0	38.70	-0.43	[17]

*References: [6] Dorogokupets and Karpov [1984]; [17] Holland and Powell [1990].

volume in reaction (4) are given in Table 1. In addition, variations in the alumina and magnesia contents of solid solutions of Bt and Opx affect their thermodynamic properties. In particular, variation in the alumina content of Bt in paragenesis with Qtz and Kfs is determined by the reactions [Perchuk and Ryabchikov, 1976, p. 83].

$$(5 + 0.5n)K_2(Mg, Fe)_5Al_4Si_5O_{20}(OH_4 + 21nSiO_2 + 3n(K_2O) + [(1-n)CO_2)] = 2K_2(Mg, Fe)_{5+0.5n}Al_{4-n}Si_{5+0.5n}O_{20}(OH)_4 + 7nKAlSi_3O_8 + (nH_2O + (1-n)CO_2), \quad (5)$$

which is meaningful within the limits of the end members of a biotite solid solution reacting with quartz:

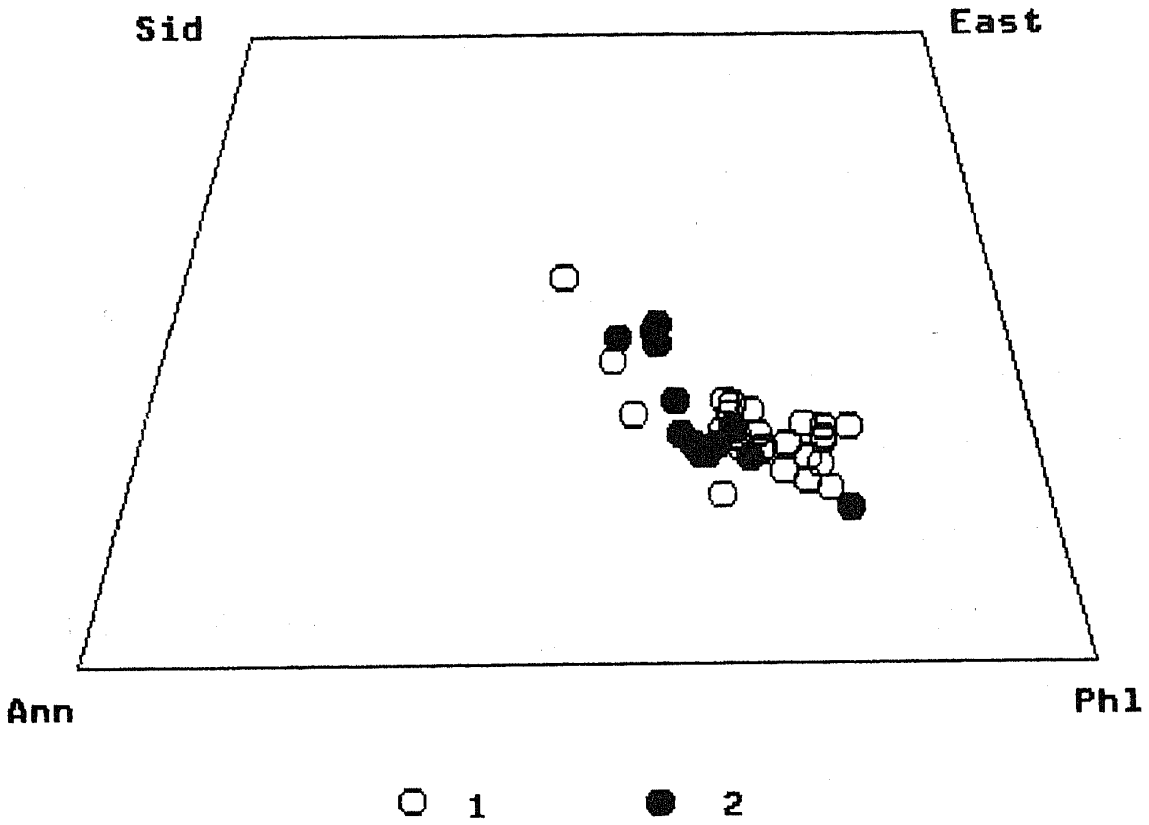

FIGURE 7. Variation in composition of biotite from enderbites and charnockites of the 1) Kansk complex, Yenisey Range [Perchuk et al., 1989] and 2) Sharyzhalgay complex [Perchuk, 1989].

$$Eas + Qtz + K_2O = Kfs + Phl + H_2O \quad (6)$$

or

$$Sid + Qtz + K_2O = Kfs + Ann + H_2O, \quad (7)$$

where K_2O and H_2O may be fully mobile components and changes in their activities lead to a change in the alumina content of Bt: an increase in the activity of potassium or decrease in a_{H_2O} lowers the alumina content of biotite in association with quartz and K-feldspar. A reduction in partial pressure of H_2O, or of its relative chemical potential $\mu_{H_2O} = RT\ln a^{fl}_{H_2O}$, may be related to an increase in the mole fraction of CO_2 in the fluid, i.e., to its becoming "dryer."

In other words, the extent of charnockitization should correlate directly with the content of the combined phlogopite-annite component in Bt. This can be checked by observational data. Figure 7 shows biotite from enderbites and charnockites varies not only in N_{Mg}, but also in alumina content; the two parameters are inversely correlated. This means that the exchange equilibrium

$$Phl + Sid = Ann + Eas \quad (8)$$

is shifted to the left, and the constant of reaction (4) should take into account the thermodynamic properties of a biotite solid solution:

$$K_{(4)} = X_{En}^{Opx} \cdot X_{Or}^{Fsp} \cdot \gamma_{En}^{Opx} \cdot \frac{\gamma_{Cr}^{Fsp}}{a_{Phl}^{Bt}} \cdot f_{H_2O}^{fl} \quad (9)$$

where for Opx with the composition (Mg, Fe, Al) (Si, Al)O_3, the excess partial molar free energy for En is determined by the relationship

$$RT\ln \gamma_{En}^{Opx} = G_{En}^{e} = X_{En}X_{Fs}\,(1.196T - 1720) + 1446 \cdot X_{En}X_{oCra} - 1931 \cdot X_{oCrn}X_{Fs},$$

where X_{En} = Mg/(Mg + Fe + Al/2)

X_{Fs} = Fe/(Mg + Fe + Al/2)

X_{oCrn} = Al/2(Mg + Fe + Al/2),

and the thermodynamic properties of a Bt solid solution, whose composition can be represented by the formula K(Mg, Fe, Al)$_3$(Al(Si, Al)$_3O_{10}(OH)_2$, is calculated from the integral equation for the Gibbs free energy

$$G_{Bt}^{e} = -3000 \cdot X_{Phl}X_{Eas} - 21967 \cdot X_{Ann}X_{Eas},$$

where X_{Phl} = Mg/[Mg + Fe + (Al-1)/2]; X_{Ann} = Fe/[Mg + Fe + (Al-1)/2]; and X_{Eas} = (Al-1)/2/[Mg + Fe + (Al-1)/2] calculated for 11 oxygens. The equation thus obtained for the activity of the phlogopite component differs somewhat from the published value [Aranovich, 1991]:

$$a_{Phl}^{Bt} = \{[Al^{IV}] \cdot X_{Mg}^{3}\,(1/3Si)^3 \exp[1 - X_{Mg}^{Bt}[Al^{VI}]\Delta G_{(8)}^{0}]\} \quad (10)$$

where Al^{IV} and Al^{VI} are the number of atoms of aluminum in fourfold and sixfold coordination; X_{Mg} = Mg/(Mg + Fe), and $\Delta G_{(i)}^{0}$ is the free energy of the internal exchange reaction (5). The mixing properties of feldspar are taken from Perchuk et al. [1990]:

$$RT\ln \gamma_{K}^{Fsp} = G_{K}^{e} = X_{Na}\,\{W_{K}^{G} + 2X_{K}\,(W_{Na}^{G} - W_{K}^{G})\}, \quad (11)$$

where X_{K}^{Fsp} = K/(K + Na) = Ab/(Ab + Or)

$$W_{Ab}^{G} = (4612 + 2982\,Z) - (2.504 + 3.427\,Z)T + (0.101 + 0.031 \cdot Z)P;$$

$$W_{Or}^{G} = (6560 + 1272\,Z) - (2.486 + 0.171\,Z)T + 0.074\,P,$$

where the degree of ordering (Z) of alkali feldspar is equal to $Z = -138.575 + 19.1353\,c_k = c_{obs} - 137.847 - 0.727\,X_{Or}^{Fsp}$ where c_{obs} is the measured value of the unit cell edge c of Kfs (for the microcline series the equation is valid in the composition range of $0.4 < X_{Or}^{Fsp} < 1$ [Hovis, 1986]. Thus, for precise calculation of reaction (4) in which Kfs takes part, it is necessary to know, at least approximately, the degree of its ordering in charnockite or gneiss.

Using these thermodynamic data, the stability fields of the mineral associations of gneisses

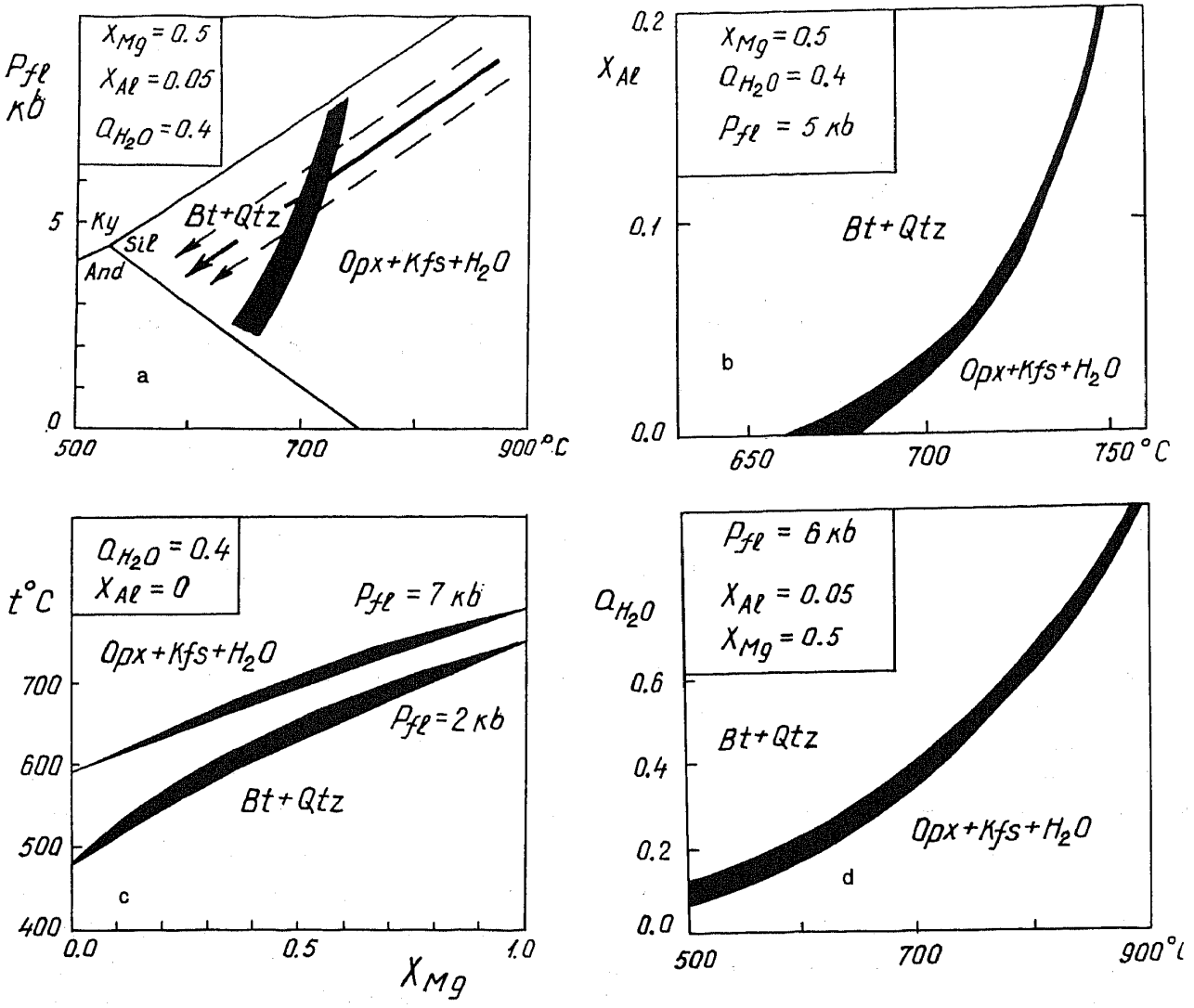

FIGURE 8. Stability fields of the mineral associations of gneisses (Bt + Qtz) and charnockites (Opx + Kfs) as a function of variable thermodynamic parameters and composition of the system. $X_{VI} = 0.5Al^e/(0.5Al^e + Fe^{2+} + Mg)$, where Al^e = Al-K-Na-Ca. $X_{Mg} = Mg/(Mg + Fe)$.

and charnockites were calculated. In Figure 8a it is seen that the *P-T* paths of retrograde metamorphism intersect a divariant field in which all four minerals of the charnockite association are stable. It is obvious that simple reduction in *T* and *P* cannot explain the replacement of biotite by orthopyroxene: the "decharnockitization" reaction would occur. Such reaction relationships of the minerals in charnockite are not uncommon and will be discussed below. Figure 8b and 8c show that, other things being equal, a decrease in aluminum and magnesium contents of the rock, as well as in $a^{fl}_{H_2O}$ (Fig. 8d) promotes the appearance of the charnockite association. The stability fields of the four-mineral association in the Figure 8 plots are very narrow. This means that even small changes in the variable parameters lead to disruption of equilibrium (4). A consequence of this, which stems from the low value of the partition coefficient of Mg, and in part of Al, is the alternation of biotite gneisses and charnockites in many metamorphic complexes, due to variations in the bulk composition of the original rocks. Still, the problem of the course of charnockitization reactions during retrograde metamorphism remains unsolved.

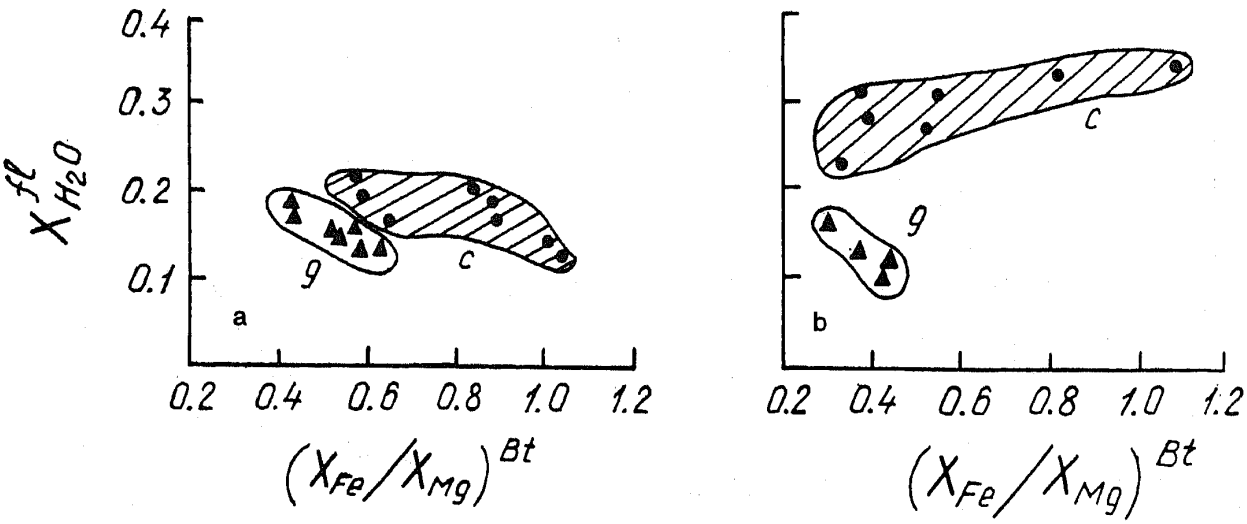

FIGURE 9. Mole fraction of water in fluid, in equilibrium with mineral associations of metapelites (g) and charnockites (c) in (a) Satnuru area and (b) Madras, India [Sen and Battacharrya, 1990].

According to the carbonate model of charnockitization (for instance, Newton [1986]), the Opx-Kfs association forms at the expense of biotite gneisses by reaction (4), due to an increase in the mole fraction of CO_2 in the fluid. As mentioned above, this conclusion is to a substantial extent in agreement with the fluid regime established [Perchuk and Gerya, 1990] for the retrograde phase of metamorphism of the granulites of East Siberia and the Soviet Far East (see Fig. 2). From the carbonate model of charnockitization it follows that X_{H_2O} in charnockites should be lower than in the associated gneisses. It turned out that an unequivocal answer can be obtained from analysis of fluid inclusions. However, Kurdyukov and Berdnikov [1987] showed that fluid inclusions in the granulites of southwest Cisbaikalia are 80-90% liquid CO_2 and no significant difference is observed in the composition of fluid inclusions in the same minerals from the gneisses and charnockites. Hansen et al. [1984] studied fluid inclusions in gneisses and charnockites from southern India and Sri Lanka. They too could find no appreciable increase in CO_2 in the fluid inclusions in charnockite compared to those in gneiss. Moreover, in one sample of coarse-grained charnockite, the concentration of water in inclusions in quartz ranged from 20 to 25%, which was not observed in the gneisses. Nevertheless, on the basis of paragenetic analysis and study of carbon isotopes, they concluded that reaction (4) and decomposition of Hbl plays the leading role in the charnockitization process. Santosh et al. [1990] likewise could find no differences in the composition of fluid inclusions in quartz from charnockites and from the associated gneisses that underwent charnockitization.

Nor has an unequivocal answer concerning the regime of water and CO_2 in the charnockitization of gneisses yet been obtained on the basis of calculating a_{H_2O} from reaction (4). Santosh et al. [1988] showed that for rocks with similar bulk compositions, a_{H_2O} in gneisses is a little higher than in associated charnockites. However, Sen and Battacharrya [1990] found precisely the opposite for the metapelites and charnockites of Satnuru and Madras. Figure 9 compiles values of $X^{fl}_{H_2O}$ for such rocks; it is seen that $X^{fl}_{H_2O}$ in charnockites is equal to or higher than that in associated gneisses. This result seemed questionable to us at first and therefore we decided to make calculations based on independent analytic and thermodynamic data.

Table 2 gives the mineral associations of gneisses and charnockites from some rock

TABLE 2. Mineral Associations in Samples Studied

Sample	Paragenesis, rock	Sampling site
Fin21g	Opx + Bt + Qtz + Kfs + Pl + Ilm, Gray charnockite	Central Finland
Fin21p	Opx + Bt + Qtz + Kfs + Pl + Ilm + Chl, Pink charnockite	" "
BL4M1	Opx + Qtz + Kfs + Pl + Ilm + Hbl + Cpx + Bt, Melanocratic charnockite	SW Cisbaikal
BL11M1	Opx + Bt + Qtz + Kfs + Pl + Ilm + Hbl + Cum + Dol + Anc + Chl + Mag, Coarse-grained charnockite	" "
Sh-I-7	Opx + Bt + Qtz + Kfs + Pl + Ilm + Grt + Dol + Cal, Charnockite	" "
BL30M9	Opx + Bt + Qtz + Kfs + Pl + Grt + Crd + Sil + Ilm, Aluminous gneiss	" "
BL3M3	Opx + Bt + Qtz + Kfs + Pl + Grt + Crd + Sil + Ilm, Aluminous gneiss	" "
A-124	Opx + Bt + Qtz + Kfs + Pl + Sil + Crd + Spl + Mag + Ilm, Aluminous gneiss	Yenisey
A-115	Opx + Bt + Qtz + Kfs + Pl + Sil + Crd + Spl + Mag + Ilm, Aluminous gneiss	"
Sln-5*	Hbl + Bt + Kfs + Pl + Qtz + Mag + Ilm, Gneiss 10 cm from patch of charnockite Sln-2	Sri Lanka
Sln-2**	Hbl + Bt + Opx + Cum + Kfs + Pl + Qtz + Mag + Ilm, Charnockite patch in gneiss Sln-5	" "
I-39/2	Bt + Opx + Kfs + Pl + Qtz + Grt + Ilm + Cal, Charnockite	India

*Sln-4.1/1/5.

**Sln-4.1/1/2—sample collected from Udadigana quarry [Kriegsman et al., 1991, pp. 38-42, stop 4.1].

associations in East Siberia, as well as in southern India, Central Finland and Sri Lanka. Table 3 gives microprobe analyses of coexisting minerals in these rocks. These data were treated thermodynamically and some results of the calculations are given in Table 4. Temperatures were determined by the orthopyroxene-biotite geothermometer (Gerya and Perchuk [1990]; Perchuk [1990]), pressures from Eq. (1), and $a^{fl}_{H_2O}$ using Eq. (9), where

$$a^{fl}_{H_2O} = \exp\left[\frac{\Delta G_{(4)}}{RT}\right],$$

where

$$\Delta G_{(4)} = RT\ln f^0_{H_2O}, + \Delta G^0_{Kfs} + \Delta G^0_{En} - \Delta G^0_{Phl} - \Delta G^0_{Qtz} + \Delta G^e_{(4)},$$

where $\Delta G_{(4)}$ is the difference in excess Gibbs energy for En and Phl in solid solutions of Opx and Bt, respectively, for given T, P and K_D (X_{Mg} = const, X_{Al} = const, X^{Kfs}_{Or} = const), using the parameters in (9)-(11). Figure 10, plotted for three samples from the Sharyzhalgay block, shows that along the P-T curve (Perchuk [1986, 1989])

$$P, \text{kb} = 0.094 \cdot t - 5.9 \cdot 10^{-5}\, t^2 - 32.61 \qquad (12)$$

at all temperatures $a^{fl}_{H_2O}$ in gneisses is higher than or equal to that in associated charnockites.

In view of those findings, we critically analyzed the results of Santosh et al. [1990], who

TABLE 3. Selected Microprobe Analyses and Crystallochemical Formulas of Coexisting Minerals from Rocks Listed in Table 2

Sample	Fin21g	Fin21g	Fin21g	Fin21p	Fin21p	Fin21p	SH-I-7	SH-I-7	Sh-I-7	Sh-I-7	BL-30
Point*	G33	G32	G36	G8	G26	G22	B17	B15	B22	B20	B38
Adjacent mineral	Center**	Bt	Kfs	Kfs	Center	Bt	Center	Kfs + Pl	Center	Bt + Qtz	Center
						Orthopyroxene					
SiO_2	49.79	50.09	50.17	50.86	50.56	50.94	50.36	50.29	50.02	49.90	50.37
Al_2O_3	3.98	4.10	3.61	3.17	3.30	3.50	1.51	1.41	1.92	1.93	2.81
FeO	25.30	25.05	25.50	23.92	24.07	23.56	29.42	29.08	29.69	30.69	27.35
MnO	0.62	0.53	0.46	0.60	0.47	0.34	0.47	0.34	0.34	0.25	0.07
MgO	20.01	19.71	19.90	21.01	21.13	21.24	17.55	18.39	17.41	16.50	18.86
CaO	0.14	0.13	0.00	0.07	0.11	0.07	0.22	0.25	0.26	0.22	0.09
Na_2O	0.00	0.17	0.14	0.00	0.04	0.14	0.07	0.00	0.00	0.16	0.27
Sum	99.85	99.78	99.79	99.63	99.67	99.77	99.59	99.76	99.63	99.66	99.82
						Formula based on 3 oxygens					
Si	0.944	0.948	0.951	0.958	0.953	0.956	0.976	0.971	0.970	0.972	0.962
Al	0.089	0.091	0.081	0.070	0.073	0.077	0.034	0.032	0.044	0.044	0.063
Fe	0.401	0.396	0.404	0.377	0.379	0.369	0.477	0.469	0.481	0.500	0.437
Mn	0.010	0.009	0.007	0.009	0.008	0.005	0.008	0.006	0.006	0.004	0.001
Mg	0.565	0.556	0.562	0.590	0.594	0.594	0.507	0.529	0.503	0.479	0.537
Ca	0.003	0.003	0.000	0.001	0.002	0.001	0.005	0.005	0.005	0.005	0.002
Na	0.000	0.006	0.005	0.000	0.001	0.005	0.002	0.000	0.000	0.006	0.010
Sum	2.012	2.009	2.011	2.006	2.011	2.008	2.008	2.013	2.008	2.009	2.012
X_{Mg}	0.579	0.578	0.577	0.604	0.605	0.613	0.511	0.527	0.508	0.487	0.551
X_{Al}	0.044	0.045	0.040	0.035	0.036	0.038	0.017	0.016	0.022	0.022	0.031

*Number of microprobe point.
**Center of grain.

TABLE 3. Continuation

Sample	BL-30	Sln-2	BL-11	BL-11	BL-3	BL-4	BL-4	I-39/2	I-39/2	A-124	A-115
Point	B37	K24	A5	A4	A24	Z6	Z5	46	44	12	58
Adjacent mineral	Bt + Qtz	Center	Center	Bt + Qtz	Bt + Qtz	Center	Bt + Qtz	Center	Bt + Qtz	Bt	Bt
						Orthopyroxene					
SiO_2	50.23	49.08	50.89	51.51	49.63	50.84	50.63	49.82	50.05	48.89	49.78
Al_2O_3	2.98	0.37	0.61	0.39	3.37	0.79	0.91	1.32	1.33	6.27	6.41
FeO	27.13	35.17	28.99	29.08	27.61	28.69	29.16	33.98	33.16	25.83	23.15
MnO	0.26	1.82	0.87	1.08	0.14	0.88	1.03	0.45	0.47	0.45	0.00
MgO	19.06	12.32	17.73	17.21	18.33	18.06	17.46	13.81	14.18	18.45	20.52
CaO	0.00	0.95	0.71	0.65	0.11	0.51	0.50	0.52	0.38	0.04	0.00
Na_2O	0.29	0.00	0.09	0.02	0.43	0.12	0.07	0.00	0.20	0.07	0.00
Sum	99.94	99.71	99.89	99.95	99.63	99.89	99.77	99.91	99.78	100.00	99.86
						Formula based on 3 oxygens					
Si	0.958	0.987	0.984	0.995	0.953	0.982	0.982	0.984	0.986	0.926	0.929
Al	0.067	0.009	0.014	0.009	0.076	0.018	0.021	0.031	0.031	0.140	0.141
Fe	0.433	0.591	0.469	0.470	0.443	0.463	0.473	0.561	0.546	0.409	0.361
Mn	0.004	0.031	0.014	0.018	0.002	0.014	0.017	0.008	0.008	0.007	0.000
Mg	0.542	0.369	0.511	0.495	0.524	0.519	0.504	0.406	0.416	0.520	0.570
Ca	0.000	0.020	0.015	0.013	0.002	0.010	0.010	0.011	0.008	0.001	0.000
Na	0.011	0.000	0.003	0.001	0.016	0.005	0.003	0.000	0.008	0.003	0.000
Sum	2.014	2.008	2.010	2.001	2.017	2.012	2.009	2.001	2.003	2.006	2.001
X_{Mg}	0.554	0.372	0.514	0.504	0.541	0.521	0.507	0.417	0.429	0.556	0.612
X_{Al}	0.033	0.004	0.007	0.004	0.038	0.009	0.010	0.016	0.016	0.070	0.070

TABLE 3. Continuation

Sample	Fin21g	Fin21g	Fin21p	Fin21p	Sh-I-7	Sh-I-7	Sh-I-7	BL-30	BL-30	Sln-5	Sln-5
Point	G34	G31	G25	G21	B18	B26	B19	B39	B36	Q52	Q51
Adjacent mineral	Center	Opx	Center	Opx	Core	Dol + Qtz	Opx + Kfs	Center	Opx	Center	Center
						Biotite					
SiO_2	37.86	38.37	38.44	39.21	39.41	40.75	39.00	37.90	38.19	37.10	37.73
TiO_2	4.82	4.82	5.15	5.15	3.72	3.07	3.52	4.68	4.61	5.09	5.61
Al_2O_3	16.57	16.65	16.12	16.24	14.09	13.62	14.41	16.88	16.88	13.25	12.85
FeO	15.16	14.55	15.00	13.81	17.55	16.84	17.46	16.68	16.23	23.49	23.46
MnO	0.06	0.02	0.14	0.09	0.00	0.08	0.00	0.00	0.00	0.26	0.27
MgO	14.38	14.90	15.23	15.20	14.66	15.01	15.04	13.21	13.91	10.25	9.89
Na_2O	0.16	0.19	0.00	0.19	0.00	0.28	0.00	0.06	0.16	0.22	0.00
K_2O	10.37	10.19	9.25	9.96	9.95	9.92	9.68	10.18	9.77	9.51	9.83
Cl	0.02	0.03	0.01	0.05	0.25	0.24	0.21	0.02	0.07	0.14	0.13
Sum	99.40	99.72	99.31	99.90	99.62	99.82	99.32	99.60	99.82	99.41	99.76
						Formula based on 11 oxygens					
Si	2.719	2.732	2.740	2.771	2.849	2.924	2.823	2.728	2.731	2.780	2.815
Ti	0.260	0.276	0.276	0.198	0.167	0.190	0.255	0.000	0.273	0.316	0.261
Al	1.402	1.397	1.354	1.352	1.200	1.151	1.230	1.432	1.423	1.170	1.130
Fe	0.910	0.866	0.893	0.816	1.060	1.010	1.057	1.003	0.970	1.471	1.463
Mn	0.004	0.001	0.008	0.005	0.000	0.005	0.000	0.000	0.000	0.017	0.017
Mg	1.538	1.580	1.617	1.600	1.578	1.605	1.622	1.416	1.482	1.155	1.100
Na	0.022	0.026	0.000	0.026	0.000	0.039	0.000	0.009	0.022	0.032	0.000
K	0.950	0.925	0.840	0.898	0.917	0.908	0.894	0.934	0.891	0.909	0.935
Sum	7.806	7.804	7.728	7.665	7.772	7.832	7.880	7.522	7.792	7.849	7.720
X_{Mg}	0.627	0.646	0.642	0.661	0.598	0.613	0.606	0.585	0.604	0.437	0.426
X_{Al}	0.076	0.075	0.066	0.068	0.037	0.028	0.041	0.082	0.079	0.031	0.025

TABLE 3. Continuation

Sample	Sln-2	BL-11	BL-11	BL-3	BL-4	BL-4	I-39/2	I-39/2	A-124	A-115
Point	K29	A8	A1	A25	Z7	Z4	47	44	11	60
Adjacent mineral	Center	Center	Opx + Qtz	Opx + Qtz	Center	Opx + Qtz	Center	Opx + Kfs	Opx + Kfs	Opx
					Biotite					
SiO_2	38.19	38.40	38.13	37.95	39.57	39.70	38.92	38.93	39.33	39.90
TiO_2	4.65	3.19	2.59	4.39	3.79	4.29	6.14	5.45	5.12	5.24
Al_2O_3	13.17	14.61	14.81	16.51	15.42	14.85	13.68	14.11	15.48	14.45
FeO	21.93	19.01	20.30	17.08	16.22	16.75	20.01	20.14	13.84	12.02
MnO	0.27	0.15	0.00	0.03	0.00	0.06	0.04	0.21	0.16	0.00
MgO	11.68	13.96	14.25	13.44	14.60	14.44	11.62	11.63	15.78	16.96
Na_2O	0.07	0.31	0.17	0.07	0.00	0.00	0.19	0.13	0.28	0.46
K_2O	9.66	9.99	9.26	9.82	9.71	9.73	9.39	9.40	9.98	10.97
Cl	0.11	0.25	0.26	0.01	n.d.	n.d.	n.d.	n.d.	n.d.	n.d.
Sum	99.72	99.87	99.77	99.29	99.31	99.82	100.00	100.00	99.97	100.00
					Formula based on 11 oxygens					
Si	2.822	2.799	2.785	2.741	2.834	2.838	2.826	2.827	2.781	2.814
Ti	0.007	0.142	0.241	0.000	0.231	0.223	0.298	0.279	0.279	0.000
Al	1.147	1.255	1.274	1.405	1.302	1.251	1.171	1.207	1.290	1.201
Fe	1.355	1.158	1.240	1.031	0.971	1.001	1.214	1.223	0.818	0.709
Mn	0.017	0.009	0.000	0.002	0.000	0.004	0.002	0.013	0.009	0.000
Mg	1.286	1.515	1.551	1.446	1.558	1.537	1.257	1.259	1.662	1.782
Na	0.011	0.044	0.024	0.009	0.000	0.000	0.027	0.018	0.039	0.063
K	0.911	0.929	0.862	0.904	0.887	0.887	0.870	0.870	0.900	0.987
Sum	7.556	7.852	7.977	7.537	7.782	7.742	7.665	7.697	7.778	7.555
X_{Mg}	0.484	0.565	0.556	0.583	0.616	0.605	0.508	0.505	0.668	0.715
X_{Al}	0.027	0.045	0.047	0.075	0.056	0.047	0.033	0.040	0.055	0.039

TABLE 3. Continuation

Sample	Fin21g	Fin21g	Fin21g	Fin21p	Fin21p	Fin21p	Sh-I-7	Sh-I-7	Sln-5	Sln-2	Sln-2	BL-11	BL-3	3BL-4
Point	G48	G35	G40	G10	G9	G14	B16	B14	Q38	K22	K23	A22	A26	C28
Adjacent mineral	Center	Opx	Pl	Center	Opx	Pl	Center	Pl + Opx	Center	Center	Pl	Center	Center	Center
							K-feldspar							
SiO_2	63.55	63.38	63.41	62.88	63.25	63.36	64.14	64.78	65.37	65.15	64.97	65.33	64.02	63.77
Al_2O_3	18.35	18.25	18.64	18.75	18.60	18.65	18.46	18.10	18.11	18.17	18.12	18.12	18.66	18.59
FeO	0.25	0.67	0.07	0.11	0.08	0.19	0.23	0.24	0.05	0.20	0.12	0.06	0.07	0.15
CaO	0.04	0.11	0.11	0.14	0.10	0.23	0.02	0.05	0.19	0.27	0.16	0.04	0.07	0.09
Na_2O	0.12	0.28	0.23	0.41	0.34	0.47	1.11	0.74	1.82	2.61	0.99	1.51	0.84	1.00
K_2O	15.95	15.79	15.98	15.40	15.57	15.42	14.61	14.81	13.79	12.81	15.17	14.56	14.59	14.75
BaO	1.67	1.43	1.51	2.03	1.91	1.53	1.38	1.18	0.48	0.30	0.47	0.35	1.76	1.43
Sum	99.93	99.91	99.96	99.72	99.86	99.84	99.96	99.92	99.80	99.49	99.99	99.96	100.00	99.77
							Formula based on 8 oxygens							
Si	2.978	2.972	2.967	2.956	2.967	2.965	2.982	3.005	3.010	3.001	3.003	3.010	2.978	2.974
Al	1.013	1.008	1.028	1.039	1.028	1.028	1.011	0.990	0.983	0.986	0.987	0.983	1.023	1.021
Fe	0.010	0.026	0.003	0.004	0.003	0.007	0.009	0.009	0.002	0.008	0.005	0.002	0.003	0.006
Ca	0.002	0.006	0.005	0.007	0.005	0.012	0.001	0.003	0.009	0.013	0.008	0.002	0.003	0.004
Na	0.011	0.026	0.021	0.037	0.031	0.043	0.100	0.067	0.162	0.233	0.089	0.134	0.076	0.090
K	0.953	0.944	0.953	0.923	0.931	0.920	0.866	0.876	0.810	0.752	0.894	0.855	0.866	0.877
Ba	0.031	0.026	0.028	0.037	0.035	0.028	0.025	0.022	0.009	0.005	0.008	0.006	0.032	0.026
Sum	4.997	5.009	5.006	5.004	5.001	5.003	4.995	4.972	4.984	4.998	4.994	4.993	4.981	4.999

TABLE 3. Continuation

Sample	Sln-2	Sln-2	BL-11	Fin21g	Fin21g	Fin21p	Fin21p	Sh-I-7	Sh-I-7	Sln-5	Sln-2	Sln-2
Point	K20	K21	A12	G37	G38	G16	G13	B24	B23	Q33	K20	K21
Adjacent mineral	Center	Kfs	Center	Center	Kfs	Center	Kfs + Opx	Center	Kfs	Center	Center	Kfs
						Plagioclase						
SiO_2	62.20	72.49	61.20	60.59	60.00	59.96	60.47	56.97	56.84	62.42	62.20	72.49
Al_2O_3	22.96	16.49	24.18	24.50	24.92	25.07	24.48	27.02	26.76	23.28	22.96	16.49
FeO	0.23	0.09	0.05	0.16	0.08	0.00	0.04	0.24	0.19	0.14	0.23	0.09
CaO	5.08	3.25	6.21	6.15	6.92	6.99	6.75	9.34	9.51	5.31	5.08	3.25
Na_2O	8.80	7.16	8.02	7.23	7.18	7.24	7.55	6.26	6.51	8.42	8.80	7.16
K_2O	0.44	0.12	0.30	1.18	0.85	0.55	0.55	0.17	0.11	0.28	0.44	0.12
BaO	n.det.	n.det.	n.det.									
Sum	99.71	99.60	99.96	99.81	99.94	99.81	99.85	100.00	99.93	99.85	99.71	99.60
						Formula based on 8 oxygens						
Si	2.773	3.140	2.723	2.709	2.681	2.679	2.700	2.559	2.559	2.772	2.776	2.665
Al	1.206	0.842	1.268	1.291	1.312	1.320	1.288	1.431	1.420	1.218	1.220	1.326
Fe	0.009	0.003	0.002	0.006	0.003	0.000	0.001	0.009	0.007	0.005	0.000	0.002
Ca	0.243	0.151	0.296	0.295	0.331	0.334	0.323	0.449	0.458	0.252	0.240	0.359
Na	0.760	0.601	0.692	0.626	0.621	0.627	0.654	0.545	0.568	0.725	0.747	0.629
K	0.025	0.007	0.017	0.067	0.048	0.031	0.031	0.010	0.006	0.016	0.007	0.011
Ba	0.000	0.000	0.000	0.000	0.000	0.000	0.000	0.000	0.000	0.000	0.000	0.000
Sum	5.016	4.743	4.997	4.993	4.998	4.991	4.998	5.003	5.019	4.989	4.991	4.992
X_{An}	0.236	0.199	0.294	0.298	0.331	0.337	0.320	0.448	0.444	0.254	0.241	0.359

TABLE 3. Continuation

Sample	Fin21g	Sh-I-7	Sln-5	Sln-2	Sln-5	Sln-2	BL-11	Sample	Sln-5	Sln-5	Sln-2	Sln-2
Point	G49	B7	Q43	K3	Q44	K2	A2	Point	Q50	Q48	K16	K17
Adjacent mineral	Center	Center	Mag	Center	Ilm	Center	Opx + Qtz	Adjacent mineral	Center	Kfs	Center	Kfs
	Ilmenite				Magnetite			Hornblende				
TiO_2	52.10	51.41	51.09	51.28	1.33	0.73	0.00	SiO_2	42.31	42.61	42.14	43.20
FeO	42.31	47.26	44.51	43.75	97.37	97.36	99.06	TiO_2	2.39	2.03	1.99	1.90
MnO	4.94	0.41	3.55	3.32	0.03	0.00	0.00	Al_2O_3	9.45	9.64	9.71	9.71
MgO	0.05	0.80	0.13	0.25	0.01	0.00	0.00	FeO	22.52	21.70	22.09	21.20
Sum	99.40	99.88	99.28	98.60	98.74	98.08	99.06	MnO	0.55	0.53	0.58	0.40
								MgO	8.20	8.57	8.19	8.76
								CaO	10.81	11.35	11.22	10.88
								Na_2O	2.06	1.63	2.13	2.09
								K_2O	1.40	1.43	1.43	1.39
								Cl	0.12	0.21	0.24	0.34
								Sum	99.80	99.68	99.71	99.87
	Formula based on 3 oxygens				Formula based on 4 oxygens			Formula based on 3 oxygens				
Ti	0.996	0.980	0.983	0.990	0.036	0.020	0.000	Si	6.450	6.477	6.436	6.533
Fe_2	0.900	1.002	0.952	0.939	0.927	0.960	1.000	Ti	0.233	0.227	0.218	0.034
Fe_3	—	—	—	—	2.000	2.000	2.000	Al	1.698	1.726	1.748	1.731
Mn	0.106	0.009	0.077	0.072	0.001	0.000	0.000	Fe	2.870	2.757	2.820	2.680
Mg	0.002	0.030	0.005	0.009	0.000	0.000	0.000	Mn	0.071	0.068	0.075	0.052
Sum	2.004	2.020	2.017	2.010	2.964	2.980	3.000	Mg	1.862	1.940	1.863	1.973
								Ca	1.764	1.848	1.836	1.761
								Na	0.608	0.480	0.631	0.611
								K	0.272	0.276	0.278	0.268
								Sum	15.286	15.800	15.905	15.644

TABLE 3. Continuation

Sample	Sln-2	BL-11	BL-11	Sample	SH-I-7	Sln-2	I-39/2	BL-11	Sh-I-7	Sh-I-7	BL-11	
Point	K26	A3	C5	Point	B30	B33	K-25	C-37	C1	B32	B28	C9
Adjacent mineral	Center	Opx + Qtz	Dol + Qtz	Adjacent mineral	Center	Dol	Cum	Opx + Qtz	Center	Cal	Bt + Qtz	Cum + Qtz
	Cummingtonite				Calcite			Dolomite				Breunnerite
SiO_2	45.34	56.25	56.81	FeO	3.76	1.16	3.34	0.39	16.33	18.83	20.18	46.23
TiO_2	0.30	0.01	0.09	MnO	0.63	0.10	23.93	0.00	1.43	0.93	1.36	3.38
Al_2O_3	7.31	0.18	0.03	MgO	2.49	0.37	0.95	0.13	28.32	27.59	27.03	48.76
FeO	31.17	23.35	21.78	CaO	90.51	96.35	70.37	98.40	53.39	51.84	50.40	1.03
MnO	2.71	0.96	0.83	Sum	97.39	97.97	98.59	98.92	99.48	99.19	98.97	99.40
MgO	8.83	18.83	20.02									
CaO	3.75	0.10	0.34									
Na_2O	0.37	0.21	0.06									
K_2O	0.20	0.05	0.04									
Cl	0.03	0.04	0.00									
Sum	100.00	100.00	100.00									
					Formula based on 3 oxygens							
Si	6.950	8.007	8.017	Fe	0.030	0.009	0.028	0.003	0.120	0.139	0.150	0.335
Ti	0.001	0.010	0.000	Mn	0.005	0.001	0.203	0.000	0.011	0.007	0.010	0.025
Al	1.320	0.031	0.005	Mg	0.036	0.005	0.014	0.002	0.369	0.363	0.359	0.630
Fe	3.994	2.779	2.569	Ca	0.929	0.985	0.755	0.995	0.501	0.491	0.481	0.010
Mn	0.352	0.116	0.099									
Mg	2.016	3.993	4.208									
Ca	0.615	0.015	0.051									
Na	0.109	0.059	0.016									
K	0.039	0.009	0.008									
Sum	15.935	15.019	14.973									
X_{Mg}	0.317	0.580	0.612									

TABLE 3. Continued

Sample	K4							
Point	Y49	Y40	Y53	Y39	Y41	Y42	Y51	Y56
Mineral	Bt	Bt	Bt	Grt	Grt	Pl	Kfs	Ilm
Contact	Opx + Qtz	Grt	Opx + Kfs	Core	Bt	Core	Opx + Bt	Core
	From rocks of Kabbaldurga area (southern India)							
SiO_2	38.17	37.83	37.94	37.09	37.35	63.81	64.36	0.11
TiO_2	4.00	3.25	1.91	0.03	0.01	0.00	0.00	49.72
Al_2O_3	16.63	16.95	18.81	20.79	20.71	22.56	18.08	0.00
FeO	19.38	20.74	19.54	34.48	34.02	0.10	0.27	48.92
MnO	0.07	0.00	0.08	1.38	1.03	0.02	0.00	0.29
MgO	11.98	11.08	13.10	3.62	3.21	0.00	0.00	0.20
CaO	0.22	0.13	0.30	2.58	3.12	4.01	0.00	0.02
Na_2O	0.13	0.07	0.38	0.00	0.31	9.16	0.29	0.27
K_2O	9.26	9.83	7.89	0.01	0.00	0.26	16.38	0.04
Cr_2O_3	0.04	0.13	0.00	0.00	0.19	0.07	0.00	0.00
BaO	0.00	0.00	0.00	0.02	0.05	0.02	0.60	0.37
	Crystallochemical formulas							
Si	2.760	2.759	2.717	2.985	3.007	2.822	3.000	0.003
Ti	0.217	0.178	0.103	0.002	0.001	0.000	0.000	0.961
Al	1.417	1.457	1.587	1.972	1.964	1.175	0.993	0.000
Fe	1.172	1.264	1.170	2.319	2.290	0.004	0.010	1.051
Mn	0.004	0.000	0.005	0.094	0.070	0.001	0.000	0.006
Mg	1.291	1.204	1.397	0.434	0.385	0.000	0.000	0.007
Ca	0.017	0.010	0.023	0.223	0.269	0.190	0.000	0.001
Na	0.018	0.009	0.052	0.000	0.049	0.784	0.026	0.014
K	0.854	0.914	0.721	0.001	0.000	0.014	0.973	0.001
O	11.000	11.000	11.000	12.000	12.000	8.000	8.000	3.000
Sum	7.750	7.795	7.774	8.028	8.035	4.990	5.003	2.044
X_{Mg}	0.523	0.488	0.543	0.152	0.140	—	—	—
X_{Al}	0.078	0.085	0.102	—	—			
X_{An}						0.192	—	—

TABLE 4. Thermodynamic Conditions of Mineral Equilibria in the Rocks Listed in Table 2

No.	Part of grain	Bt	Opx	$t°$ C*	P, kb**	$a^{fl}_{H_2O}$***
Fin21g	center	G34	G33	720	5.9	0.382
Fin21g	rim	G31	G32	685	5.3	0.317
Fin21p	center	G25	G26	759	6.6	0.458
Fin21p	rim	G21	G22	734	6.1	0.400
BL4M1	center	Z7	Z6	622	4.2	0.235
BL4M1	rim	Z4	Z5	630	4.3	0.261
BL-11M1	center	A8	A5	719	5.9	0.413
BL-11M1	rim	A1	A4	711	5.7	0.398
Sh-I-7	center	B18	B17	671	5.0	0.345
Sh-I-7	rim	B19	B20	607	3.9	0.247
BL30M	center	B39	B38	724	5.9	0.381
BL30M	rim	B36	B37	697	5.5	0.335
BL3M3	rim	A25	A24	720	5.9	0.393
Sln-2	center	K29	K24	587	3.6	0.279
I-39/2	center	47	46	639	4.5	0.341
I-39/2	rim	44	44	663	4.9	0.368
A124	rim	11	12	644	4.6	0.292
A115	rim	60	58	685	5.3	0.363

*Temperature determined from Opx-Bt geothermometer.
**Pressure determined from Eq. (1)
***Activity of water calculated from Eq. (12).

obtained the opposite relationships. For this purpose we recalculated the P-T parameters of th mineral equilibria in some of the samples they studied. The results are given in Table 5. Estimate of temperature from the biotite-garnet thermometer were exceptionally stable both in gneisses (689° C ± 2) and in charnockites (642.5° C ± 1.5). Moreover, bringing orthopyroxene into the calculations leads to considerable distortion of the equilibrium temperature values (see Table 5). Although the Bt-Opx and Grt-Opx geothermometers are mutually consistent (Gerya and Perchuk [1990]; Perchuk [1990]). This may just be related to local disequilibrium of Opx, for instance due to oxidation-reduction reactions, as will be discussed below.

Thus if CO_2 makes a substantial contribution to the transformation of gneisses, there are no grounds for claiming that its volatility controls charnockitization of granulite complexes in various parts of the world. The more so, as so far no substantial increase in f_{CO_2} or f_{H_2O} has been found along the whole path (1); for the gneisses and charnockites of southwest Cisbaikalia (Perchuk [1989]) this relationship has been shown to increase only up to 4 to 3.5 kbar, and to stabilize below that. Apparently there is some other independent parameter that governs charnockitization of gneisses.

Chemical potential of K_2O. It looks as though in some cases it is impossible to reduce to calculations Korzhinskiy's idea [1962] concerning the role of $\mu^{fl}_{K_2O}$ in the formation of the charnockite paragenesis. According to his model, an increase in the activity coefficient of potassium may be an acid-base interaction effect of metamorphic fluid migrating from a granitic melt into metamafic rocks. And as the biotite in gneisses is never phlogopite, the reaction occurs:

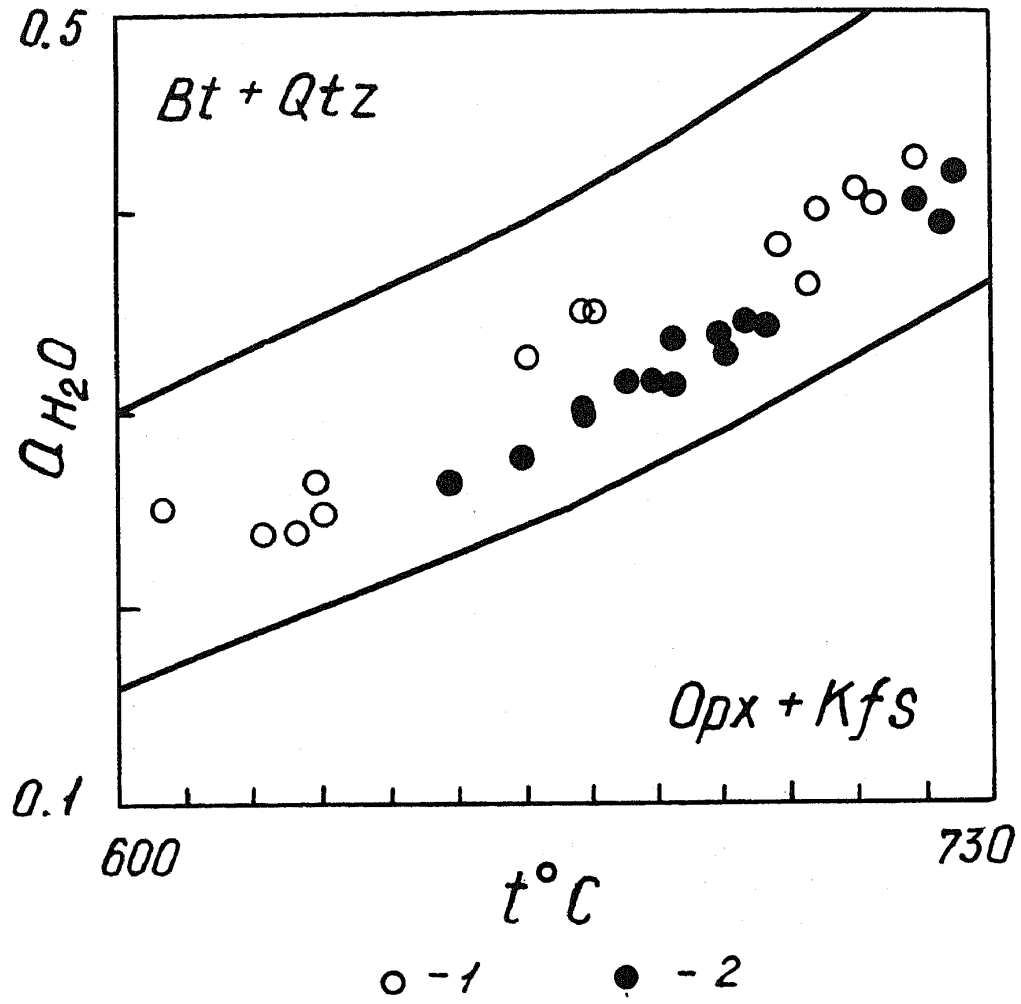

FIGURE 10. Relationship of $a^{fl}_{H_2O}$ in gneisses (1) and charnockites (2) of southwest Cisbaikalia along the *P-T* path of retrograde metamorphism, Eq. (12).

$$Bt + Qtz + (K_2O) = Or + Opx + (H_2O), \quad (13)$$

i.e., in the presence of quartz the alumina content of biotite is reduced according to reaction (5). It is obvious that reaction (5) should be accompanied by a decrease in the quartz content in gneisses, while the amount of biotite does not change significantly. Of course, such observations are practically never made in nature. In any case, they cannot answer the question: Does reaction (13) really take place in gneisses, or is the decisive factor an increase in the activity of CO_2 in the fluid?

Thus, not one of the reactions considered above in which biotite participates can be an effective indicator that potassium or CO_2 in the fluid is decisive in the charnockitization process. Therefore we must find independent reactions that would be unequivocal indicators of the influence of some specific intensive parameters on the process. One such indicator might be the reaction

$$CaAl_2Si_2O_8 \cdot nNaAlSi_3O_8 + (0.5mK_2) = CaAl_2Si_2O_8 \cdot (n\text{-}m)NaAlSi_3O_8 + mKAlSi_3O_8 + (0.5mNa_2O), \quad (14)$$

TABLE 5. Calculated Thermodynamic Parameters for Mineral Associations of Charnockites and Gneisses from Quarry in Mannatala Area (S. India) According to Microprobe Data of Santosh et al.

No.	Sample	Rock	Mineral	$t°$ C*		P, kb**	$a^{fl}_{H_2O}$***
1	M-2	Gneiss	Bt + Grt (rim)	691	*BG*	5.9	—
2	M-2	Gneiss	Bt + Grt (rim)	686	*BG*	5.9	—
3	M-3	Gneiss	Bt + Grt (center)	690	*BG*	5.9	—
4	M-3	Gneiss	Bt + Grt (rim)	689	*BG*	5.9	—
5	M-4	Charnockite	Bt + Grt (center)	644	*BG*	5.1	—
6	M-4	Charnockite	Bt + Grt (rim)	641	*BG*	5.0	—
7	M-4	Charnockite	Bt + Grt (center), Opx-1	644	*BG*	5.0	0.560
8	M-4	Charnockite	Bt + Grt (center), Opx-2	644	*BG*	5.0	0.493
9	M-4	Charnockite	Bt + Grt (rim), Opx-1	641	*BG*	5.0	0.545
10	M-4	Charnockite	Bt + Grt (rim), Opx-2	641	*BG*	5.0	0.481
11	M-4	Charnockite	Bt + Opx-1	480	*BO*	1.8	—
12	M-4	Charnockite	Bt + Opx-2	504	*BO*	2.3	—
13	M-4	Charnockite	Grt (center) + Opx-1	888	*GO*	9.9	—
14	M-4	Charnockite	Grt (center) + Opx-2	836	*GO*	8.9	—
15	M-4	Charnockite	Grt (rim) + Opx-1	878	*GO*	9.7	—
16	M-4	Charnockite	Grt (rim) + Opx-2	827	*GO*	8.7	—

*Bt-Grt (*BG*), Bt-Opx (*BO*) and Grt-Opx (*GO*) geothermometers [Perchuk & Lavrent'yeva, 1963, 1990; Gerya & Perchuk, 1990].
**From Eq. (1).
***From Eq. (12).

which does not involve the volatiles H_2O and CO_2, but is shifted to the right with increasing $\mu^{fl}_{K_2O}$. This means that the basicity of plagioclase would increase, and according to reaction (5), the alumina content of coexisting biotite would decrease. Such a correlation is shown in Figure 11, compiled from microprobe data (see Table 3) on biotite and plagioclase associated with orthopyroxene, quartz and K-feldspar in the gneisses and charnockites of the Sharyzhalgay complex [Perchuk, 1989] and of the Yenisey Ridge [Perchuk et al., 1989]. The position of the regression lines on the diagrams is determined by temperature pressure, $\mu^{fl}_{H_2O}$ and the bulk composition of the rocks. If N_{Al} does not correlate with the alumina content of the rock, it is obvious that reactions (5) and (12) occur. The slope of the regression lines on the diagrams is related to kinetic parameters (completeness of the diffusion or growth profile), or to the character of the diffusion profiles.

The correlations given in Figure 11 should be the usual ones in the many granulite complexes of the world where charnockitization has occurred. It indicates the behavior of potassium during that process and the effect of variation in its chemical potential on the composition of the newly formed minerals. For example, in Sri Lanka and southern India the plagioclase in the gneisses and in the charnockites formed from them have the same composition, and the alumina contents of biotite likewise do not change [Hansen et al., 1987]. This unequivocally indicates that potassium is inert during charnockitization of gneisses, although Hansen et al. [1987] accept the possibility that charnockites of the Kabbal type could form under open-system conditions. In contrast, no such charnockites occur in the gneiss complexes of East Siberia and Ukraine, where

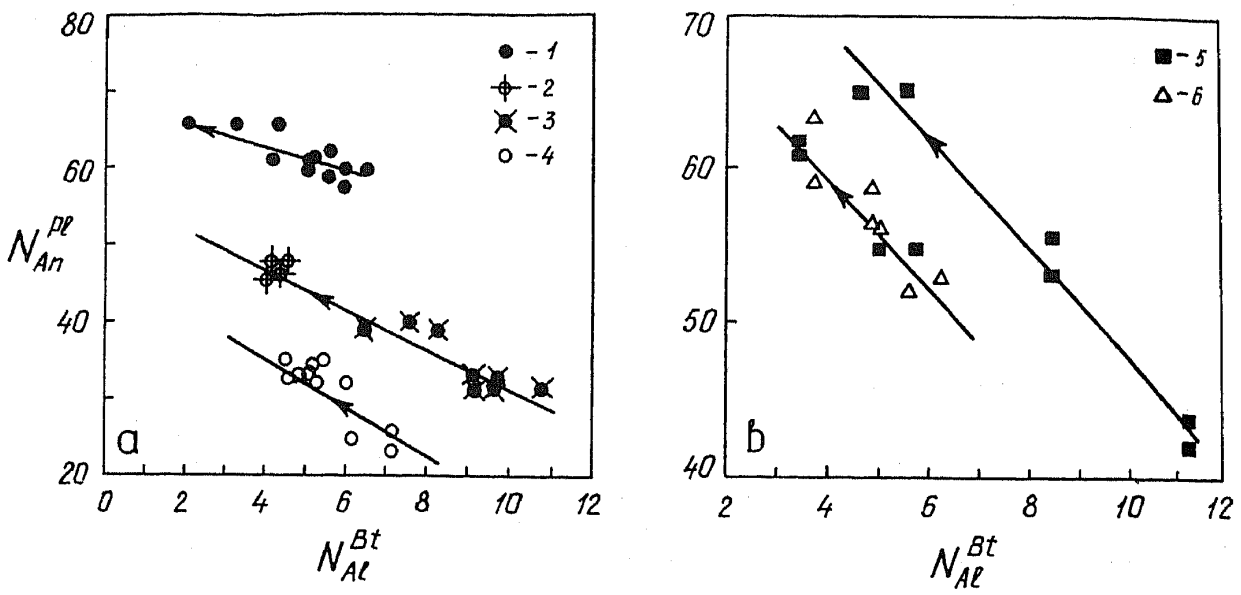

FIGURE 11. Conjugate reactions (13) and (14) in charnockitic gneisses of (a) the Sharyzhalgay complex, Cisbaikalia and (b) the Kansk complex, Yenisey Range, East Siberia, demonstrated by the systematic variation in composition of coexisting biotite and orthoclase: 1) garnet-bearing charnockitic gneisses with carbonates; 2) metapelites; 3) migmatites; 4) igneous charnockites; 5) charnockitized migmatites of various bulk compositions; 6) charnockitized gneisses.

K_2O behaved as a completely mobile component during charnockitization of gneisses and metamafites (see Figs. 11 and 12).

Korzhinskiy [1962] believed that reaction (14) cannot be an indicator of variation in potassium activity during charnockitization, as sodium is present in the fluid and the increase in total alkalinity of the fluids when they react with metamafites and gneisses leads to an increase in the activity coefficients of both alkalis. Moreover, he attached no importance to reactions of type (5). Not having enough chemical analyses of minerals from charnockites and associated gneisses at that time, Korzhinskiy could not check his hypothesis that potassium plays a leading role in charnockitization. For instance, it was difficult to predict that in addition to (14), the reaction

$$(Fe, Mg)_2Si_2O_6 \cdot (1\text{-}n)Al_2Al_2O_6 + (1\text{-}n)\,(K_2O) = (1\text{-}n)KAlSi_3O_8 + (Mg, Fe)_2Si_2O_6$$

or

$$SiO_2 + oCrn + (K_2O) = Kfs \qquad (15)$$

also can be an independent indicator of the effect of $\mu^{fl}_{K_2O}$ on the charnockite reaction, as the alumina content in hypersthene in charnockites does not exceed 1.5 wt%. However, it is easy to show that variations in Al_2O_3 in Opx in association with plagioclase and K-feldspar is directly dependent on μ_{K_2O}, if potassium is completely mobile. Indeed, the existence of such a relationship indicates its mobility, and its absence, its inertness. Mobility of K_2O can be demonstrated in the charnockite gneisses of central Finland. Here orthopyroxenes and coexisting plagioclases were carefully analyzed (see Tables 2 and 3) and their equilibrium parameters determined (see Table 4). In Figure 12 it is seen that with constant bulk composition of a rock, the oCrn content

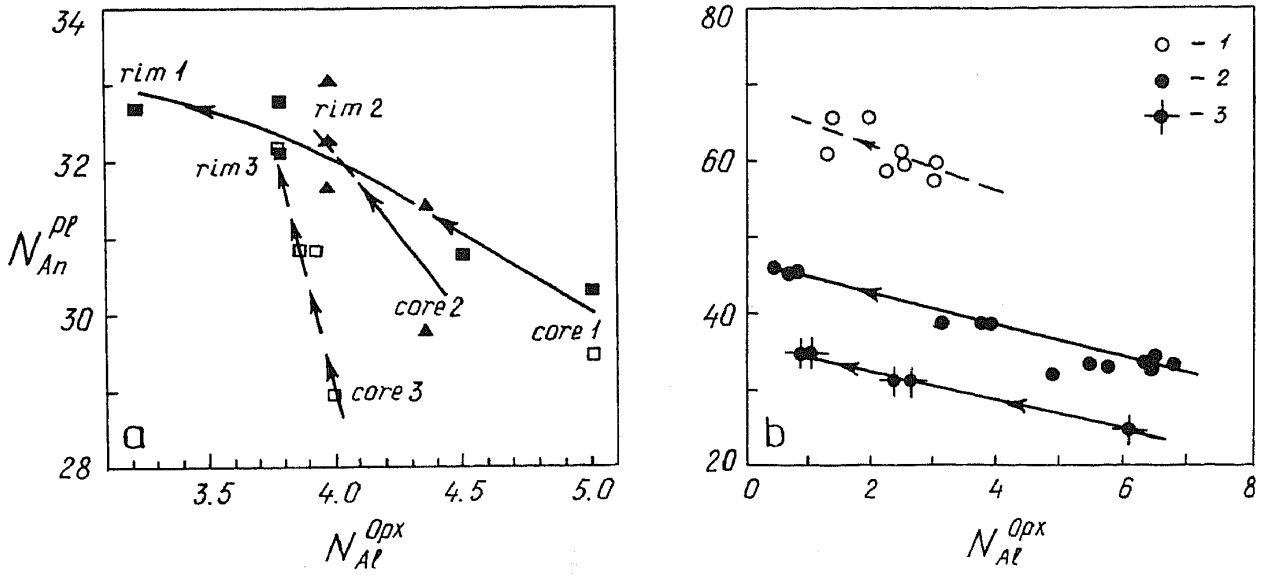

FIGURE 12. Systematic variation in composition of coexisting orthopyroxene and plagioclase, reflecting conjugate reactions (15) and (14) in charnockitic gneisses of central Finland (a) and southwest Cisbaikalia (b): 1) garnet-bearing charnockitic gneisses with carbonates; 2) metapelites; 3) migmatites.

decreases toward the edges of Opx grains, and the basicity of coexisting Pl increases. This is an unequivocal indication that μ_{K_2O} increases during charnockitization of gneisses.

According to Korzhinskiy's theory of open systems, high mobility of potassium and an increase in its chemical potential due to an increase in its activity coefficient during acid-base interaction would not necessarily lead to a sharp increase in K_2O in a rock. A positive correlation between total alkalies and the potassium concentration can be an indicator of this effect even when potassium is removed from the rock in the final stages of the process.

The distinct correlation between the compositions of biotite and of plagioclase in accordance with reactions (5) and (13)-(15) indicates that charnockites and charnockite gneisses can form as products of the metasomatism of ordinary gneisses or amphibolites during retrograde metamorphism, due to introduction of water-carbon dioxide fluids in which $\mu^{fl}_{K_2O}$ increases when those fluids react with mafic rocks. In other words, not only relatively low activity of water, but also a high chemical potential of potassium in the fluid promotes the formation of charnockites. It cannot be ruled out that the fluid evolved during crystallization of a granite magma during the retrograde phase of metamorphism [Perchuk, 1970; Letnikov, 1975] can have a high $\mu^{fl}_{K_2O}$ from the start, which leads to the formation of the orthopyroxene-orthoclase paragenesis in granulites, transforming them into charnockites.

Charnockitization of metapelites corresponds to reaction (3). But if potassium is mobile and the alumina concentration is high in the original metapelite, reaction (15) is possible. The sequence of charnockite reactions as a function of the alumina content in metapelites is shown in the composition-paragenesis diagram, Figure 13, and a few of the most likely reactions are listed in Table 6. In one way or another, as Figure 13 shows, orthopyroxene in charnockites always would be depleted in the tschermakite component. However, in some cases, if potassium activity is low, reactions (2) and (3) occur in metapelites and the development of symplectites after garnet, consisting of cordierite and aluminous orthopyroxene [Perchuk, 1989, Fig. 3], can be

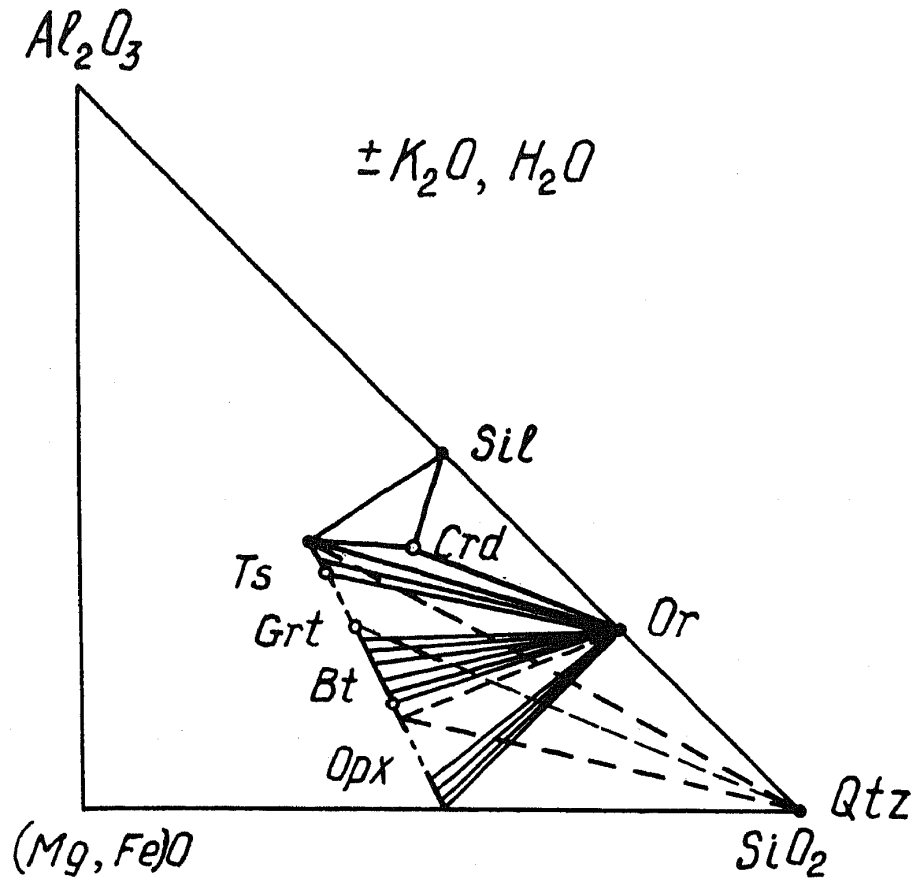

FIGURE 13. Order of reactions of charnockitization of metapelites and gneisses as a function of their alumina content.

observed. And despite the high chemical potential of CO_2 and replacement of biotite by cordierite and plagioclase, the charnockite reaction is virtually not observed.

Calculations by Sen and Battacharrya [1990], on the correlation of $\mu^{fl}_{H_2O}$ in metapelites and charnockites in the Satnuru and Madras regions of southern India, have been discussed above. It is difficult to decide whether the relatively high activity of H_2O in charnockites developed after metapelites is systematic. But such relationships are observed in the Baikal rocks (see Fig. 10).

Metamafites and Amphibolites

Little work, either theoretical or experimental, has been done on the charnockitization of mafic rocks. Nevertheless, it is clear that when fluids percolate through mafic rocks, the chemical potentials of the alkalies in the fluids would increase [Korzhinskiy, 1962], and the stronger the base, the more substantial its increase. For instance, the basicity of potassium is higher than that of sodium. Therefore, according to reaction (14), in metamafites there should be an increase in the basicity of plagioclase, accompanied by the formation of K-feldspar and a decrease in the alumina content of hornblende, according to the reactions:

$$\underset{\text{edenite}}{NaCa_2Mg_5AlSi_7O_{22}(OH)_2} + 4SiO_2 + {}^1/_2(K_2O) = \underset{\text{tremolite}}{Ca_2Mg_5Si_8O_{22}} + \underset{\text{orthoclase}}{KAlSiO_8} + ({}^1/_2Na_2O) \quad (16)$$

TABLE 6. Charnockite Reactions Caused by Dehydration of Biotite Under the Influence of Alkali-Carbon Dioxide Fluid

	Reaction	Agent
Enderbitization	$KMg_3AlSi_3O_{10}(OH)_2 + 3SiO_2 + (CO_2) = KAlSi_3O_8 + 3MgSiO_3 + (H_2O \cdot CO_2)$ *Phl + Qtz + (CO₂) = Kfs + En + fluid*	CO_2
	$KMg_2Al_3Si_2O_{10}(OH)_2 + 3SiO_2 + (CO_2) = KAlSi_3O_8 + Mg_2Al_2Si_2O_9 + (H_2O \cdot CO_2)$ *Eas + Qtz + (CO₂) = Kfs + Mg-Ts(Opx) + fluid*	CO_2
Charnockitization	$3KMg_2Al_3Si_2O_{10}(OH)_2 + 21SiO_2 + (3K_2O) = 7KAlSi_3O_8 + 2KMg_3AlSi_3O_{10}(OH)_2 + (H_2O)$ *Eas + Qtz + (K₂O) = Kfs + Phl + fluid*	K_2O
	$Mg_2Al_2Si_2O_9 + 3SiO_2 + (K_2O) = 2KAlSi_3O_8 + 2MgSiO_3$ *Mg-Ts(Opx) + Qtz + (K₂O) = Kfs + En*	K_2O

or

$$\underset{\text{pargasite}}{NaCa_2Mg_4Al_3Si_6O_{22}(OH)_2} + \underset{\text{enstatite}}{MgSiO_3} + \underset{\text{quartz}}{6SiO_2} + (K_2O) = \underset{\text{edenite}}{NaCa_2Mg_5AlSi_7O_{22}(OH)_2} + \underset{\text{orthoclase}}{2KAlSi_3O_8} \quad (17)$$

If these reactions actually take place in rocks of the amphibolite and granulite facies, there should be a fairly marked negative correlation N_{An}^{Pl} and N_{Al}^{Hbl} in charnockitized metamafites. To check this, we carefully analyzed amphibole-plagioclase-orthoclase rocks from zones of charnockitization of mafic schists in the Baikal section of the Sharyzhalgay complex. Figure 14 shows that the composition of hornblende in rocks of the metamafite-enderbite-charnockite series from this complex changes fairly systematically: below $X_{Ca}^{Hb} = 0.9$, the content of the actinolite component increases sharply, with a slight reduction of the alumina content of hornblende. In granitoids with and without orthopyroxene, the alumina content of hornblende also decreases due to reactions (16) and (17). In this case the basicity of plagioclase increases, as the albite component in it is replaced by orthoclase and the feldspar unmixes.

Figure 15 illustrates the negative correlation between the anorthite content in plagioclase and the alumina content of coexisting hornblende. This means that an increase in the chemical potential of potassium in the fluid plays an important role in the charnockitization of metamafic rocks. Nevertheless, the position of enderbites in the granite-charnockite-enderbite-metamafite section typical of the structure of the domes of the Sharyzhalgay complex, is not clear [Petrova and Levitskiy, 1984; Kurdyukov, 1989; Perchuk, 1989]. Likewise unclear are the conditions of formation of the amphibole-free charnockites and enderbites that are common in virtually all granulite complexes of the world.

Table 7 gives the reactions of decomposition of hornblende (associated with quartz) under the influence of alkali-carbonate fluids. Depending on the activity of the chemical agent, they can occur both in the case of an increase in $\mu_{K_2O}^{fl}$ and in the case of a decrease in μ_{H_2O} (for instance, due to a high content of CO_2 in the fluid). From this point of view, the charnockite reactions listed

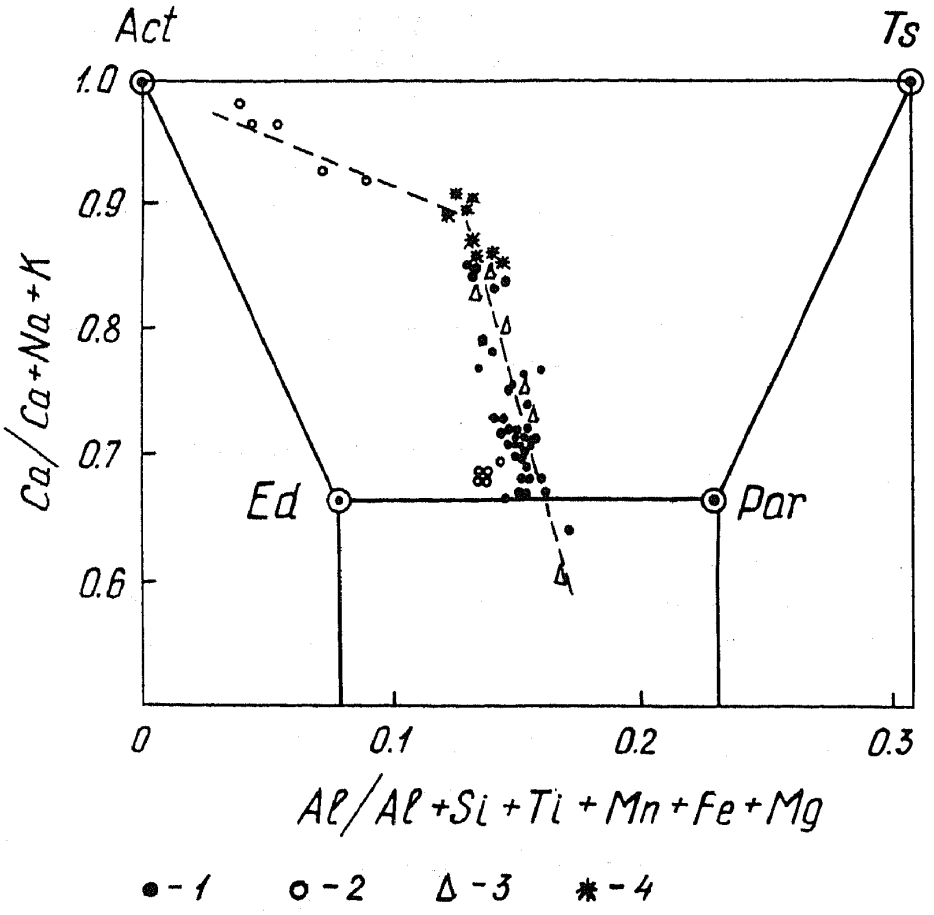

FIGURE 14. Variations in composition of hornblendes from rocks of the Sharyzhalgay complex: 1) schists and enderbites, 2) granitoids, 3) charnockites and enderbites, 4) xenoliths of metamafic rocks in intrusive enderbite bodies.

in Table 7 are of very great interest. The plot of $\mu^{fl}_{K_2O}$ versus $\mu^{fl}_{H_2O}$ (Fig. 16) illustrates conditions of metapelites and gneisses into charnockites, according to Korzhinskiy's calculations [1962].

In zoned charnockite complexes, enderbites often are situated between a zone of charnockite and a zone of metamafic rocks. For this type of section it is important to ascertain the relationships of the intensive parameters during charnockitization. Under constant T and P conditions, the main factors in the mineral equilibria in these rocks are the alkalies and the H_2O/CO_2 ratio in the fluids. Under open-system conditions, the chemical potentials of these components govern the mineral parageneses of charnockites and enderbites. The plot of $\mu^{fl}_{H_2O}$ versus $\mu^{fl}_{K_2O}$ (Fig. 17) illustrates the relationships between charnockites and enderbites formed after amphibolites (or any other metamafic rocks), under constant T and P. This plot illustrates the two main reactions of charnockitization and enderbitization. It is seen that the latter occurs at lower values of $\mu^{fl}_{H_2O}$ and $\mu^{fl}_{K_2O}$. Consequently, with relatively high $\mu^{fl}_{Na_2O}$, $a^{fl}_{CO_2}$ is favorable for the formation of enderbite after amphibole-bearing gneisses at the front of the percolating fluids. Behind this front, charnockites can develop. This relationship is seen in many metamorphic complexes. Subjected to attack by alkali-carbonate solutions, the appropriate metamorphic zoning is

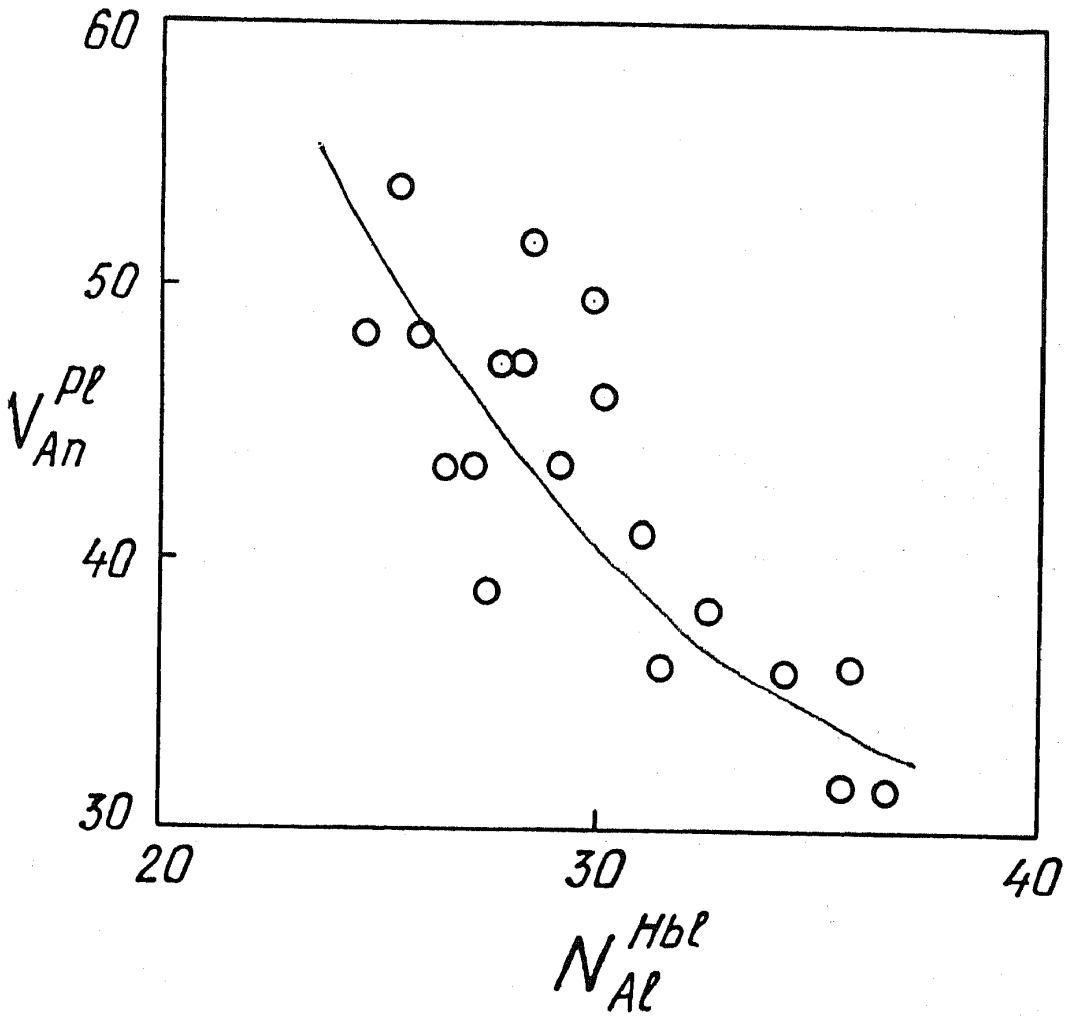

FIGURE 15. Negative correlation between basicity of plagioclase and alumina content of coexisting hornblende in association with quartz and K-feldspar in charnockitized schists, southwest Cisbaikalia. N_{An}^{Al} increases according to reaction (15), and N_{Al}^{Hbl} decreases according to reactions of the type of (16) and (17). N_{An}^{Pl} = An/(An + Ab); N_{Al}^{Hbl} = atl/(Al + Fe + Mg + Mn + Ti).

produced in them. The inner zones of transformation of amphibolites into typical charnockites develop against a background of high $\mu_{K_2O}^{fl}$.

If alkalies are inert, the influx of carbon dioxide fluids into a sequence consisting of interbedded biotite gneisses and amphibolites leads to dehydration, with the formation of a rock association in which boundaries between interlayered charnockite and enderbite are sharp.

In some cases, charnockitization of gneisses can be regulated by oxidation-reduction reactions. For instance, in a quarry near the village of Diagan (Kandy area, Sri Lanka), metagranites are replaced by carbonate- and graphite-bearing charnockites, under the influence of a reduced carbon-dioxide fluid, according to the reaction $CO_2 = Gr + O_2$. Quartz probably reacts with magnetite and calcite, forming iron-rich clinopyroxene and siderite according to the reaction:

$$\underset{\text{magnetite}}{2Fe_3O_4} + \underset{\text{quartz}}{6SiO_2} + \underset{\text{calcite}}{3CaCO_3} = \underset{\text{clinopyroxene}}{3FeCaSi_2O_6} + \underset{\text{siderite}}{3FeCO_3} + O_2 \qquad (18)$$

TABLE 7. Reactions of Dehydration of Amphiboles in the Presence of Quartz, Taking Place in Metamafic Rocks Under the Influence of Alkali-Carbonate Fluids

	Reaction	Agent
Enderbitization	$Na_2Mg_3Al_2Si_8O_{22}(OH)_2 + SiO_2 + (CO_2) = 2NaAlSi_3O_8 + 3MgSiO_3 + (CO_2 \cdot H_2O)$ *Gln + Qtz + (CO₂) = Pl + Opx + fluid*	CO_2
	$NaCa_2Mg_5AlSi_7O_{22}(OH)_2 + 3SiO_2 + (CO_2) = NaAlSi_3O_8 + 3MgSiO_3 + 2CaMgSi_2O_6 + (CO_2 \cdot H_2O)$ *Ed + Qtz + (CO₂) = Pl + Opx + Cpx + fluid*	CO_2
	$Ca_2Mg_3Al_4Si_6O_{22}(OH)_2 + SiO_2 + (CO_2) = 2CaAl_2Si_2O_8 + 3MgSiO_3 = (CO_28H_2O)$ *Ts + Qtz + (CO₂) = Pl + Opx + fluid*	CO_2
	$NaCa_2Mg_4Al_3Si_6O_{22}(OH)_2 + 4SiO_2 + (CO_2) = NaAlSi_3O_8 + CaAl_2Si_2O_8 + 3MgSiO_3 + CaMgSi_2O_6 + (CO_2 \cdot H_2O)$ *Prg + Qtz + (CO₂) = Pl + Opx + Cpx + fluid*	CO_2
Charnockitization	$NaCa_2Mg_4Al_3Si_6O_{22}(OH)_2 + 9SiO_2 + (1.5K_2O) = 3KAlSi_3O_8 + 2MgSiO_3 + 2CaMgSi_2O_6 + (H_2O \cdot 0.5Na_2O)$ *Prg + Qtz + (K₂O) = Or + Opx + Cpx + fluid*	K_2O
	$NaCa_2Mg_5AlSi_7O_{22}(OH)_2 + 3SiO_2 + (0.5K_2O) = KAlSi_3O_8 + 3MgSiO_3 + 2CaMgSi_2O_6 + (H_2O \cdot 0.5Na_2O)$ *Ed + Qtz + (K₂O) = Kfs + Opx + Cpx + fluid*	K_2O
	$Ca_2Mg_3Al_4Si_6O_{22}(OH)_2 + SiO_2 + (K_2O) = 2CaAl_2Si_2O_8 + 3MgSiO_3 + (K_2O \cdot H_2O)$ *Ts + Qtz + (K₂O) = Pl + Opx + fluid*	K_2O

In such cases the association of iron-rich pyroxene (Opx or Cpx) and graphite should be observed in the charnockites. Actually, in all the arrested charnockites of Sri Lanka and India, as well as in the ordinary charnockites of the Sharyzhalgay complex, N_{Fe}^{Opx} is at least 8-10 mole percent higher than in the associated gneisses and/or metamafites. For instance, according to the data of Hansen et al. [1987, p. 232], N_{Fe}^{Opx} in the Udadigana gneiss (sample D4-K1) is 43%, while in charnockite $N_{Fe}^{Opx} = 0.56\%$. However, an elevated iron content of Opx in charnockites is not necessarily the result of reduction of iron. It could also be the result of melting of the rock as its composition approaches the eutectic in preliminary metasomatism of the gneiss by water-carbon dioxide fluids.

Examples of Reaction Textures in Charnockites and Charnockitic Gneisses

The main alternative reactions of charnockitization of gneiss complexes have been determined above, and the possible transformation of the mineral composition of the charnockites themselves pointed out. Thus a basis has been created for explaining the reaction textures observed in rocks of the charnockite series. Here we encounter both prograde and retrograde reaction textures. By "prograde," we mean the formation of a charnockite paragenesis due to a change in some thermodynamic parameter, and destabilization of that paragenesis reflects the process of decharnockitization due to retrograde reactions.

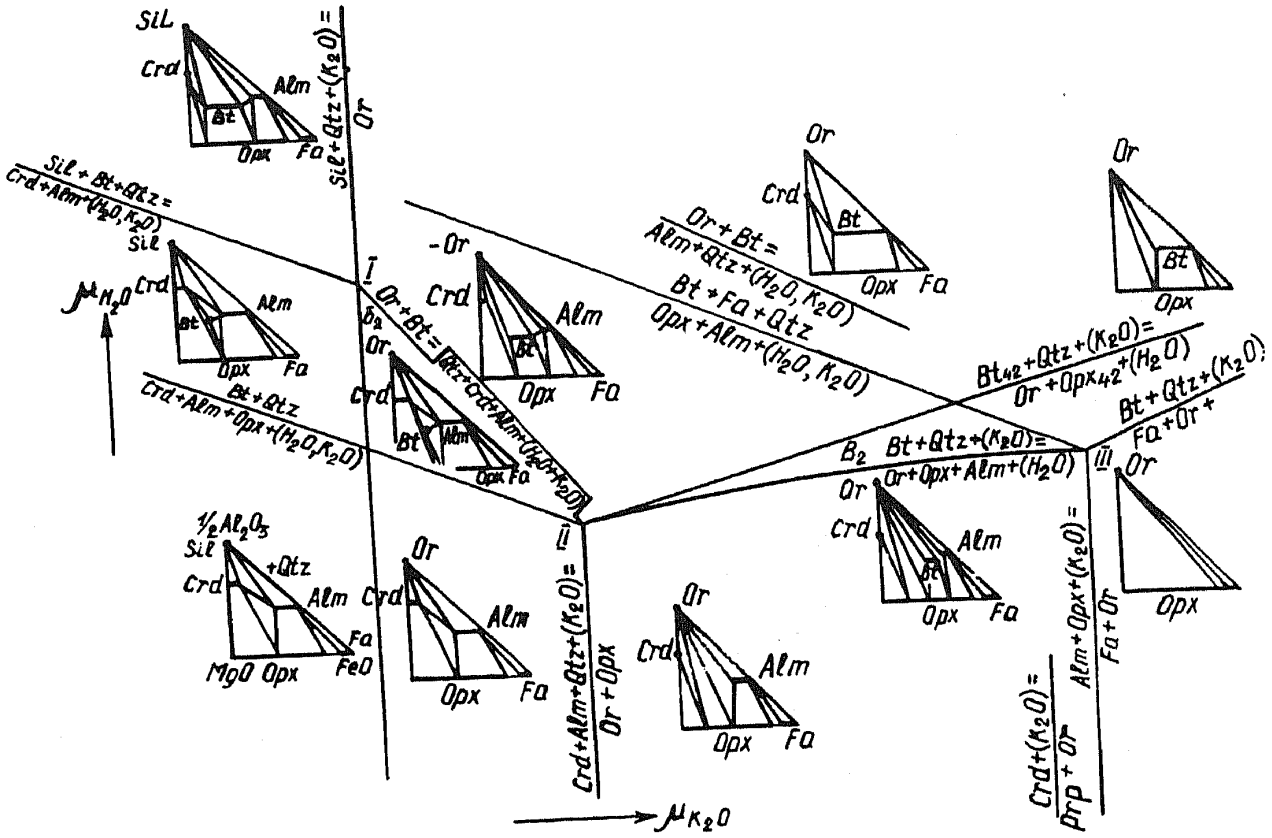

FIGURE 16. Diagram of chemical potentials of H_2O and K_2O, illustrating the role of alkalinity in the formation of charnockitic gneisses [Korzhinskiy, 1962].

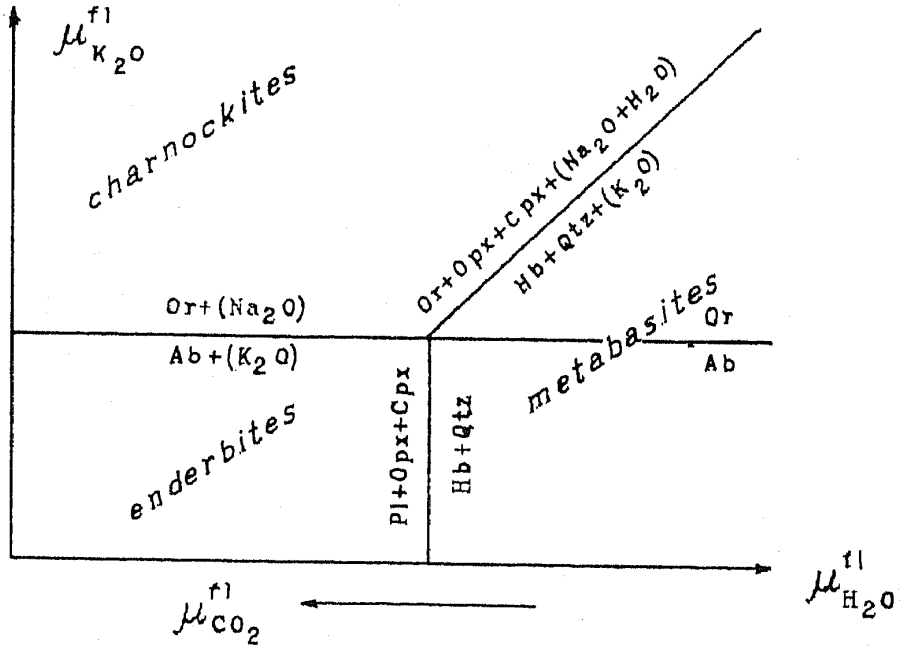

FIGURE 17. Conditions of transformation of amphibolites into charnockites and enderbites as a functio of the chemical potentials of H_2O and K_2O, at constant P and T.

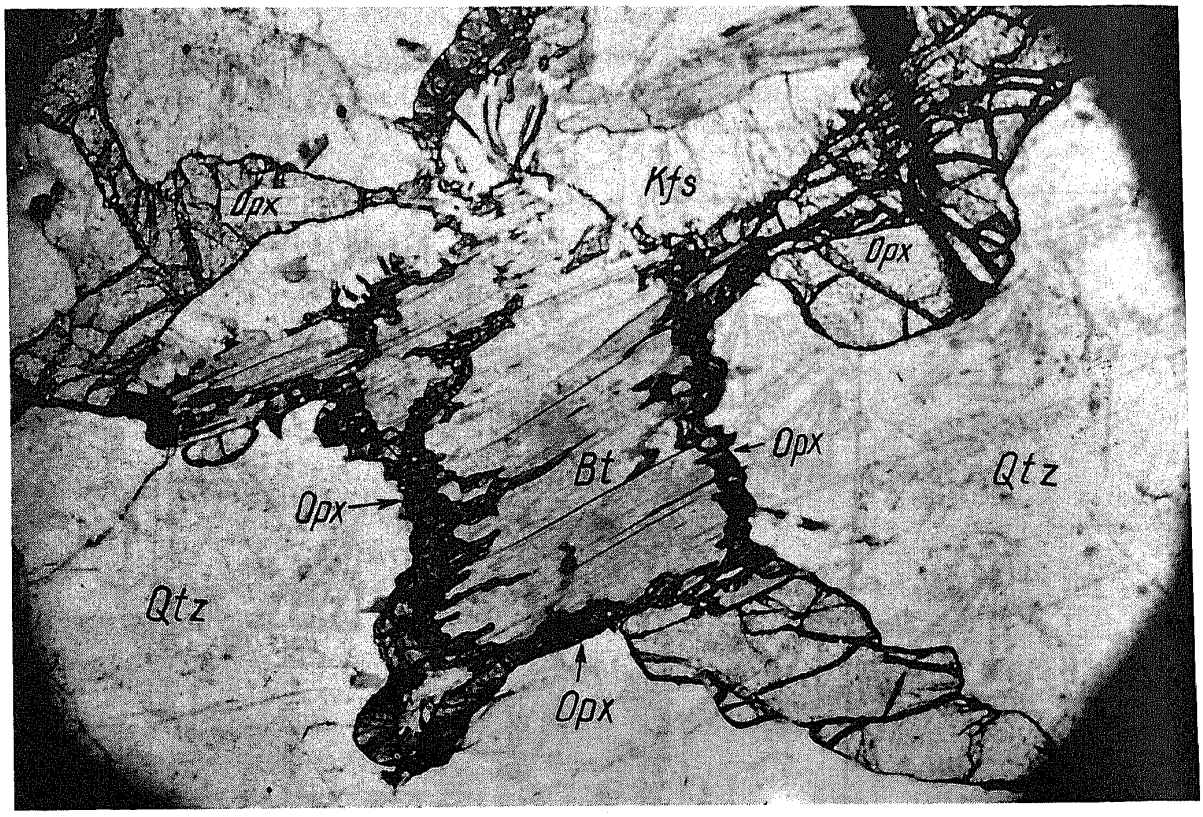

Fig. 18a

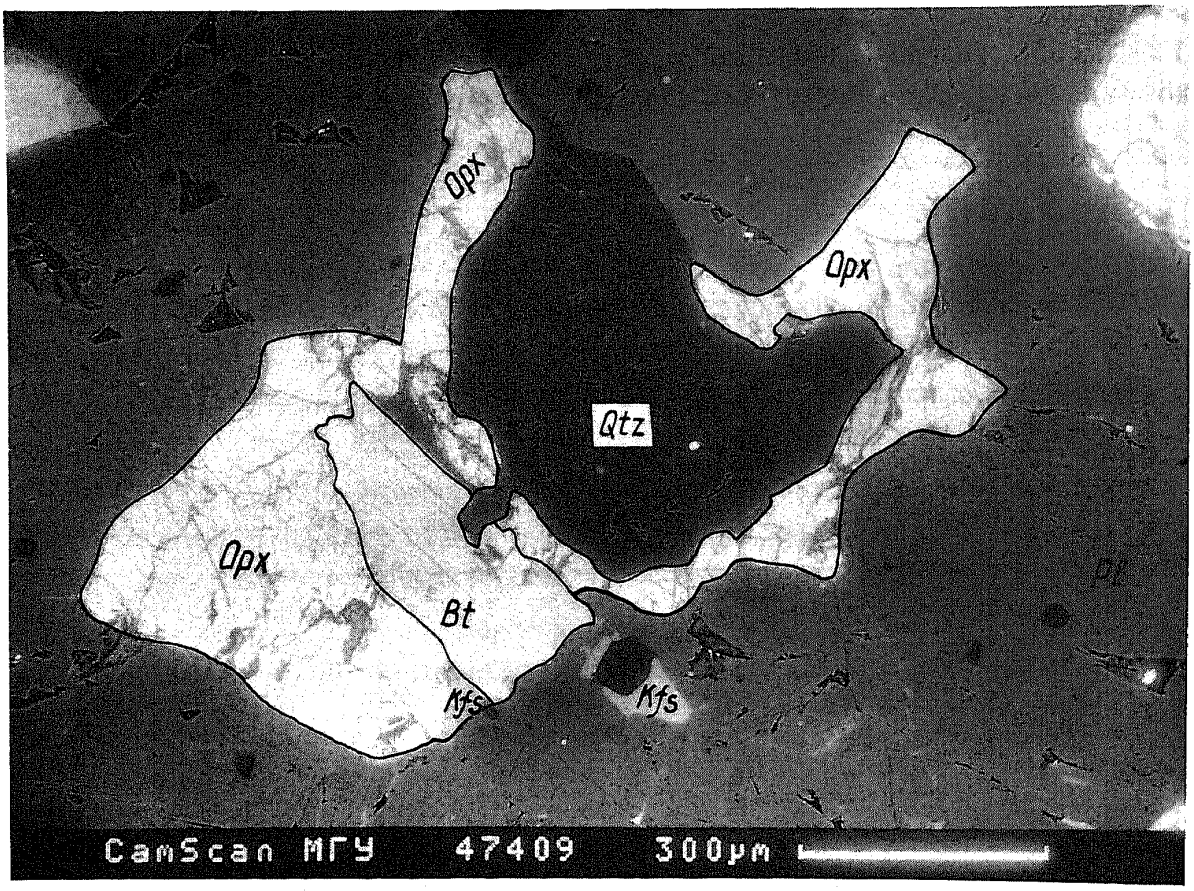

Fig. 18b

Charnockitization

The formation of Opx + Kfs reaction rims around biotite grains (Fig. 18a), described in granulites of the Sutam complex on the Aldan shield [Korikovskiy and Kislyakova, 1975; Perchuk et al., 1985], reflects a shift in reaction (4) to the right. The appearance of the biotite + quartz paragenesis at the contact between orthopyroxene and K-feldspar grains indicates displacement of this reaction to the left. Usually, both types of reaction rims occur in rocks of the charnockite series. They are not always easy to find. However, in close investigation of samples under the optical and/or electron microscope, very distinct reaction relationships between the minerals in reaction (4) can be ascertained. Figure 18b gives a photomicrograph of part of an area in a charnockite gneiss where the development of narrow rims of orthopyroxene at the contact between biotite and quartz grains is clearly seen. These rims are not more than 120 μm wide. The possible reasons for a shift in reaction (4) to the right were discussed in a previous section of this paper.

One of the most important factors in charnockitization, an increase in the activity of carbon dioxide in the fluid, is proven by the development of high-temperature carbonates in charnockite gneisses. In rocks of the charnockite series of many regions, carbonates of very different compositions are common. In some cases, two carbonates and quartz coexist. The shape of the carbonate grains and their relationships to silicates (Opx, Bt, Qtz) indicate relatively high temperatures during their formation. Moreover, some carbonates are stable in the presence of quartz and contain high concentrations of impurities, which indirectly indicates relatively high T and $a^{fl}_{CO_2}$ during their formation. The sample of Opx-Kfs gneiss in Figure 19 is an example, where Cal and Dol contain impurities (see Table 3), are in euhedral crystals and coexist with Qtz and Mag. However, such textures do not occur in charnockites proper. Carbonates form in the late stages of the process, or even during diaphthoresis. They have low contents of minor components and persistent stoichiometry. They include, for instance, Dol developed after Opx (Fig. 20). No prograde reactions were found in the charnockites we studied. Evidently they crystallized from a melt.

"Decharnockitization"

Destabilization of the Opx + Qtz paragenesis defines the process of decharnockitization in the most general sense of that term. It corresponds to a shift to the right in the reaction

$$\underset{\text{Opx}}{3MgSiO_3} + \underset{\text{Kfs}}{KAlSi_3O_8} + H_2O = \underset{\text{Bt}}{Mg_3AlSi_3O_{10}(OH)_2} + \underset{\text{Qtz}}{3SiO_2}$$

due to a local increase in $a^{fl}_{H_2O}$, probably during diaphthoresis. Hansen et al. [1987, p. 235] gave an example of such metamorphism in charnockites from the Arni area, South Arcot, in the state of Tamil Nadu, India. Here scattered bodies of gneiss formed within charnockite patches as biotite replaced hypersthene during diaphthoresis, Hansen et al. [1987] suggested that this diaphthoresis was related to the emplacement of young granites, greatly separated in time from the charnockitization process proper. Two examples of "decharnockitization," i.e., reaction (4a),

FIGURE 18. Reaction rims of orthopyroxene at the contact between quartz and biotite grains in charnockitized gneisses: a) Sutam block, Aldan shield, optical photomicrograph, plain light (from Korikovskiy and Kislyakova [1976], and b) central Finland, electron micrograph, sample Fin21g.

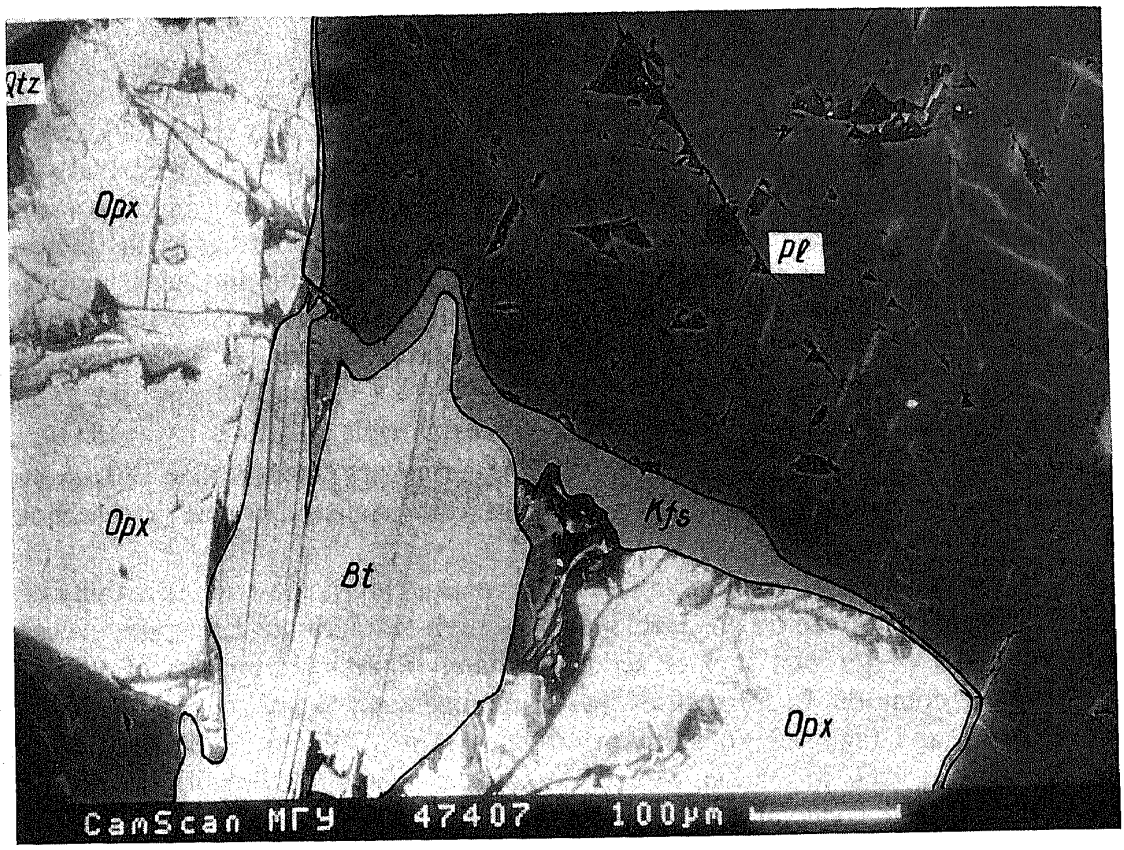

Fig. 19a

Fig. 19b

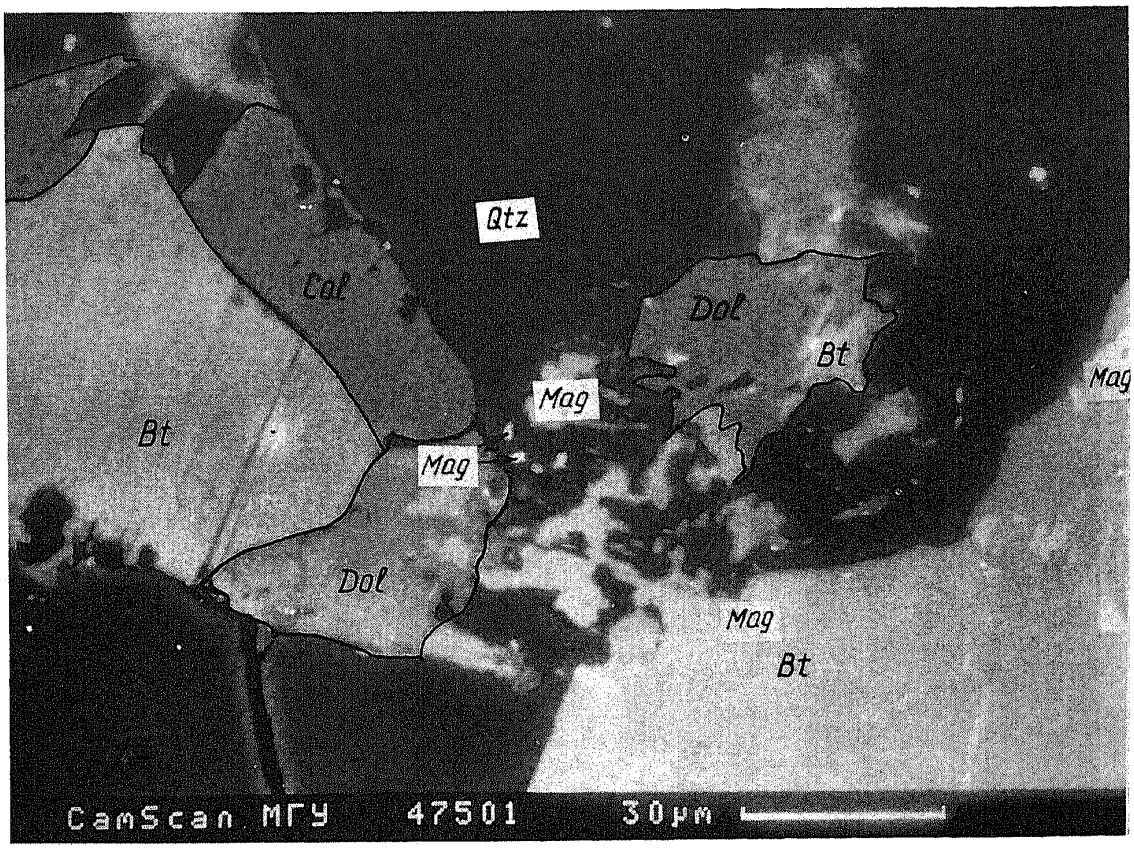

FIGURE 20. Development of carbonates + magnetite after biotite + quartz in charnockite gneiss Sh-I-7 from the Sharyzhalgay complex. Parameters of the process given in Table 4.

in charnockites and gneisses are shown in Figure 21. Moreover, the development of biotite and quartz due to the reaction of hypersthene with K-feldspar can occur not only as a result of a change in composition of the fluid; it can be accomplished as a result of a decrease in temperature and pressure along the path of retrograde metamorphism (see Fig. 8a), while the composition of the fluid remains constant.

Practically any reactions of hydration and/or carbonatization of charnockites essentially govern the process of decharnockitization. They include development of reaction rims of amphibole at the contact between orthopyroxene and calcite grains, according to the reaction

$$\underset{\text{Opx}}{8FeSiO_3} + \underset{\text{Cal}}{CaCO_3} + H_2O = \underset{\text{Ank}}{CaFeCO_3} + \underset{\text{Gru}}{Fe_7Si_8O_{22}(OH)_2} \qquad (19)$$

An example of this reaction is shown in Figure 22. Here orthopyroxene is unstable not only with K-feldspar, but also with other minerals, being replaced by iron-rich amphibole of the cummingtonite-grunerite series. In parallel with reaction (4a), in this same stage of the transformation of a charnockite the paragenesis muscovite + quartz forms, due to the reaction (see Fig. 22)

FIGURE 19. Charnockitization of gneisses in central Finland. Reaction rims of K-feldspar formed at the expense of "orthocorundum" in orthopyroxene (reaction 15) and the albite component of plagioclase (reaction 14), with elevated chemical potential of potassium. In this case, plagioclase becomes more calcic toward the rim and orthopyroxene, less aluminous (see Fig. 12a). Parameters of the process in Table 4, sample Fin21g.

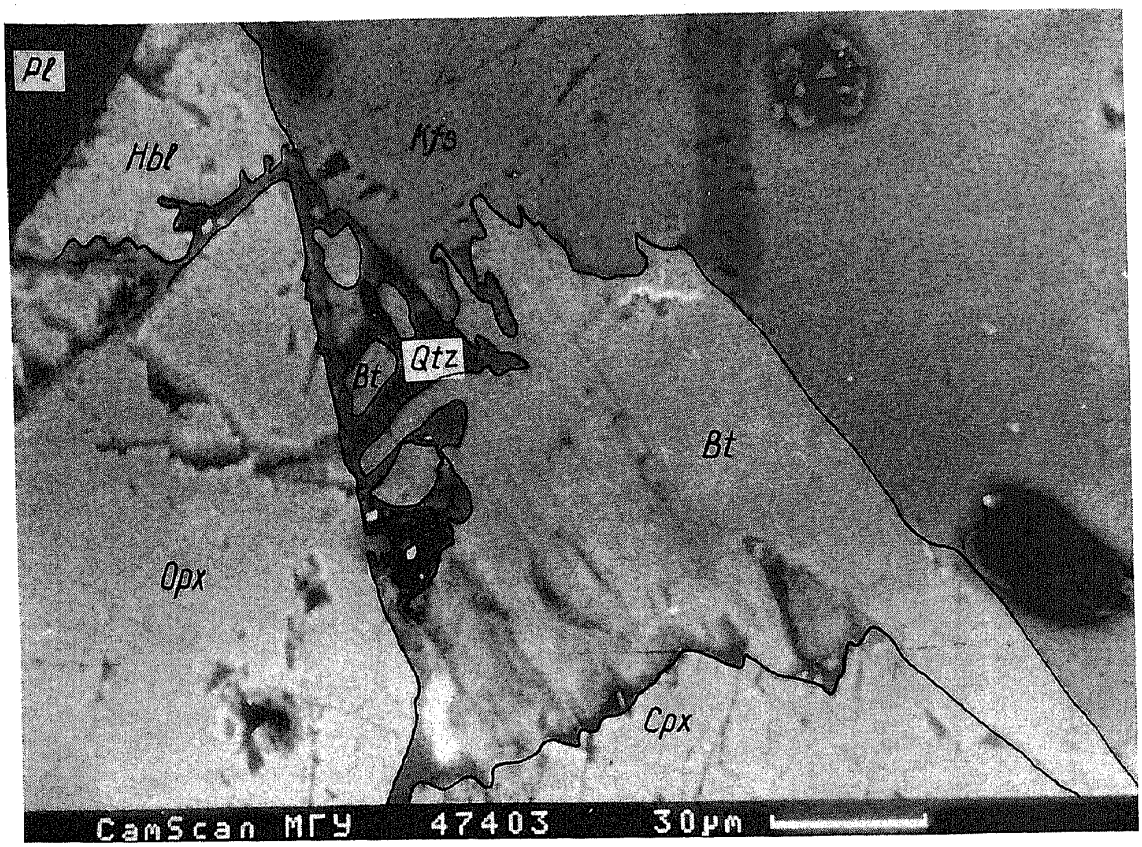

Fig. 21a

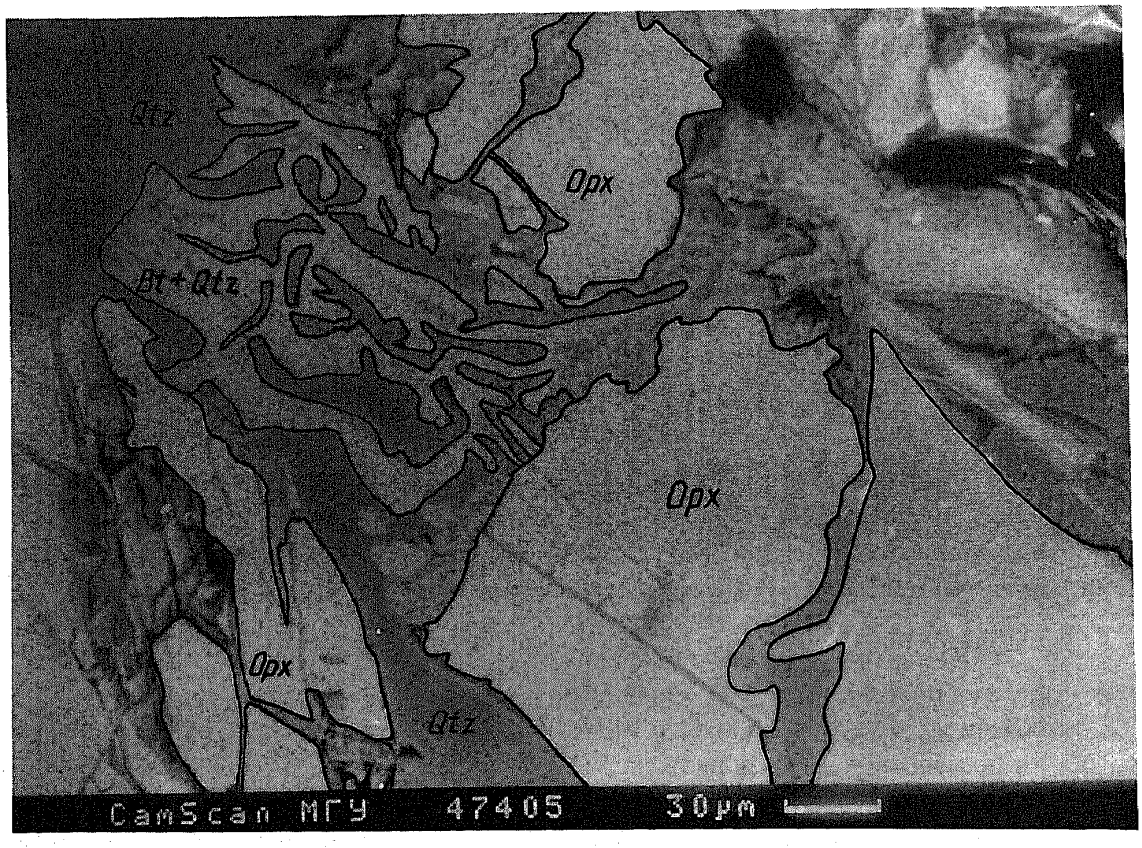

Fig. 21b

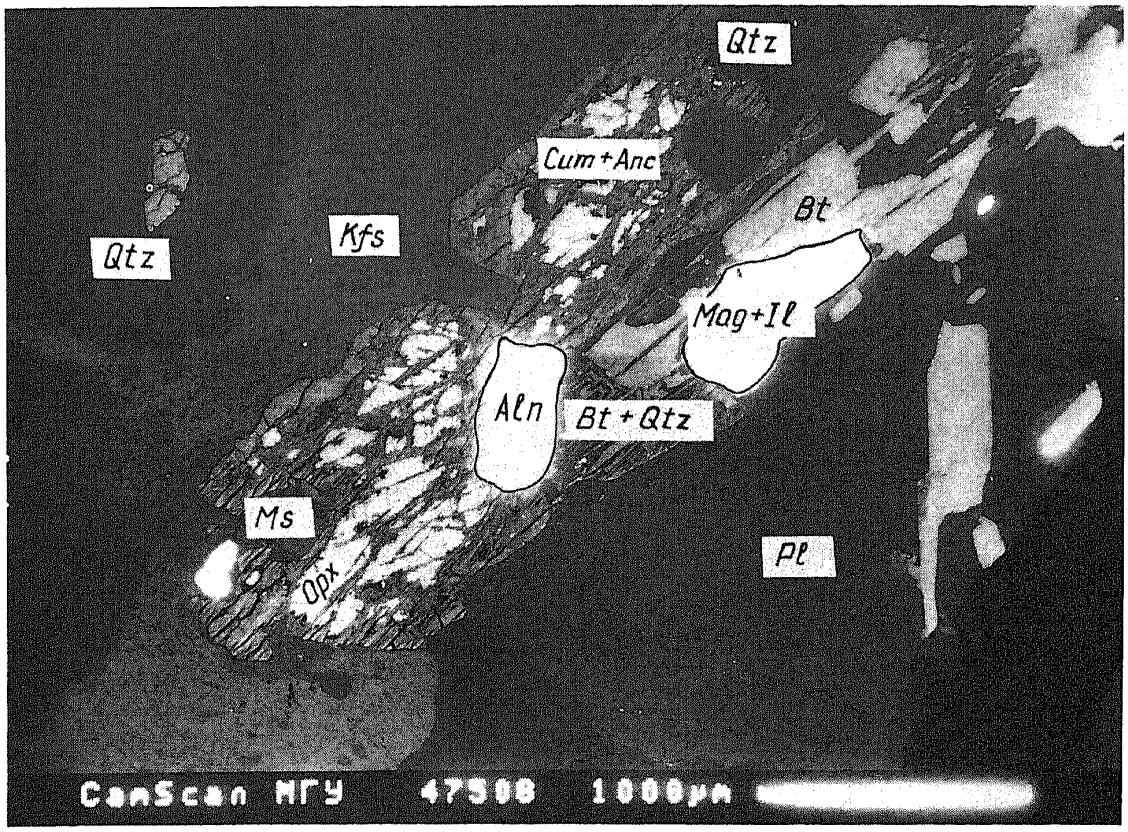

FIGURE 22. Reaction rims of iron-rich cummingtonite around orthopyroxene grains in charnockite from Sri Lanka, sample Sln-2 (see Table 4), formed by reaction (21). Also seen are symplectites of Cum + Ank and Bt + Qtz.

$$\underset{\text{An}}{CaAl_2Si_2O_8} + \underset{\text{Kfs}}{KAlSi_3O_8} + H_2O + CO_2 = \underset{\text{Ms}}{KAl_3Si_3O_{10}(OH)_2} + \underset{\text{Cal}}{CaCO_3} + \underset{\text{Qtz}}{2SiO_2} \qquad (20)$$

In many cases reaction textures developed in the late stages of the evolution of rocks of the charnockite series reflect the following reaction of carbonatization of orthopyroxene:

Reaction		Sample	Fig.
$\underset{\text{Opx}}{(Mg, Fe)SiO_3} + CO_2 = \underset{\text{Brn + Qtz}}{(Mg, Fe)CO_3 + SiO_2}$	(21)	BL3M3	23
$(Mg, Fe)SiO_3 + \underset{\text{Opx + Cal}}{CaCO_3} + CO_2 = \underset{\text{Dol + Qtz}}{Ca(Mg, Fe)(CO_3)_2 + SiO_2}$	(22)	BL22M1	—
$8FeSiO_3 + \underset{\text{Opx + Cal}}{CaCO_3} + H_2O = \underset{\text{Ank + Cum}}{CaFeCO_3 + Fe_7Si_8O_{22}(OH)_2}$	(23)	Sln-2	24

FIGURE 21. Symplectic rims of biotite + quartz separating grains of orthopyroxene from K-feldspar: a) mafic charnockite of the Sharyzhalgay complex (specimen BL4M1); b) decharnockitization of charnockitized gneiss, central Finland (specimen Fin21g). Parameters of reaction given in Table 4.

FIGURE 23. Rim of breunnerite around orthopyroxene grain from charnockitized gneiss (sample BLZM3 in Tables 2 and 4).

Characteristically, in most cases carbonatization reactions in charnockites proceed simultaneously with hydration reactions during the late stages of retrograde metamorphism, which indicates that f_{CO_2} increases along the *T-P* path.

In charnockites of the Sharyzhalgay complex, cummingtonite-magnetite rims develop around orthopyroxene grains:

$$\underset{\text{Opx}}{48FeSiO_3} + O_2 + 6H_2O = \underset{\text{Cum}}{6Fe_7Si_8O_{22}(OH)_2} + \underset{\text{Mag}}{2Fe_3O_4} \qquad (24)$$

during the late phases of the regressive stage of metamorphism (see Fig. 24).

Melting

It was stated above that charnockites and enderbites may be the products of various processes,

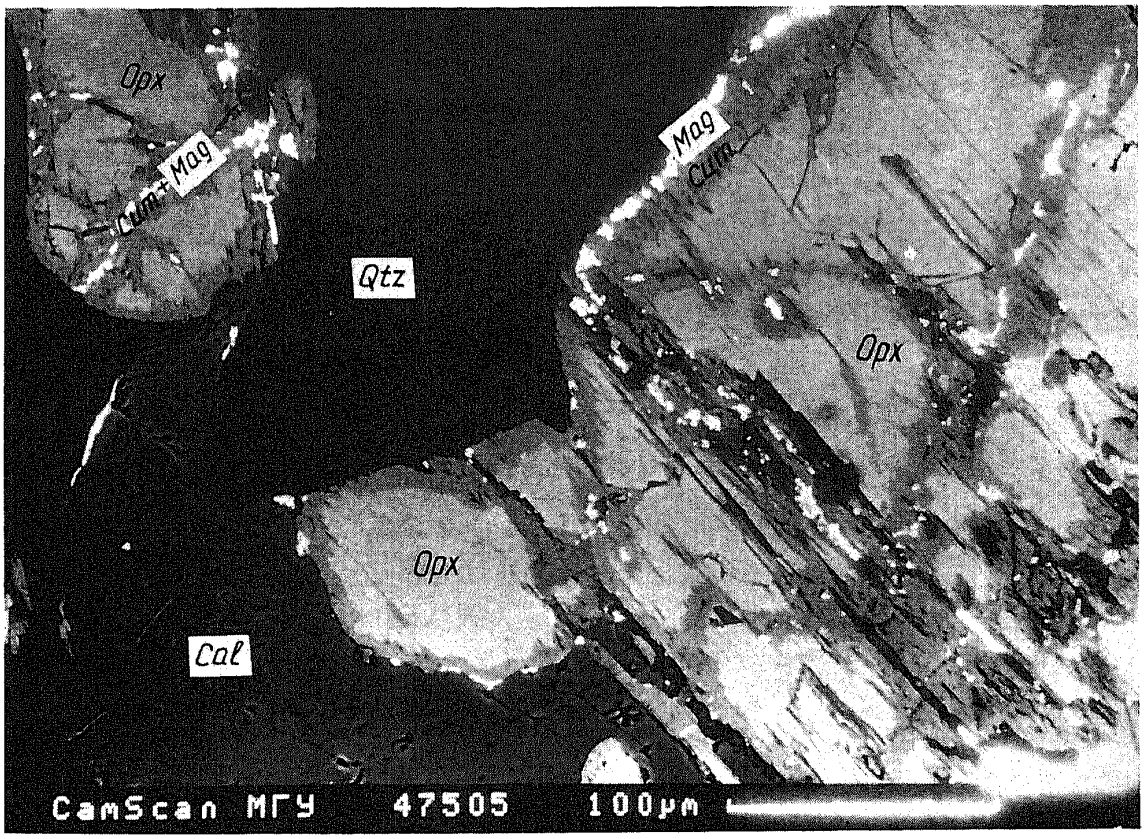

FIGURE 24. Cummingtonite-magnetite reaction rims around orthopyroxene grains in charnockite sample BL11M1 (see Tables 2 and 4) from the Sharyzhalgay complex, formed by reaction (25).

including magmatic ones. In some cases unequivocal evidence can be found of the intrusive nature of charnockites and enderbites, such as the order of crystallization of minerals and the presence of melt inclusions in them, the morphology of the intrusive bodies, etc. For instance, in the Kabbaldurga area in southern India, thick bodies (up to 1 m) of pegmatitic charnockite are emplaced in gneisses with no visible contact metamorphism. In the pegmatite veins, large (up to 3 cm) crystals of orthopyroxene contain inclusions of biotite, and in turn are rimmed by later biotite, apparently of a somewhat different composition. The texture and shape of the veins and their cross-cutting relation to the host gneisses suggest that they are igneous. Their relationship to the arrested charnockites, situated a few centimeters from the veins, could not be established, but it is clear that these two rock types are syngenetic. Along with pegmatites and arrested charnockites, the *in situ* formation of charnockite melts, capable of migrating in a very limited space, can be observed here (see Figs. 25 and 26).

In many cases it cannot be proven that any melt appeared in the central parts of the charnockite "patches" (see Figs. 3 and 6) as a product of partial melting of the gneisses. Chemical analyses show, however, that charnockites fall somewhat closer to the granite eutectic than gneisses and enderbites. This means that at the beginning of the charnockitization process the gneisses could have been metasomatically prepared for partial melting, i.e., their bulk composition shifted toward the eutectic (Sudovikov's model [1954]). This conclusion can also be drawn from the analytical data of Milisenda et al. [1991], who carefully analyzed for a large number of chemical elements in rocks along a gneiss-charnockite-gneiss profile 34.5 cm long. They found that, besides SiO_2 and alkalies, virtually all the components (including rare earths) are removed from charnockite at the contact with gneisses, forming a so-called transition zone. However, the

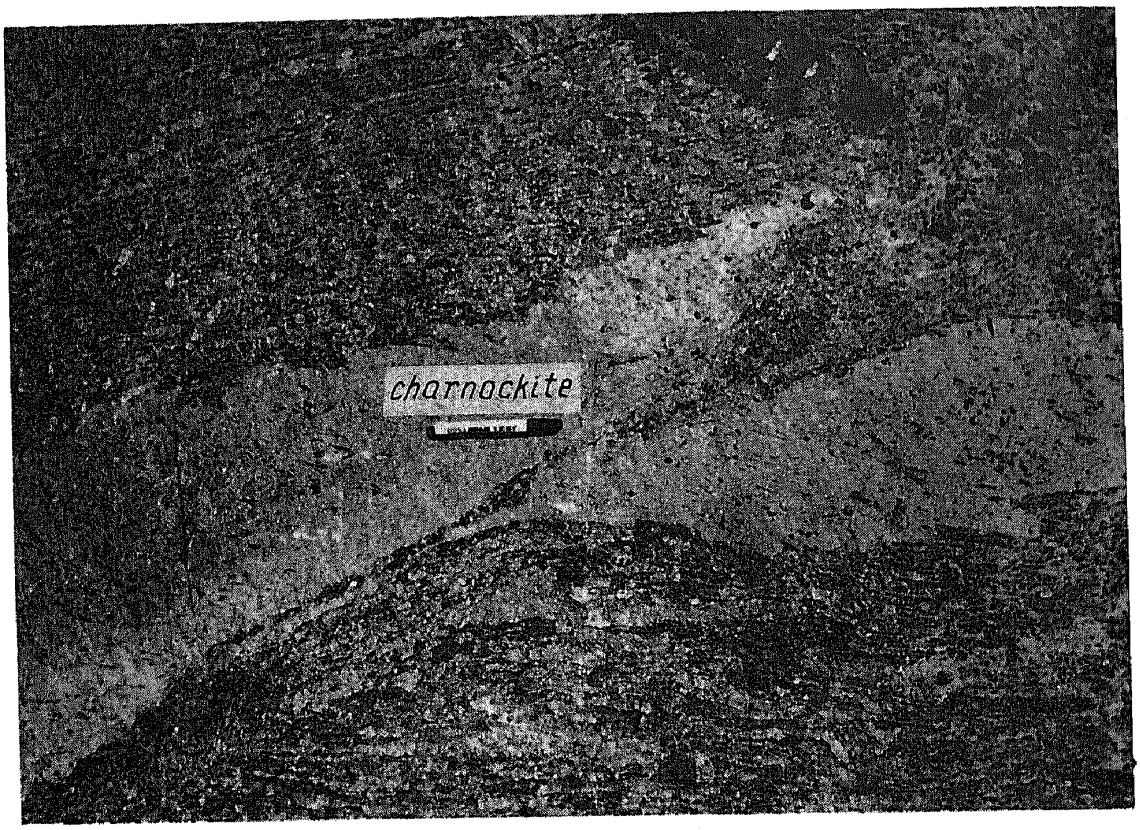

FIGURE 25. Generation of melt of charnockite composition in the Kabbaldurga gneiss complex, southern India, under the influence of water-carbon dioxide fluids. Relict foliation (linearity, banding and other elements of structural orientation), unconformable with the foliation of the host rocks, is preserved in the charnockite bodies.

amount of elements removed is strictly controlled by the composition of the fluid (at a given T and P), and the composition of the charnockite is close to the granite eutectic.

Figure 27 shows the variation in iron content of the rocks, through a patch of charnockite along the same profile: gneiss - transition zone - charnockite - transition zone - gneiss. The mineralogical and chemical zoning along the profile is:

gneiss: Bt + Hbl + Pl + Kfs + Qtz + Mag + Ilm;

transition zone: Bt + Hbl + Pl + Kfs + Qtz + Cum (after Opx) + Mag + Ilm;

charnockite (near transition zone): Opx + Kfs + Bt + Hbl + Pl + Qtz + Mag + Ilm;

charnockite (center of patch): (Bt) + Opx + Pl + Kfs + Qtz + (Mag + Ilm);

It is seen that toward the center of the patch, N_{Fe} increases in charnockite, mainly reflecting a change in N_{Fe}^{Opx} at relatively low temperature (~650° C). And this in turn may reflect an increase in iron content of the rock due to partial melting of the host gneiss, metasomatically prepared by an H_2O-CO_2-F_2 fluid. Figure 27 illustrates only the increase in iron toward the center of a charnockite "patch." However, both components, MgO and FeO, are removed metasomatically into the transition zone [Milisenda et al., 1991]. The behavior of alkalies during this process is

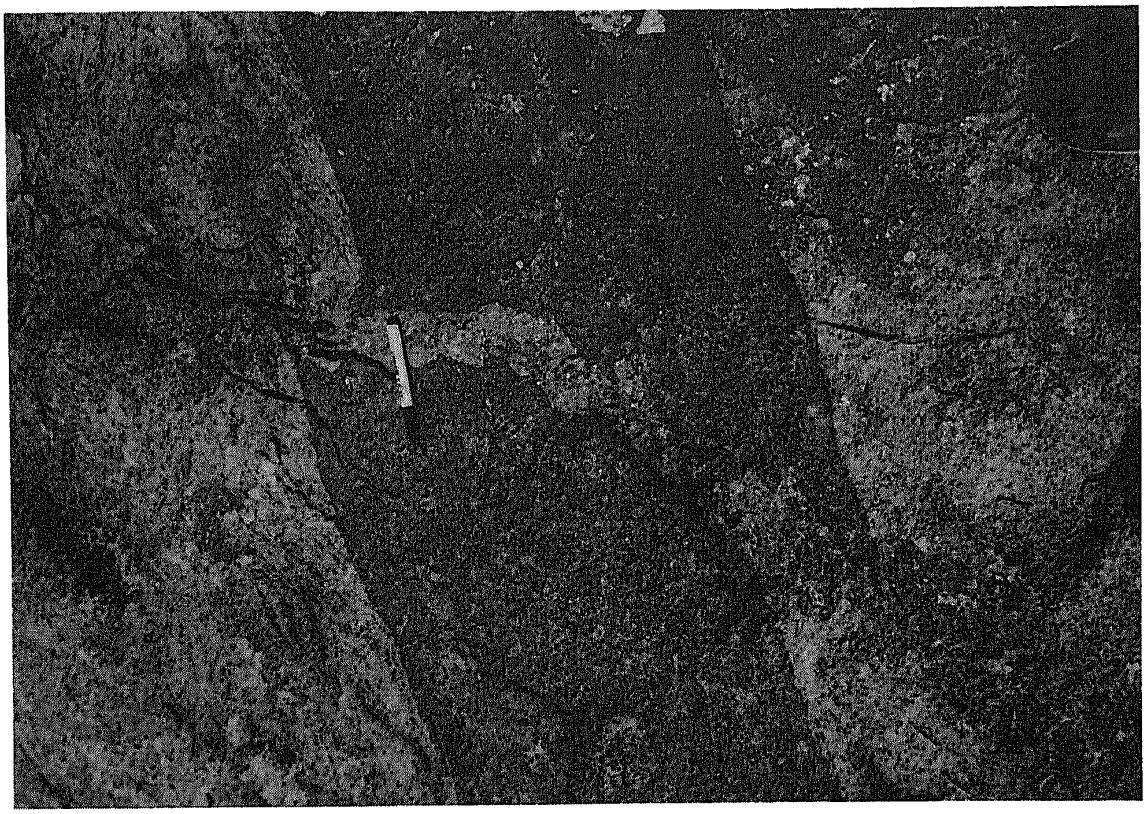

FIGURE 26. Emplacement of charnockite melt along fracture in boudin of metadolerite in orthogneiss, Kabbal, southern India.

ambiguous. In some cases they are removed from the charnockite, in others they accumulate in it. Figure 28 shows the relationships of the alkalies in charnockite and associated gneiss from southern India. Here it is seen that in most cases, the alkalies accumulate in the charnockite, although some samples show a deficit in K_2O (i.e., a shift toward enderbite, see Fig. 5). This also indicates that the central parts of charnockite patches tend toward a eutectic composition.

The degree of metasomatism of the charnockite gneisses varies, depending on many parameters, both thermodynamic and rheological. Hansen et al. [1987] studied this question by calculating charnockitization reactions and the mass balance of the components. They showed that in some cases, for instance in the Ponmudi area, charnockitization occurred under closed-system conditions, i.e., with no introduction or removal of components, while in the Kabbaldurga area, a purely metasomatic process prevailed (with introduction and removal of components). Our investigations confirm that conclusion, although their formulations are not precise. In all cases the system is open for volatiles and, in part, for silica. However, the mobility of other components

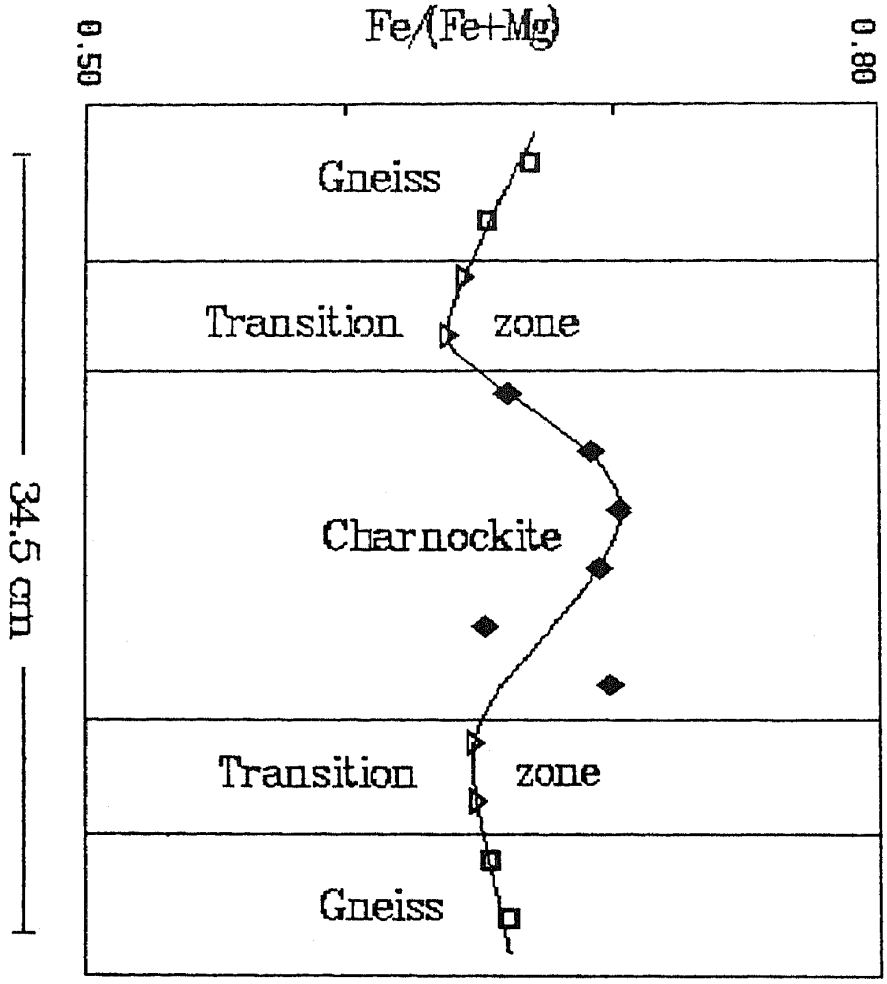

FIGURE 27. Variation of iron/magnesium ratio of rocks along a profile through a charnockite patch, plotted from analytical data of Milisenda et al. (1991): Genetic types of charnockite: 1) Kabbal, 2) Ponumudi.

during charnockitization may vary. If they are highly mobile, they are metasomatically redistributed within each patch by diffusion, with the formation of a zone of accumulation of bases such as Fe, Mg, Ca and Al [Milisenda et al., 1991]. It is interesting that in this case, the typical metasomatic zones are not formed. But in the case of melting, the rear zone is represented by melt (the analog of a monomineralic zone in the metasomatic column) [Korzhinskiy, 1922].

A bulk composition of a rock close to the eutectic is a necessary, but not sufficient, condition for melting to occur. The temperature, pressure and composition of the fluid phase must correspond to eutectic values. Looking at Table 4, as well as using estimates of these parameters for arrested charnockites [Chacko et al., 1987; Hansen et al., 1987; Santosh et al., 1988, 1991], it can be seen that in some cases a temperature of 720-740° C is reached in charnockites, at a pressure of about 5.5 kbar. This corresponds to the conditions of melting in reaction (4) in a KMAS system. Peterson and Newton [1990] made an experimental study of melting by this reaction in the presence of an equimolar H_2O-CO_2 fluid. They found the melting temperature of reaction (4) to be ~700° C or lower at a pressure of 6 kbar and $X^{fl}_{CO_2} = 0.4$. This is even lower than the melting temperature in a purely aqueous system (see Fig. 29). And if it is taken into account that the iron content of charnockites is very high (the iron number can be as high as 0.93 [Prime,

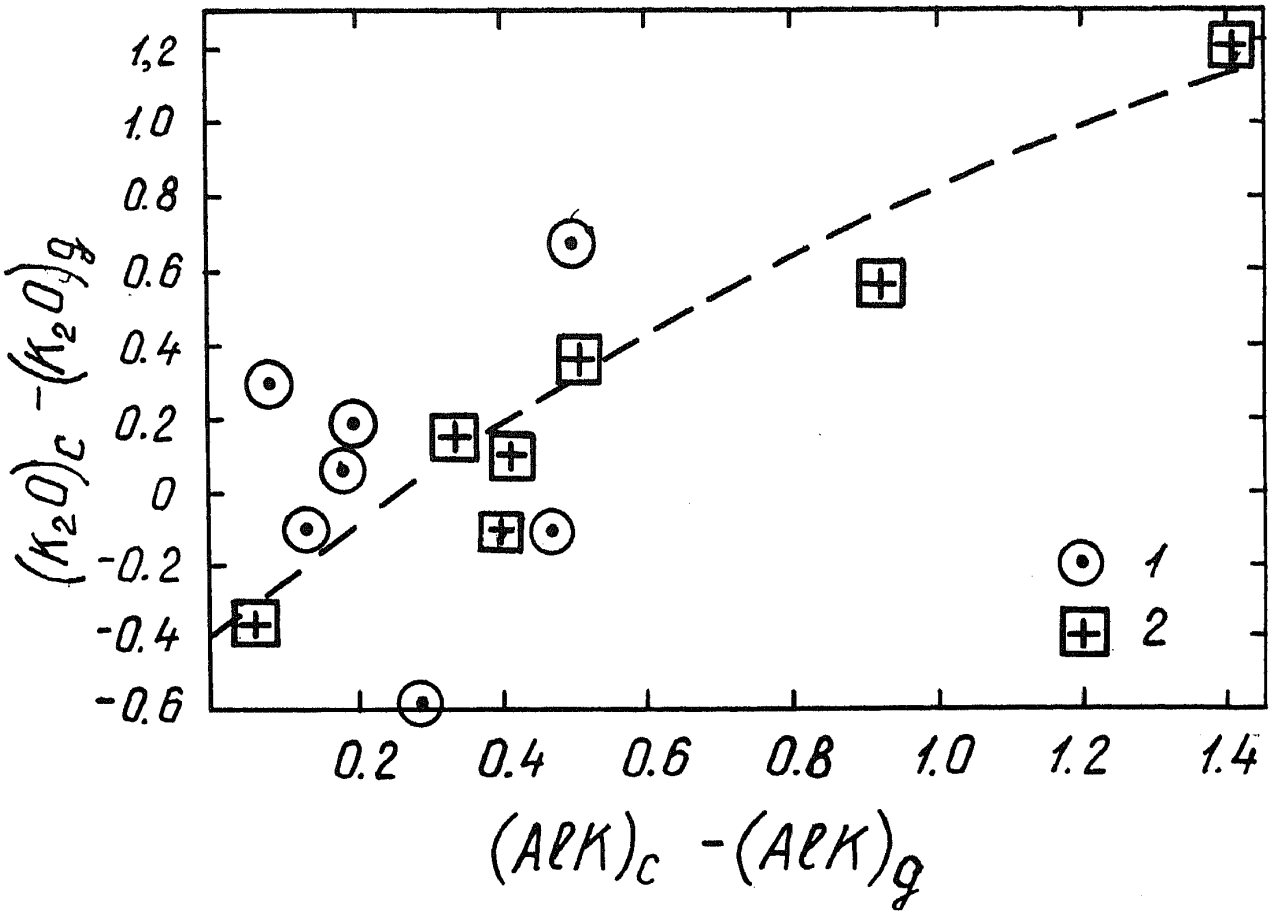

FIGURE 28. Correlation of differences in total alkalies, $(Alk)_c$-$(Alk)_g$, and of calcium $(K_2O)_c$-$(K_2O)_g$ in gneisses (g) and charnockites (c) of the Kabbal type (1) and the Ponumudi type (2) of southern India [Hansen et al., 1988].

1991]), there can be no doubt that melting of charnockite can occur in nature at a temperature on the order of 650° C. Thus the experiments by Peterson and Newton [1990] showed that there are no physicochemical barriers to the formation of granite magma in the regressive phase of metamorphism [Perchuk, 1969, 1973; Letnikov, 1975; Perchuk, 1977].

Metasomatic processes within the domain of local melting during charnockitization are obvious, and today few would dispute them. However, they are not so obvious in the case of regional charnockitization. Korzhinskiy's model [1962] is very applicable here; according to it, charnockitization takes place at the front of magmatic replacement of mafic schists by enderbite and charnockite. Enderbites, as it were, are analogs of the transition zone in the formation of charnockite patches. For the two gneiss-enderbite-charnockite complexes in the USSR, the *CNM* classification diagram in Figure 30, proposed in the first part of this paper (see Fig. 5), illustrates the shift of the bulk composition of charnockites toward the granite eutectic. In essence, Korzhinskiy's model [1962] is realized in this shift, but he did not specially discuss the role of high $X^{fl}_{CO_2}$ of the fluids. In addition, his μ-μ plot (Fig. 16) unambiguously indicates a low chemical potential of H_2O during the charnockitization process.

Judging from the morphology of the charnockite and enderbite bodies in the Ukrainian crystalline massif (observations by L.L.P., as well as Nalivkina [1964]), in the Yenisey Range [Gerya et al., 1986] and in the Sharyzhalgay complex of southwest Cisbaikalia [Letnikov, 1976;

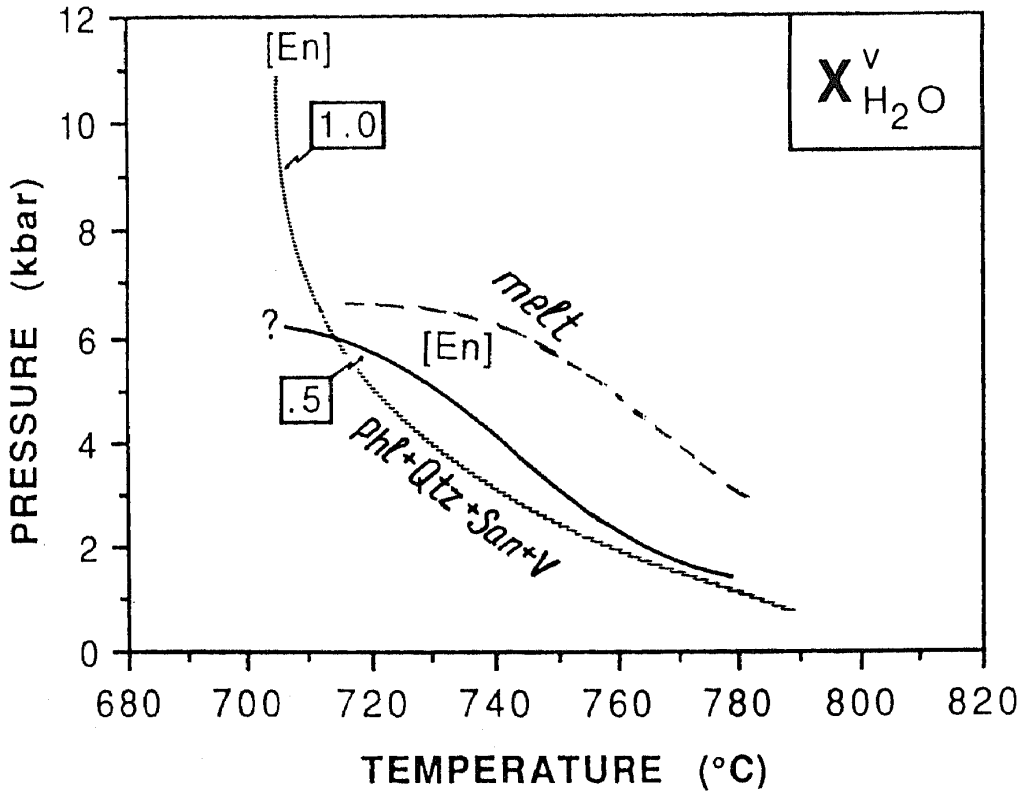

FIGURE 29. *P-T* diagram of melting of mineral association by the reaction Phl + Qtz + San = En + melt, for X_{H_2O}:X_{CO_2} = 1 in the equilibrium fluid (from data of Peterson and Newton, 1990).

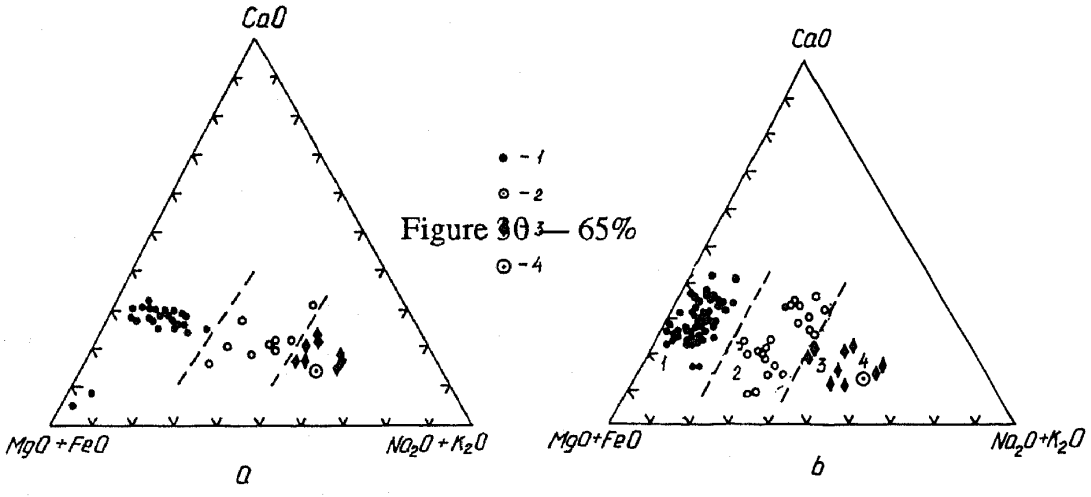

FIGURE 30. Projection of rock compositions on the *CNM* triangle (see Fig. 5): a) along the Bug R. (Ukraine) and Belorussia (from data of Fayouz al-Mukhana (1991)); b) Sharyzhalgay complex (authors' data); 1) mafic schists; 2) enderbites; 3) charnockites, 4) average (Zavaritskiy, 1960).

Petrova and Levitskiy, 1984; Perchuk, 1989], a very consistent pattern of local appearance of charnockite and enderbite melts at the granitization front is observed. For instance, in southwest Cisbaikalia the core of granite gneiss domes consists of biotite granite, replaced by charnockite and enderbite toward the country rock schists [Kurdyukov, 1989; Perchuk, 1989]. The relationship of charnockitization to granite melts is obvious here: It was the granite melts that were the

TABLE 8. Chemical Compositions and CIPW Norms of Dike Rocks Cutting Kabbaldurga Gneisses, Southern India

Oxide	Kab-9		Kab-10		Norm	Kab-9	Kab-10
	wt%					CIPW norms	
SiO_2	58.98	±0.39	52.90	±0.74	Qtz	8.748	0
TiO_2	0.67	±0.22	0.70	±0.2	Or	6.94	7.94
Al_2O_3	8.23	±0.28	7.79	±0.18	Ab	18.93	21.20
FeO	9.84	±0.33	13.50	±2.88	An	9.25	5.49
MgO	9.66	±0.43	9.99	±0.47	Ne	—	0.74
CaO	8.14	±0.18	9.84	±0.10	Di	15.98	19.6
Na_2O	2.20	±0.45	2.81	±0.70	Hed	10.12	16.5
K_2O	1.15	±0.97	1.33	±0.22	En	17.00	7.44
CO_2	0.71	±0.12	0.88	±0.09	Fs	—	6.72
H_2O	0.54	±0.01	0.80	±0.01	Fo	—	5.99
					Il	0.71	1.32
Sum	99.87*		98.85*				

*Excluding water and carbon dioxide.

carriers of the heat energy and juvenile water-carbon dioxide fluids that caused the charnockitization and enderbitization.

We should note that the importance of deep-seated magmatic melts and the fluids accompanying them is recognized by many petrologists. The divergences between the various models are not large and mainly are related to the nature of the fluids. By far the majority of investigators believe that these fluids are of juvenile, i.e., mantle, origin [Korzhinskiy, 1952, 1962, 1972; Perchuk, 1970; Petrova and Levitskiy, 1984; Frost and Frost, 1977; Frost et al., 1979; Santosh et al., 1988, 1991; Jayananda and Mahabaleswar, 1991; Chacko et al., 1987; Stähle et al., 1987 and many others]. Carbon isotope ratios from fluid inclusions and from the associated gneisses and charnockites themselves provide firm evidence of the juvenile nature of the carbon dioxide fluids [Jackson et al., 1988; Jiang et al., 1982; Santosh et al., 1988, 1991].

Some also believe (for instance, Glassly [1983]) that the source of the CO_2 should be sought in carbonate rocks undergoing granulite-facies metamorphism in the lower part of the crust. However, this model does not account for the rather high fluorine content of biotite in charnockites [Hansen et al., 1988]: the carbonate rocks in Precambrian sequence do not contain high concentrations of fluorine. Of course, solving the problem of the source of CO_2 is not essential for understanding the charnockitization process itself. It is clear that charnockitization can occur in the pressure range of 2.5 to 6 kbar, which corresponds to a depth range of 8 to 20 km. We have already presented proof of the relatively shallow depth of this process [Perchuk, 1989]. As we remarked in the Introduction, many others have come to this same conclusion. For instance, on the basis of study of the density and composition of fluid inclusions and of the P-T parameters of generation of the Closepet granites in southern India, Bantosh et al. [1991] determined the possible range of charnockitization as 2 to 5 kbar. Friend [1981], and later Jayandanda and Mahabaleswar [1991], established that the charnockites of the Kabbaldurga area are the products of alteration of orthogneisses by carbon dioxide fluids genetically related to the Closepet granites. The depths of generation of the granite magma correspond to the middle crust.

FIGURE 31. Dolerite dike in charnockitized gneisses at Kabbal, southern India. Charnockitization is evident along the contacts of the dike (some areas are circled), but there is no evidence of influx of carbon dioxide fluids from crystallizing mafic melt into the orthogneisses.

Jayananda and Mahabaleswar [1991] distinguished two stages of charnockitization: at ~2900 and ~2500 Ma (isotopic determinations). The former differ from the latter in the development of post-charnockite structural ordering. Our field observations in this same area, as well as in the highlands of Sri Lanka, also confirm the possibility of twofold occurrence of charnockitization. And still, dislocated "arrested" charnockites are very rare in the exposures studied.

In the Kabbaldurga quarry it can be seen how the charnockitization of the gneisses was accompanied by the emplacement of a post-tectonic dike of dolerite-basalt (Fig. 31). The chemical composition of the rock is given in Table 8. Its texture and mineralogic composition are very variable. In most thin-sections, rather fresh glass can be seen, in which phenocrysts of clinopyroxene, olivine, plagioclase and sanidine are present, the olivine often rimmed with clinopyroxene. But in some samples (for instance, K10-k), the glass is slightly devitrified, and it contains equant grains of olivine, clinopyroxene and orthoclase. The amount of glass locally

reaches 60%, which indicates a high degree of quenching. In some cases, most of the phenocrysts are plagioclase or K-feldspar. With the contents of most rock-forming components (except silica) close to the rest of the samples (see Table 8), that order of crystallization indicates a high chemical potential of potassium, which changed the order of precipitation of crystals.

Development of arrested charnockites and accompanying structural homogenization of the orthogneisses can be seen everywhere at the contacts of the dikes (Fig. 31). We do not wish to make an unequivocal claim that the charnockitization was related to the introduction of carbon dioxide fluids from the dolerite magma. In not one case, however, could the dolerite dike be seen to cut a charnockite patch. These observations suggest that the source of the carbon dioxide should indeed be sought in the mantle, where the mafic magmas were generated. Possibly, the influx of heat and fluids into the upper crust should be related precisely to mantle magmatism. Nor is it ruled out that this magmatism illustrates the process of advection in the granulite complexes of southern India, i.e., it leads to gravitational redistribution of material in the crust, as has been demonstrated for the granites of East Siberia [Perchuk, 1989, 1991].

Conclusions

Several thermodynamic parameters (T, P_s, $\mu^{fl}_{K_2O}$, $\mu^{fl}_{CO_2}$, $\mu^{fl}_{H_2O}$, f_{O_2}) and the bulk composition of the rocks govern the charnockite reaction (4) in Precambrian gneiss complexes. In general, it is caused by the influx of alkali-carbon dioxide fluids during the retrograde metamorphism. These fluids may lead to dehydration due to high activities of potassium and/or CO_2. Paragenetic analysis and thermobarometry of hypersthene granulites show that these chemical agents can determine the appearance of the Kfs + Opx association (charnockite) or Pl + Opx (enderbite) in the case of constant or falling temperature (along retrograde T-P trends). Geobarometry, taking into account the reaction textures in charnockite and enderbite gneisses, provides the possibility of unequivocally determining the role of each of the thermodynamic parameters listed above in charnockitization in specific complexes. In particular, mineral thermometry and barometry indicate that charnockitization occurs at shallow depths and relatively low temperatures, along the path of retrograde metamorphism. This is also indicated by petrographic and geologic observations (for instance, Hiroi et al. [1990]). Some of the most important evidence for the post-granulite origin of arrested charnockites is the *homogenization texture*, "erasure" of textural elements of all previous stages of deformation during charnockitization.

Reaction (4) has proven a reliable indicator of the thermodynamic factors governing charnockitization. In the granite-charnockite-enderbite-metamafite-gneiss complexes of ancient shields, charnockitization is accompanied by an increase in basicity of plagioclase along with a reduction in aluminum content of biotite and/or hornblende. In the case of charnockitization of hypersthene gneisses, a reduction in the aluminum content of Opx according to reaction (15) is established. These trends confirm Korzhinskiy's model of charnockitization which assigns a leading role to an increase in activity of potassium as the fluids percolate through a sequence of mafic rocks. However, in contrast to the situation in zoned complexes, in the formation of the arrested charnockites of Sri Lanka and southern India, $\mu^{fl}_{K_2O}$ does not govern the charnockite reaction (i.e., potassium is inert). In all complexes and rock associations studied, the activity of water was lower in the charnockites as they formed than in the associated gneisses. Moreover, in all charnockite associations without exception, replacement of hypersthene by biotite and/or grunerite is almost ubiquitous, which indicates that *decharnockitization* occurred (increase in $\mu^{fl}_{H_2O}$) in the late stages of retrograde metamorphism.

The relationships considered limit the applicability of the carbon dioxide model for the genesis of charnockites, including arrested charnockites (Newton's model), but rather a completely different role of fluids in the charnockitization process emerges. These fluids are not only the carriers of heat, but at the same time provide metasomatic mass transfer of practically all the components of the rock subjected to charnockitization. During metasomatism of gneiss or schist, the greater part of the major oxides are removed, guaranteeing that the composition will move close to the granite eutectic. Such metasomatism can occur at the front of formation of a melt in the inner zone, which resembles the development of a metasomatic column with a monomineralic rear zone. This is promoted by the composition of the fluid, which sharply lowers the temperature of the eutectic [Peterson and Newton, 1990]. This conclusion is based on calculation of the thermodynamic parameters of charnockitization and the finding of a correlation between Fe and SiO_2 in "arrested" charnockites, for which the possibility of melting with preliminary metasomatism and a shift of the bulk composition toward the granite eutectic has been demonstrated. Geologic observations of dikes and small bodies unequivocally demonstrate local migration of charnockite and enderbite melts.

Acknowledgements. The Institute of Experimental Mineralogy of the USSR Academy of Sciences and the International Geologic Correlation Program under Projects 235 and 304 funded the collection of material from several granulite-charnockite complexes in East Siberia, Ukraine, Sri Lanka and southern India. K. Korsman made possible our sampling of the charnockite gneisses of central Finland. L. Ya. Aranovich provided some of the microprobe analyses of minerals from the charnockites and gneisses of the Baikal section of the Sharyzhalgay block, made in the Laboratory of Electron Microscopy and Microanalysis of the Department of Petrology at Moscow University. The contribution of the personnel of this laboratory to this work was invaluable.

References

Al-Muhana, Fayrouz, 1991, Petrology of the rocks of the Bug complex of the Ukraine and of the Belorussian crystalline massif. Dissertation, Candidate's Degree in Geol.-Min. Sciences, Moscow University.

Aranovich, L. Ya., 1991, *Mineral'nyye ravnovesiya mnogokomponentnykh tverdykh rastvorov (Mineral Equilibria of Multicomponent Solid Solutions)*: Nauka Press, Moscow.

Chacko, T., Ravindra Kuma, G. R., and Newton, R. C., 1987, Metamorphic *P-T* conditions of the Kerala (S. India) khondalite belt, a granulite facies supracrustal terrain: *Jour. Geology*, Vol. 95, pp. 343-358.

Condie, K. C., Allen, P., and Narayana, B. L., 1982, Geochemistry of the Archean low- to high-grade transition zone, southern India: *Contributions to Mineralogy and Petrology*, Vol. 81, No. 3, pp. 157-167.

Dolgov, Yu. A., Makagon, V. M., and Sobolev, V. S., 1967, Fluid inclusions in kyanite from metamorphic rocks and pegmatites of the Mama area (Northeast Trans-Baikal): *Doklady AN SSSR*, Vol. 175, No. 2, pp. 444-447.

Dorogokupets, P. I. and Karpov, I. K., 1984, *Termodinamika mineralov i mineral'nykh ravnovesiy (Thermodynamics of Minerals and Mineral Equilibria)*: Nauka Press, Novosibirsk.

Friend, C. R. L., 1981, Charnockite and granite formation and influx of CO_2 at Kabbaldurga: *Nature*, Vol. 294, No. 5841, pp. 550-551.

Friend, C. R. L., 1983, The link between charnockite formation and granite production: Evidence from Kabbaldurga, Karnataka, South India. In M. P. Atherton and C. D. Gribble (Eds.), *Migmatites, Melting, Metamorphism* (pp. 246-276): Shiva Press, Nantwich.

Friend, C. R. L., 1985, Evidence for fluid pathways through Archean crust and the generation of the Closepet granite, Karnataka, South India: *Precambrian Research*, Vol. 25, Nos. 1-3, pp. 239-250.

Frost, B. R. and Frost, C. D., 1987, CO_2 melts and granulite metamorphism: *Nature*, Vol. 327, No. 6122, pp. 503-506.

Frost, B. R., Frost, C. D., and Touret, J. L. R., 1979, Magmas as a source of heat and fluids in granulite metamorphism. In D. Bridgewater (Ed.), *Fluid Movements, Element Transport and Composition of the Deep Crust* (pp. 1-18): Kluwer Academic Press.

Gerya, T. V., Datsenko, V. K., Zabolotskiy, K. A., et al., 1986, *Dokembriyskiye kristallicheskiye kompleksy Yeniseyskogo kryazha (Putevoditel' Yeniseyskoy ekskursii) [Precambrian Crystalline Complexes of the Yenisey Range (Road Log of Yenisey Excursion)]*: Institute of Geology and Geophysics, Siberian Branch of the Academy of Sciences of the USSR, Novosibirsk.

Gerya, T. V. and Perchuk, L. L., 1990, GEOPATH: a new computer program for geothermometry and related calculations with the IBM IPC computer. In E. Ghent, D. Pattison and T. Gordon (Eds.), *Metamorphic Styles in Young and Ancient Orogenic Belts*: Calgary University Press, Program and Abstracts.

Glassley, W. E., 1983, Deep crustal carbonates as CO_2 fluid sources: evidence from metasomatic reaction zones: *Contributions to Mineralogy and Petrology*, Vol. 84, Nos. 1-2, pp. 15-24.

Glossary of Geology, 1972: American Geological Institute, Alexandria, Virginia [Russian translation of second edition, Mir Press, Moscow, 1978].

Hansen, E. C., Newton, R. C., and Janardhan, A. S., 1984, Fluid inclusions in rocks from amphibolite-facies gneiss to charnockite progression in southern Karnataka, India: direct evidence concerning the fluids of granulite metamorphism: *Jour. Metamorphic Geology*, Vol. 2, No. 3, pp. 249-264.

Hansen, E. C., Janardhan, A. S., Newton, R. V., Prime, W. K. B. N., and Kumar, G. R. R., 1987, Arrested charnockite formation in southern India and Sri Lanka: *Contributions to Mineralogy and Petrology*, Vol. 96, No. 2, pp. 225-244.

Hiroi, Y., Asami, M., Curray, P. G., et al., 1990, Arrested charnockite formation in Sri Lanka: field and petrographical evidence for low-pressure conditions: *Proc. NIPR Symposium on Antarctic Geoscience*, No. 4, pp. 213-230.

Holland, T. J. B. and Powell, R., 1990, An enlarged and updated internally consistent data set with uncertainties and correlations: the system K_2O-Na_2O-CaO-MgO-MnO-FeO-Fe_2O_3-Al_2O_3-TiO_2-C-H_2-O_2: *Journal of Metamorphic Petrology*, Vol. 8, No. 1, pp. 869-890.

Hovis, G. L., 1986, Behavior of alkali feldspars: crystallographic properties, charnockitization of composition and Al-Si distribution: *American Mineralogist*, Vol. 71, No. 7-8, pp. 869-890.

Hutton, D. H. W., Dempster, T. J., and Decker, S. D., 1990, A new mechanism of granite emplacement: intrusion in active extensional shear zone: *Nature*, Vol. 343, No. 6257, pp. 452-455.

Jackson, D. H., Mattey, D. P., and Harris, N. B. W., 1988, Carbon isotope compositions of fluid inclusions in charnockites from southern India: *Nature*, Vol. 333, No. 6169, pp. 167-170.

Janardhan, A. S., Newton, R. S., and Smith, J. V., 1970, Ancient crustal metamorphism at low P_{H_2O}: charnockite formation at Kabbaldurga, South India: *Nature*, Vol. 278, No. 5704, pp. 511-514.

Janardhan, A. S., Newton, R. S., and Hansen, E. S., 1982, The transformation of amphibolite facies gneiss to charnockite in southern Karnataka and Northern Tamil Nadu, India: *Contributions to Mineralogy and Petrology*, Vol. 79, No. 2, pp. 130-149.

Jayananda, M. and Mahabaleswar, B., 1991, Relationship between shear zones and igneous activity: the Closepet granite of southern India: *India Acad. Sci. Proc., Earth and Planetary Sciences*, Vol. 100, No. 1, pp. 31-36.

Jiang, J., Clayton, R. N., and Newton, R. S., 1988, Fluids in granulite metamorphism: A comparative oxygen isotope study on the South India and Adirondack high-grade terrains: *Journal of Geology*, Vol. 96, No. 5, pp. 517-533.

Korikovskiy, S. P. and Kislyakova, N. G., 1975, Reaction textures and phase equilibria in the hypersthene-sillimanite schists of the Sutam complex on the Aldan shield. In *Metasomatism i orudneniye (Metasomatism and Mineralization)* (pp. 314-341): Nauka Press, Moscow.

Korzhinskiy, D. S., 1940, Factors in mineral equilibria and mineralogical depth facies: *Trudy Inst. Geol. Nauk*, No. 12 (AN SSSR Press, Moscow).

Korzhinskiy, D. S., 1952, Granitization as magmatic replacement: *Izvestiya AN SSSR, seriya geologicheskaya*, No. 2, pp. 56-69.

Korzhinskiy, D. S., 1962, The role of alkalinity in the formation of charnockite gneisses. In *Geologiya i petrologiya dokembriya. Obshchiye i regional'nyye problemy (Precambrian Geology and Petrology: General and Regional Problems)* (pp. 50-61): *Trudy Vostochno-Sibirskogo Geologicheskogo Institute, No. 5, ser. geol.* (AN SSSR Press, Moscow).

Korzhinskiy, D. S., 1972, Flows of transmagmatic solutions and problems of granitization. In *Magmatizm, formatsii krystallicheskikh porod i glubiny Zemli (Magmatism, Crystalline Rock Associations and the Depths of the Earth)* (pp. 144-153): Nauka Press, Moscow.

Korzhinskiy, D. S., 1982, *Teoriya metasomaticheskoy zonal'nosti 2-ye isdaniye (Theory of Metasomatic Zoning, 2nd Edition)*: Nauka Press, Moscow.

Kriegsman, L., Kroner, A., and Milisenda, C. C., 1991, Excursion 4: Kurunegala and Dambula Areas, Wanni Complex and Central Granulite Belt (CGB). In G. Voll and L. Kleinschrodt (Eds.), *The Crystalline Crust of Sri Lanka. Part II (Excursion Guide)* (pp. 38-48): *Geological Survey Department of Sri Lanka*, Prof. Papers, Vol. 6.

Kurdyukov, Ye. V., 1989, Evolution of metamorphism and granitization in the Precambrian of the Sharyzhalgay block (Baikal area). Author's abstract of Candidate's dissertation, Moscow University.

Kurdyukov, Ye. B. and Berdnikov, N. V., 1987, *P-T* conditions of metamorphism and granitization of the Sharyzhalgay complex (southwest Cisbaikalia): *Izvestiya AN SSSR, seriya geologicheskaya*, No. 12, pp. 42-49.

Lamb, W. and Valley, J. W., 1984, Metamorphism of reduced granulites in low-CO_2 vapor-free environment: *Nature*, Vol. 312, No. 5989, pp. 56-58.

Letnikov, F. A., 1975, *Granitoidy glibovykh oblastey (Granitoids of Shield Regions)*: Nauka Press, Moscow.

Marakushev, A. A., 1965, *Problemy mineral'nykh fatsiy metamorficheskikh i metasomaticheskikh porod (Problems of the Mineral Facies of Metamorphic and Metasomatic Rocks)*: Nauka Press, Moscow.

Marakushev, A. A., 1968, *Termodinamika metamorficheskoy gidratatsii mineralov (Thermodynamics of Metamorphic Hydration of Minerals)*: Nauka Press, Moscow.

McLelland, J., Hunt, W. M., and Hansen, E. C., 1988, The relationship between metamorphic charnockite and marble near Speculator, Central Adirondack mountains, New York: *Journal of Geology*, Vol. 96, No. 4, pp. 455-467.

Milisenda, C. C., Pohl, J. R., and Hofmann, A. W., 1991, Charnockite formation at Kurunegala, Sri Lanka. In *Summary of Research of the German-Sri Lankan Consortium: Geological Survey Department of Sri Lanka, Prof. Papers*, Vol. 5, pp. 141-159.

Nalivkina, E. B., 1964, *Charnokity yugo-zapadnoy chasti Ukrainskogo kristallicheskogo massiva*

i ikh genezis (Charnockites of the Southwestern Part of the Ukrainian Crystalline Massif and Their Origin): Nedra Press, Moscow.

Newton, R. C., 1986, Fluids of granulite facies metamorphism. In *Fluid-Rock Interactions during Metamorphism* (pp. 36-49): (*Advances in Physical Chemistry*, Vol. 5), Springer-Verlag, New York.

Perchuk, L. L., 1970, Thermodynamic conditions of granitization of metapelitic sequences. In *Ocherki fiziko-khimicheskoy petrologii (Outlines of Physicochemical Petrology)* (pp. 188-214): Nauka Press, Moscow.

Perchuk, L. L., 1973, *Termodinamicheskiy rezhim glubinnogo petrogenezisa (Thermodynamic Regime of Deep-Seated Petrogenesis)*: Nauka Press, Moscow.

Perchuk, L. L., 1976, Gas-mineral equilibria and a possible geochemical model of the Earth's interior: *Physics of the Earth and Planetary Interiors*, Vol. 13, No. 3, pp. 232-239.

Perchuk, L. L., 1977, Thermodynamic control of metamorphic processes. In S. K. Saxena and S. Bhattacharji (Eds.), *Energetics of Geological Processes* (pp. 285-352): Springer Verlag, New York.

Perchuk, L. L., 1985, Metamorphic evolution of shields and fold belts: *Geologicky Zbornik—Geologia Carpatica*, Vol. 36, Pt. 2, pp. 179-189.

Perchuk, L. L., 1986, The course of metamorphism: *International Geology Review*, Vol. 28, No. 12, pp. 1377-1400.

Perchuk, L. L., 1989, *P-T*-fluid regimes of metamorphism and related magmatism with specific reference to the Baikal granulites. In S. Daly, B. Yardley and B. Cliff (Eds.) *Evolution of Metamorphic Belts* (pp. 275-291): Geological Society of London, Special Publication.

Perchuk, L. L., 1990, Derivation of thermodynamically consistent system of geothermometers and geobarometers for metamorphic rocks and magmatic. In L. L. Perchuk (Ed.) *Progress in Metamorphic and Magmatic Petrology* (pp. 93-112): Cambridge University Press, Cambridge.

Perchuk, L. L., 1991, Studies in magmatism, metamorphism and geodynamics: *International Geology Review*, Vol. 33, No. 4, pp. 311-374.

Perchuk, L. L., Aranovich, L. Ya., Podlesskii, K. K., Lavrent'eva, I. V., Gerasimov, V. Yu., Fed'kin, V. V., Kitsul, V. N., and Karsakov, L. P., 1985, Precambrian granulites of the Aldan shield, eastern Siberia, USSR: *Journal of Metamorphic Geology*, Vol. 3, No. 3, pp. 265-310.

Perchuk, L. L. and Gerya, T. V., 1990, Regime of CO_2 and H_2O in some granulite facies rocks: *The Baltic Shield. Second Symposium (Abstracts)*: Lund, Sweden, pp. 72-73.

Perchuk, L. L., Podlesskii, K. K., and Aranovich, L. Ya., 1990, Thermodynamics of some framework silicates and their equilibria: application to geothermometry. In L. L. Perchuk (Ed.) *Progress in Metamorphic and Magmatic Petrology* (pp. 131-166): Cambridge University Press, Cambridge.

Perchuk, L. L. and Ryabchikov, I. D., 1976, *Fazovoye sootvetstviye v mineral'nykh sistemakh (Phase Relations in Mineral Systems)*: Nedra Press, Moscow.

Peterson, J. W. and Newton, R. C., 1990, Experimental biotite-quartz melting in the KMASH-CO_2 system and the role of CO_2 in petrogenesis of granites and related rocks: *American Mineralogist*, Vol. 75, Nos. 9-10, pp. 1029-1042.

Petrova, Z. I. and Levitskiy, V. I., 1984, *Petrologiya i geokhimiya granulitovykh kompleksov Pribaykal'ya (Petrology and Geochemistry of the Granulite Complexes of the Cisbaikal Area)*: Nauka Press, Moscow.

Prime, W. K. B. N., 19??, Petrology of the Kataragama complex, Sri Lanka: Evidence for high T, P granulite-facies metamorphism and subsequent isobaric cooling. In A. Kroner (Ed.),

The Crystalline Crust of Sri Lanka. Part I. Summary of Research of the German-Sri Lankan Consortium: Geological Survey Department of Sri Lanka, Prof. Papers, Vol. 5, pp. 200-224.

Raith, M., Hoernes, S., Klatt, E., and Stähle, H. J., 1989, Contrasting mechanisms of charnockite formation in the amphibolite to granulite grade transition zones of southern India. In D. Bridgewater (Ed.) *Fluid Movements, Element Transport and Composition of the Deep Crust*: NATO ASI Series C, Vol. 281, pp. 29-38.

Santosh, M., Harris, N. B. W., Jackson, D. H., and Mattey, D. P., 1990, Dehydration and incipient charnockite formation: a phase equilibria and fluid inclusions study from South India: *Journal of Geology*, Vol. 98, No. 6, pp. 915-926.

Santosh, M., Jayananda, M., and Mahabaleswar, B., 1991, Fluid inclusions in the Closepet Granite: a magmatic source for CO_2 in charnockite formation at Kabbaldurga?: *Jour. Geol. Soc. India*, Vol. 38, No. 1, pp. 55-65.

Sen, S. K. and Battacharrya, A., 1990, Granulites of Satnuru and Madras: a study of different behavior of fluids. In D. Vielzeuf and P. Vidal (Eds.), *Granulites and Crustal Evolution* (pp. 367-384): Kluwer Academic Press, NATO Advanced Study Institute Series.

Stähle, H. J., Raith, M., Hoernes, S., and Delfs, A., 1987, Element mobility during incipient granulite formation of Kabbaldurga, southern India: *Journal of Petrology*, Vol. 28, No. 6, pp. 1-32.

Sudovikov, N. G., 1954, Tectonics, metamorphism, migmatization and granitization of rocks of the Ladoga association: *Trudy Laboratorii geologii i geokhronologii dokembriya*, No. 4; AN SSSR Press, Leningrad.

Tomilenko, A. A. and Chupin, V. P., 1983, *Termobarogeokhimiya metamorficheskikh kompleksov (Thermobarogeochemistry of Metamorphic Complexes)*: Nauka Press, Moscow.

Touret, J., 1981, Fluid inclusions in high grade metamorphic rocks. In L. S. Hollister and M. L. Crawford (Eds.), *Short Course in Fluid Inclusions: Application to Petrology* (pp. 182-208): Mineralogical Association of Canada, Ottawa.

Walther, J. V. and Orville, P. M., 1982, Volatile production and transport in regional metamorphism: *Contributions to Mineralogy and Petrology*, Vol. 79, No. 3, pp. 242-247.

Waters, D. J. and Whales, C. J., 1985, Dehydration melting and the granulite transition in metapelites from southern Namaqualand, South Africa: *Contrib. Mineralogy and Petrology*, Vol. 88, No. 3, pp. 269-275.

Yardley, B. W., 1989, *An Introduction to Metamorphic Petrology*: Longman Scientific and Technical Press, New York.

Zavaritskiy, A. N., 1960, *Pereschet khimicheskikh analizov izverzhennykh gornykh porod (Recalculation of Chemical Analyses of Igneous Rocks)*: Gosgeoltekhizdat, Moscow.